Department of Built Environment

Assessing water and sediment balances in clayey agricultural fields in high-latitude conditions

Mika Turunen

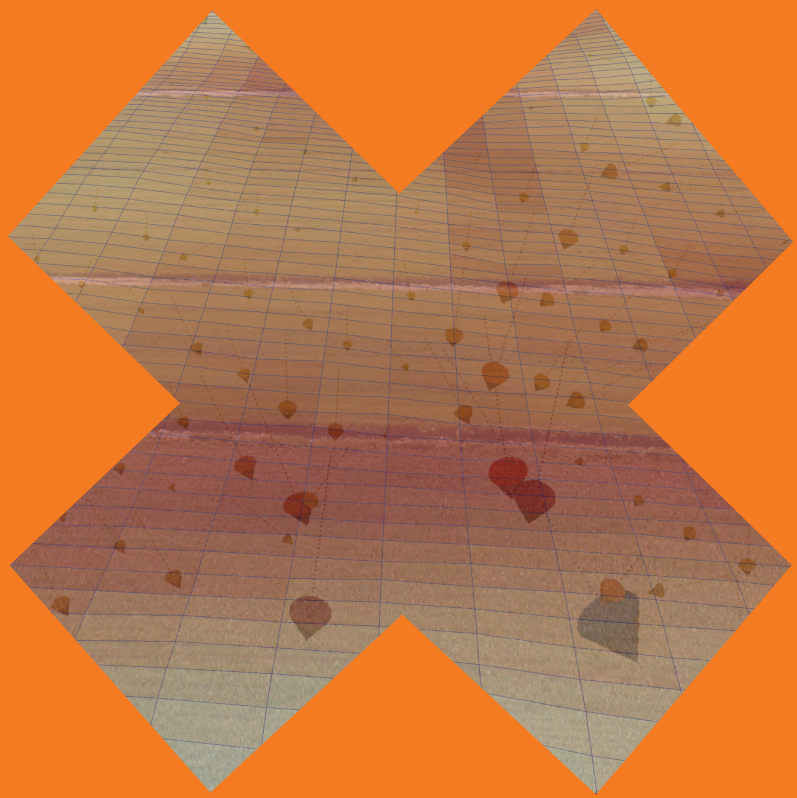

Aalto University

DOCTORAL DISSERTATIONS

Aalto University publication series
DOCTORAL DISSERTATIONS 67/2017

Assessing water and sediment balances in clayey agricultural fields in high-latitude conditions

Mika Turunen

A doctoral dissertation completed for the degree of Doctor of Science (Technology) to be defended, with the permission of the Aalto University School of Engineering, at a public examination held at the lecture hall R1 of the school on 28 April 2017 at 12.

Aalto University
School of Engineering
Department of Built Environment
Water and Environmental Engineering

Supervising professor
Professor Harri Koivusalo

Thesis advisor
Dr. Lassi Warsta

Preliminary examiners
Professor John L. Nieber, University of Minnesota, USA
Dr. Lillian Øygarden, Bioforsk, Norway

Opponent
Professor Emeritus Per-Erik Jansson, KTH Royal Institute of Technology, Sweden

Aalto University publication series
DOCTORAL DISSERTATIONS 67/2017

ISBN 978-952-60-7379-8 (printed)
ISBN 978-952-60-7378-1 (pdf)
ISSN-L 1799-4934
ISSN 1799-4934 (printed)
ISSN 1799-4942 (pdf)
http://urn.fi/URN:ISBN:978-952-60-7378-1

Unigrafia Oy
Helsinki 2017

Finland

441 697
Printed matter

Aalto University

Abstract

Aalto University, P.O. Box 11000, FI-00076 Aalto www.aalto.fi

Author
Mika Turunen

Name of the doctoral dissertation
Assessing water and sediment balances in clayey agricultural fields in high-latitude conditions

Publisher School of Engineering

Unit Department of Built Environment

Series Aalto University publication series DOCTORAL DISSERTATIONS 67/2017

Field of research Water and Environmental Engineering

Manuscript submitted 19 December 2016 **Date of the defence** 28 April 2017

Permission to publish granted (date) 13 February 2017 **Language** English

☐ **Monograph** ☒ **Article dissertation** ☐ **Essay dissertation**

Abstract

Comprehensive knowledge of hydrological processes controlling water flow, erosion and transport of substances is a prerequisite for the design of water management procedures for sustainable crop production. Knowledge gaps currently exist regarding hydrological processes and flow paths of water and sediment in subdrained clayey soils in high-latitude conditions.

This thesis aimed to quantify the dominating water and sediment balance components in subdrained clayey soils in different drainage, topographic and hydrometeorological conditions. Moreover, the thesis aimed to quantify the dominating erosion processes and evaluate the capability of a three-dimensional (3D) dual-permeability model to tackle the preceding objectives.

The simulation results and data covered a range of experimental conditions and produced a closure of water and sediment balances. Lateral preferential groundwater outflow, which has not been quantified in previous studies, was shown to form a major water balance component, and terrain slope was shown to control its magnitude. Due to the groundwater flow processes, field areas were linked to non-local processes. Topography of the field areas and the surrounding areas were shown to have an impact on the hydrological effects of drainage installations. Evapotranspiration (ET) dominated the annual water balances. However, the results suggested that standard ET estimation methods have to be adjusted to accurately estimate ET in high-latitude conditions. During the growing seasons, groundwater outflow formed the highest outflow component. Most water and sediment outflow occurred outside the growing seasons when ET was minimal. Drain discharge was the highest outflow component during the dormant seasons, and subsurface components dominated the water outflow. The results suggest that tillage layer runoff (TLR) typically occurred due to saturation a excess mechanism. Typically, soil frost did not have a high impact on runoff generation, although occasionally frost conditions increased the amount of TLR.

Subsurface transport pathways dominated the sediment loads. Load via subdrains formed the highest load component, and load via groundwater outflow contributed to the simulated load generation. Simulations provided a quantification of sediment balances and demonstrated that the majority of the eroded particles at the field surface did not form load. Three model structures demonstrated how structural uncertainties can impact the simulation results. The 3D dual-permeability approach was found to be a suitable method for water and sediment balance analyses. More detailed analyses would require detailed data on hydraulic properties in deep soil layers and erosion and sediment transport processes within the fields. The results suggest that the design of drainage and water protection measures should focus more on subsurface flow and load pathways.

Keywords drainage, preferential flow, groundwater outflow, erosion, sediment transport, dual-permeability model, 3D model, hydrological connection

ISBN (printed) 978-952-60-7379-8 **ISBN (pdf)** 978-952-60-7378-1

ISSN-L 1799-4934 **ISSN (printed)** 1799-4934 **ISSN (pdf)** 1799-4942

Location of publisher Helsinki **Location of printing** Helsinki **Year** 2017

Pages 173 **urn** http://urn.fi/URN:ISBN:978-952-60-7378-1

Tekijä
Mika Turunen

Väitöskirjan nimi
Vesi- ja kiintoainetaseiden määritys savipelloilla pohjoisissa olosuhteissa

Julkaisija Insinööritieteiden korkeakoulu

Yksikkö Rakennetun ympäristön laitos

Sarja Aalto University publication series DOCTORAL DISSERTATIONS 67/2017

Tutkimusala Vesi- ja ympäristötekniikka

Käsikirjoituksen pvm 19.12.2016 **Väitöspäivä** 28.04.2017

Julkaisuluvan myöntämispäivä 13.02.2017 **Kieli** Englanti

☐ **Monografia** ☒ **Artikkeliväitöskirja** ☐ **Esseeväitöskirja**

Tiivistelmä

Veden virtausta, eroosiota ja aineiden kulkeutumista hallitsevien prosessien tunteminen on ennakkoedellytys tehokkaiden ja ympäristön kannalta kestävien vesienhallintatoimenpiteiden suunnittelulle. Nykyisellään hydrologisten prosessien tuntemuksessa pohjoisten ilmasto-olosuhteiden salaojitetuissa savimaissa on puutteita. Tämän työn tavoitteena oli estimoida hallitsevat vesi- ja kiintoainetaseen komponentit salaojitetuilla savipelloilla erilaisissa maankuivatuksen, topografian ja hydrometeorologian olosuhteissa. Tavoitteena oli myös määrittää hallitsevat eroosioprosessit ja arvioida kolmiulotteisen (3D) monihuokosmallin soveltuvuutta vesi- ja kiintoainetaseiden sekä eroosioprosessien estimoimiseen savipelloilla.

Simulaatio- ja mittaustulokset kahdelta koekentältä tuottivat arvion vesi- ja kiintoainetaseista. Horisontaalisten oikovirtausreittien kautta virtaava pohjavesivalunta osoittautui laskelmissa oleelliseksi vesitaseen komponentiksi, jonka määrää kontrolloi maaston topografia. Pohjavesivaluntaprosessien vuoksi peltoalueet kytkeytyivät niitä ympäröiviin alueellisiin hydrologisiin systeemeihin. Siten tutkittujen peltojen ja niitä ympäröivien alueiden topografia vaikutti monitoroitujen alojen hydrologiaan. Evapotranspiraatio hallitsi vuotuisia vesitaseita. Tulosten mukaan standardimenetelmiä täytyy kuitenkin kalibroida, jotta ne pystyvät arvioimaan haihduntaa tarkasti pohjoisissa olosuhteissa. Kasvukausien aikana pohjavesivalunta muodosti suurimman valuntakomponentin. Suurin osa valunnasta ja kuormista tapahtui kasvukauden ulkopuolella ja salaojavalunta muodosti suurimman valuntakomponentin. Pintakerrosvaluntaa tapahtui pääasiassa maaperän vesivaraston kyllästymisen yhteydessä. Maan jäätymisellä ei ollut suurta vaikutusta valuntojen muodostumiseen, mutta yksittäisinä keväinä routa lisäsi pintakerrosvalunnan muodostumista.

Suurin osa kiintoainekuormasta muodostui maanpinnan alapuolisia virtausreittejä pitkin. Salaojien kautta tuleva kuorma muodosti suurimman kuormituskomponentin ja huomattava osa laskennallisesta kuormasta tapahtui pohjavesivalunnan kautta. Simulaatiot muodostivat arvion kiintoainetaseista ja osoittivat, että suuri osa maan pinnalla erodoituneesta materiaalista ei muodostanut kuormaa. Kolme mallirakennetta demonstroivat kuinka rakenteelliset epävarmuudet voivat vaikuttaa simulaatiotuloksiin.

3D monihuokosmalli osoittautui sopivaksi menetelmäksi vesi- ja kiintoainetaseiden analyyseihin. Kattavampi analyysi vaatisi syvien maakerrosten hydraulisten ominaisuuksien tarkempaa määrittämistä ja peltolohkojen sisäisiä mittaushavaintoja eroosiosta sekä kiintoaineen kulkeutumisesta. Tulosten mukaan maankuivatuksen ja vesiensuojelun suunnittelun tulisi fokusoitua aiempaa enemmän maanpinnan alapuolisiin virtaus- ja kuormitusreitteihin.

Avainsanat maankuivatus, oikovirtaus, pohjavesivalunta, eroosio, kiintoaineen kulkeutuminen, monihuokosmalli, 3D malli, hydrologinen yhteys

ISBN (painettu) 978-952-60-7379-8 **ISBN (pdf)** 978-952-60-7378-1

ISSN-L 1799-4934 **ISSN (painettu)** 1799-4934 **ISSN (pdf)** 1799-4942

Julkaisupaikka Helsinki **Painopaikka** Helsinki **Vuosi** 2017

Sivumäärä 173 **urn** http://urn.fi/URN:ISBN:978-952-60-7378-1

Acknowledgements

It was a pleasure and a privilege to work with many great people and to conduct this doctoral thesis in the Water and Environmental Engineering research group. I am very happy that all my colleagues, especially those at the coffee table, created an enjoyable working environment. I enjoyed this journey and learned a lot.

Conducting this thesis would not have been possible without the support of various funders. I greatly acknowledge Drainage Foundation sr, Maa- ja vesitekniikan tuki ry, Aalto University School of Engineering, Sven Hallin Research Foundation sr, Ministry of Agriculture and Forestry and Tekniikan edistämissäätiö for supporting this work.

I would like to sincerely thank my supervisor Prof. Harri Koivusalo and instructor Dr. Lassi Warsta for sharing their knowledge of hydrology. I really appreciate the effort that Harri puts into instructing his students and the Lassi's guidance was a key element during this thesis. I also would like to acknowledge Lic. Sc. Maija Paasonen-Kivekäs who, together with Lassi, instructed my master's thesis, gave me my first experiences in hydrological research and also significantly contributed to my doctoral thesis work. The help of Jyrki Nurminen particularly with the field data was also invaluable. Many comments and insights from the PVO, PVO2 and TOSKA groups are greatly acknowledged. Many thanks to Helena Äijö for many discussions and comments and for organizing all those good meetings at the Finnish Field Drainage Association. I am also thankful to Prof. Laura Alakukku, Merja Myllys, Markku Puustinen, Heidi Salo and Markus Sikkilä for many great conversations and comments. Many thanks belong also to Prof. Emer. Pertti Vakkilainen, who originally initiated the project where I started my thesis work. I also wish to acknowledge the CSC - IT Center for Science, Finland, for the allocation of computational resources.

I also wish to sincerely thank Prof. John Nieber and Dr. Lillian Øygarden for the pre-examination of this thesis. Prof. Emer. Per-Erik Jansson is acknowledged for accepting the invitation to act as the opponent.

The support of family members and friends was also invaluable during this thesis work. The guys from Puunlatva, Niittoväki and Hot made many days very funny. My mother, father, brother and grandmothers have always been there to support me. Most special thanks belong to Eeva for all those good moments, love, support and steady nerves.

Mikkeli, March 2017.
Mika Turunen

Contents

List of abbreviations

1D	one-dimensional
2D	two-dimensional
3D	three-dimensional
CDD	cumulative effective degree days
D	difference between simulated and measured annual accumulations
DD/TD	proportion of drain discharge to the sum of tillage layer runoff and drain discharge
MAE	mean absolute error
N-S	Nash-Sutcliffe coefficient
N-S_m	modified Nash-Sutcliffe coefficient where the squared values of the original Nash-Sutcliffe equation are replaced with absolute values (Legates and McCabe 1999)
LGT	level of the groundwater table
PET	potential evapotranspiration
PET_o	potential evapotranspiration for reference surface
PET_{o7}	potential evapotranspiration of a cropped surface estimated with a constant calibrated crop coefficient
PET_{ClassA}	potential evapotranspiration estimated with Class A data and an adjustment function
PET_{Cropc}	potential evapotranspiration of a cropped surface estimated with temporally varying crop coefficients
SD	standard deviation
SSCC	soil shrinkage characteristic curve
SWE	snow water equivalent
TDR	time domain reflectometry
TLR	tillage layer runoff
TSS	total suspended sediment
WRC	water retention curve

List of symbols

A_s	[m^2]	surface area of the sink
c	[-]	empirical parameter of the van Genuchten (1980) function
C	[-]	correction coefficient
C_c	[-]	proportion of soil covered by canopy cover
C_T	[g m^{-3}]	threshold value controlling TSS concentrations in the subsurface domain
d	[m]	half-width of the matrix structure or the characteristic radius
d_l	[-]	constant (121 in leap years and 120 in regular years)
D_r	[m]	median raindrop diameter
F_w	[-]	overland water depth correction factor
H_c	[m]	hydraulic head in the subsurface grid cell containing a sink term
h_f	[m]	hydraulic pressure head in the soil matrix system
h_m	[m]	hydraulic pressure head in the soil macropore systems
H_s	[m]	hydraulic head in the sink
h_w	[m]	overland water depth
I	[mm h^{-1}]	rainfall intensity
J	[-]	Julian day
K_A	[m h^{-1}]	hydraulic conductivity of the interface between the matrix and macropore systems
k_i	[-]	empirical constant
k_r	[h^2 kg^{-1} m^{-2}]	raindrop splash soil erodibility coefficient
K_{sat}	[m h^{-1}]	saturated hydraulic conductivity
M_r	[kg^2 h^{-3}]	momentum squared for rainfall
q	[m^3 h^{-1}]	volumetric flux to the sink
r_e	[kg m^{-2} h^{-1}]	raindrop splash erosion
α	[m^{-1}]	empirical parameter of the van Genuchten (1980) function
α_w	[m^{-1} h^{-1}]	water exchange coefficient
β	[-]	geometry coefficient
γ	[-]	scaling coefficient
θ	[m^3 m^{-3}]	soil water content

θ_r	[$m^3\ m^{-3}$]	residual water content
θ_s	[$m^3\ m^{-3}$]	saturated water content
θ_w	[$m^3\ m^{-3}$]	water content at wilting point
λ	[m]	calibrated entrance parameter, which can be interpreted as an equivalent length for flow path
τ	[h^{-1}]	water exchange rate between the pore systems
ψ	[m]	suction pressure
w_{fs}	[-]	volumetric fraction of macropores in the subsoil layers (depth >1.05 m)

List of appended papers

This doctoral dissertation consists of a summary and of the following publications, which are referred to in the text by their numerals:

I Turunen, M., Warsta, L., Paasonen-Kivekäs, M., Nurminen, J., Myllys, M., Alakukku, L., Äijö, H., Puustinen, M., Koivusalo, H., 2013. Modeling water balance and effects of different subsurface drainage methods on water outflow components in a clayey agricultural field in boreal conditions. Agricultural Water Management 121, 135–148.

II Turunen, M., Warsta, L., Paasonen-Kivekäs, M., Nurminen, J., Koivusalo, H., 2015. Simulating water balance and evapotranspiration in a subsurface drained clayey agricultural field in high-latitude conditions. Acta Agriculturae Scandinavica, Section B—Soil & Plant Science 65(sup1), 44–57.

III Turunen, M., Warsta, L., Paasonen-Kivekäs, M., Nurminen, J., Alakukku, L., Myllys, M., Koivusalo, H., 2015. Effects of terrain slope on long-term and seasonal water balances in clayey, subsurface drained agricultural fields in high latitude conditions. Agricultural Water Management 150, 139–151.

IV Turunen, M., Warsta, L., Paasonen-Kivekäs, Koivusalo, H. Computational assessment of sediment balance and suspended sediment transport pathways in subsurface drained clayey soils. Revised manuscript. Under review at Soil & Tillage Research (submitted on 7 Oct 2016).

Author's contribution

Paper I:

The author was responsible of the simulations and had the main responsibility for the model application design, the interpretation of the results, and the writing of the paper. Dr. Warsta and Prof. Koivusalo participated in the design of the model application. Paasonen-Kivekäs, Nurminen, Myllys and Äijö were responsible for the design of the experimental setup. Nurminen and Myllys were responsible for the data acquisition. All co-authors contributed to the interpretation of the results and the writing of the paper.

Paper II:

The author was responsible for the hydrological simulations and mainly responsible for the interpretation of the results and writing of the paper. Dr. Warsta and Prof. Koivusalo participated in the model application design. All co-others participated in the interpretation of the results and the writing of the paper.

Paper III:

The author was mainly responsible for the hydrological modelling, interpretation of the results and the writing of the paper. Dr. Warsta and Prof. Koivusalo participated in the design of the model application. Paasonen-Kivekäs and Nurminen were responsible for the design of the experimental setup. Nurminen was responsible for the data acquisition. All co-authors participated in the interpretation of the results and the writing of the paper.

Paper IV:

The author had the main responsibility for the model application design, the simulations, the interpretation of the results and the writing of the manuscript. Dr. Warsta and Prof. Koivusalo participated in the model application design. Paasonen-Kivekäs was responsible for the experimental setup design. All co-authors contributed to the interpretation of the results and the writing of the paper.

1. Introduction

1.1 Background, motivation and focus

Population growth is increasing the demand for food production and water resources while agricultural activities are causing environmental impacts, including the eutrophication of water bodies (Tilman et al. 2011). A comprehensive understanding of the hydrological processes that control water flow, erosion and the transport of substances in agricultural fields is a prerequisite for the management of water for sustainable crop production. These soil-water-atmosphere systems are complex due to the interconnections between different processes such as water flow, plant growth, soil erosion and transport of substances. Furthermore, the processes are subject to temporally and spatially varying hydrometeorological conditions, farming operations, soil properties and catchment features. Due to the complex and dynamic nature of the systems, their management and comprehension have proven to be challenging (e.g. Jarvis 2007; Skaggs et al. 2006; Skaggs et al. 2005). Moreover, changing climate conditions are expected to further complicate water management in agricultural areas (Iglesias and Garrote 2015).

Local climatic conditions are one dominant factor that sets requirements for agricultural water management methods. In high-latitude agricultural fields, the hydrological conditions are characterized by snow-covered winter periods, rapid snowmelt events, and high soil moisture conditions during spring, relatively short growing seasons, and wet autumn periods with lower evapotranspiration demand than precipitation (e.g. Jin and Sands 2003). In these conditions, annual precipitation amount exceeds the evapotranspiration demand (e.g. Hintikka et al. 2008; Jin and Sands 2003; Johnsson and Jansson 1991). During growing seasons, the amount of evapotranspiration is typically higher than the amount of precipitation and thus water outflow and environmental loads from agricultural fields occur mostly during the dormant season (Vagstad et al. 2004; Jin and Sands 2003).

Due to the hydrometeorological conditions of the high-latitude areas, proper drainage practices are essentially needed during the wet spring and autumn seasons to facilitate optimal soil moisture conditions for crop growth, as well as to ensure trafficability and workability of the soil with a minimal risk of soil compaction. Drainage is particularly needed in fine-textured soils (e.g. Wright and Sands 2001) due to their relatively low hydraulic conductivity and ability to retain a high amount of water (Kätterer et al. 2006; Rawls et al. 1982; van Genucthen 1980). Fine-textured clayey agricultural soils are abundant, e.g., in northern Europe (Panagos et al. 2012; Eriksson et al. 1999; Puustinen et al. 1994).

Hydrological processes function differently in fine-textured soils than in homogeneous frictional soils (Jarvis 2007). Fine-textured soils with clay content of

≥15% tend to form an aggregate structure (Oades, 1993) which facilitates the formation of preferential flow paths called macropores. These flow paths are normally composed of biopores, structural cracks, and layers of coarse soil materials; and the macropores facilitate fast water flow compared to the surrounding soil matrix, which consists of smaller micropores (e.g. Jarvis 2007). Rapid bypass flow via preferential flow paths in structured soils can have a major impact on water flow and the transport of substances in the soil (Frey et al. 2016; Warsta et al. 2013a; Koestel et al. 2012; Jarvis 2007). In addition to solutes, preferential flow paths have also been noted to convey suspended solids (Warsta et al. 2013b; Turtola et al. 2007; Øygarden et al. 1997), which highlights their importance in the context of environmental loads. Numerous studies have assessed the vertical preferential flow, whereas lateral preferential flow paths have been studied much less (e.g. Beven and Germann 2013; Allaire et al. 2009; Jarvis 2007).

Even though previous studies have assessed hydrological processes in clayey high-latitude fields (e.g. Hintikka et al. 2008; Johnsson and Jansson 1991), comprehensive knowledge of water flow and transport of substances remains incomplete (King et al. 2015; Sharpley et al. 2015; Beven and German 2013; Jarvis 2007). Some water balance components, such as precipitation, drain discharge and tillage layer runoff (TLR), are routinely monitored at experimental sites (e.g. Turtola et al. 2007), but groundwater outflow and evapotranspiration are challenging to estimate accurately (Widmoser 2009; Weiler and McDonnell 2007). All water balance components are interlinked, and thus the design of water management methods in high-latitude clayey fields could benefit from a more comprehensive understanding of the role of the different water balance components and the impacts of different factors on their temporal and spatial distribution. Regarding environmental loads, the transport pathways are also not known in detail (e.g. Sharpley et al. 2015). Since water flow controls the transport of substances in agricultural fields (Zhang et al. 2007; Vagstad et al. 2004), water management and the transport of substances need to be studied in an integrated manner (van den Eertwegh et al. 2006). Due to the potential for soil particles to sorb substances, the load generation processes are also linked to soil erosion and sediment transport, and erosion is further driven by the hydrological processes (Warsta et al. 2013b; Quinton and Katt 2007; McDowell et al. 2001). As erosion and transport of suspended solids largely contribute to the generation of environmental loads, assessing water balances, soil erosion and sediment loads in an integrated manner is a worthwhile research focus and basis for future studies regarding the transport of substances.

1.2 Water flow and drainage

The water balance of subdrained fields can be divided into the following major components: (1) precipitation, (2) evapotranspiration, (3) accumulation and melt of snow, (4) surface runoff, (5) soil water storage, (6) seepage to open ditches, (7) subsurface drain discharge and (8) groundwater outflow (water seepage across the field boundaries below the artificial drainage networks) (e.g. van der Velde et

al. 2010; Jin and Sands 2003). Different drainage methods, mainly open ditches and subsurface drains, are commonly applied to modify the water balance of agricultural fields to facilitate optimal soil moisture conditions for crop growth and cultivation operations by conveying excess water from the field.

Nowadays subsurface drains are the standard method to convey excess water from fields in high-latitude regions (Deelstra 2015; Deelstra et al. 2014; Sands et al. 2015; Puustinen et al. 1994). Subsurface drains are a profitable means for drainage because they provide a larger cultivation area and improved trafficability compared to drainage with open ditches. They have also been noted to have a positive impact on soil structure (e.g. Nuutinen et al. 2001) and crop yields (e.g. Kladivko et al. 2005).

Drainage efficiency is controlled by several design parameters. Drain spacing and drain depth are among the most important parameters, and subsurface drains are typically installed with a drain spacing of 10–30 m and a depth of 0.6–1.2 m (Deelstra et al. 2014; Blann et al. 2009; Paasonen-Kivekäs et al. 2009; Saavalainen 1984). Other drainage parameters include drain inner diameter, envelope material and trench backfill materials. Typical envelope materials can be classified as mineral, organic and synthetic envelopes, which have different impacts on water conductivity and filtration of suspended solids (Stuyt et al. 2005). Different trench backfill materials are occasionally applied together with the original soil material to facilitate better water conductivity above the drains (e.g. Turtola and Paajanen 1995; Aura 1990). In addition to the drainage materials and parameters, the drain installation method can also have an impact on drainage efficiency (Spoor and Fry 1983; Vakkilainen and Suortti-Suominen 1982; Boels 1978). Trench and trenchless installation methods are the most common installation methods, and they have mostly replaced manual installation (Ritzema et al. 2006). With the trench method, a trench with a certain depth and grade is excavated, and the drain pipe is placed at the bottom of the trench. The trench is then backfilled. The trenchless method does not excavate a trench, but a plough blade temporarily displaces the soil column upwards, sideways and forwards while the drain pipe is laid in its place. The soil thereafter falls back around the drain pipe when the installation machine moves forward. In structured soils, a trenchless drain installation has been observed to have a higher impact on the soil physical properties than the trench installation method (Boels 1978). The trenchless installation has been noted to decrease soil hydraulic conductivity (Boels 1978; Olesen 1978; Naarding 1978) and to induce a decrease in macroporosity and soil loosening in structured soils (Spoor and Fry 1983).

Before the 1960s, ongoing research concerning drainage concentrated on developing efficient and economic methods to convey excess water from the fields (Stuyt et al. 2005; Wilson 2000). In the 1960s, the environmental impacts of the ongoing agricultural intensification were recognized (e.g. Matson 1997), and research on the environmental impacts of drainage systems were initiated (Wilson 2000).

Numerous studies have assessed environmental loads from subdrained fields (e.g. Øygarden et al. 1997; Gustafson 1988; Seuna and Kauppi 1981) and further studies have demonstrated how drainage procedures impact both water outflow

pathways and load generation processes (e.g. Dalzell et al. 2011; Skaggs et al. 2005; Mendez et al. 2004). These findings have further generated attempts to optimize drainage design parameters to minimize environmental loads and to maximize yields at the same time. The topic has been studied especially in the US (e.g. Sands et al. 2015; Skaggs et al. 2006; Mendez et al. 2004). One of the primary problems of drainage optimization in clayey high-latitude fields, where preferential flow processes dominate the water flow in the soil, is insufficient knowledge of the relevant water balance components and hydrological processes.

The preferential flow processes have clear implications for the water balance of subdrained clayey soils, discerning them from frictional soils. A rapid vertical flow of water and the transport of particles and dissolved substances via soil macropores have been demonstrated in numerous studies (Beven and German 2013; Koestel et al. 2012; Jarvis 2007). Furthermore, the impact of the preferential flow on drainage and transport of substances to subsurface drains has been recognized to be substantial. Many empirical and modelling studies (e.g. Warsta et al. 2013b; Ulén et al. 2014; Uusitalo et al. 2001; Villholth and Jensen 1998; Øygarden et al. 1997) have demonstrated that water, suspended sediment and dissolved substances can bypass the soil matrix (having relatively low hydraulic conductivity) and flow directly to the subsurface drains via preferential flow paths. Moreover, many previous studies have indicated that preferential flow paths can dominate the water flow to subsurface drains in clayey fields (Frey et al. 2016; Warsta et al. 2013a; Hintikka et al. 2008; Gärdenäs et al. 2006; Koivusalo et al. 1999), which demonstrates the importance of macropores on the water balance of subdrained fields.

Compared to vertical preferential flow, the impact of lateral preferential flow on field water balances has been studied less (e.g. Allaire et al. 2009), and field-scale studies typically neglect the groundwater outflow component (e.g. Weiler and McDonnell 2007). Field-scale studies can be particularly important from the point of view of determining the outflow components, since catchment-scale studies are practically unable to quantify outflow pathways without internal catchment data (Gallart et al. 2007). Overall, the lateral preferential flow is a complex process, and Weiler and McDonnell (2007) even claimed the conceptualization and parameterization of lateral preferential flow to be one of the greatest challenges of hillslope hydrology. Despite the complexity of the issues, some studies (Hintikka et al. 2008; Gärdenäs et al. 2006; Larsson and Jarvis 1999) have indicated that lateral flow processes have an impact on the hydrology of high-latitude clayey fields. Even though empirical evidence about hydraulic properties of deep soil layers is scarce, observations support the assumption that lateral preferential flow can occur in structured soils. For example, Kessler et al. (2012), Yli-Halla et al. (2009), and Klint and Gravesen (1999) have noticed that preferential flow paths, such as permeable sand lenses and structural cracks prevail in the deep soil layers below the subsurface drain networks. Nielsen et al. (2010), who studied water flow paths in a structured soil with dye tracers, also noted that vertical macropores can be directly connected to horizontal preferential flow paths below subsurface drains. Moreover, a recent simulation study by Nieber and Sidle (2010) demonstrated that discontinuous soil macropores (e.g. Kessler et al. 2012)

can also facilitate preferential flow in structured soils. Sidle et al. (2001) also claimed that preferential flow paths may tend to self-propagate in the downslope direction. Thus, lateral preferential flow can hypothetically contribute to the water balance of clayey high-latitude fields, but a quantification of groundwater outflow has not been conducted in previous studies. If topography impacts the magnitude of lateral flow, it likely also has an impact on drain discharge (Gärdenäs et al. 2006; Fipps and Skaggs 1989) due to the interconnection of the water balance components. Field areas might also be hydrologically connected (e.g. Bracken et al. 2013) to adjacent regions via groundwater flow, which could further complicate the optimization of drainage design parameters and link field hydrology to nonlocal processes (Vereecken et al. 2016). In empirical hydrological studies in agricultural fields, observations are often conducted in adjacent field plots (e.g. Äijö et al. 2014; Turtola et al. 2007), and the impacts of the potential groundwater flow connection on the observations are difficult to decipher and are often neglected. Moreover, groundwater outflow in clayey soils may also contribute to nutrient leaching, much like in sandy soils (Rozemeijer et al. 2010a). Thus, studying lateral flow processes has the potential to benefit the design of water management and protection measures.

A comprehensive understanding of field water balances would require knowledge of surface runoff generation processes in different topographic and hydrological conditions during different seasons. Surface runoff tends to occur from variable source areas within the fields (e.g. Needelman et al. 2004; Srinivasan et al. 2002) and the location and occurrence of the source areas are likely linked to drainage conditions and groundwater outflow processes. Water flow on field surface is further controlled by both terrain topography and microtopography (including small channels and depressions) (Appels et al. 2011). Field microtopography is, however, typically spatially and temporally variable, and it is challenging to identify the factors influencing the surface flow directions on the field surface (Antoine et al. 2009). In high-latitude conditions, soil freezing and melt further impact runoff generation processes (Stähli et al. 1996; Lundin 1990), and it is not known how surface runoff is controlled by different hydrometeorological and topographic conditions in clayey soils.

Evapotranspiration is typically the dominating water balance component during the growing season in high-latitude agricultural fields (e.g. Jin and Sands 2003). Therefore, to comprehensively assess field water balance components, it is essential to estimate evapotranspiration relatively accurately. The method of Allen et al. (1998) (also called the FAO-56 method) is among the most widely adopted means to estimate evapotranspiration from cropped surfaces (e.g. Pereira et al. 2015), and it provides a standard method to estimate evapotranspiration from cropped surfaces in a wide range of climatic and agricultural conditions. The FAO-56 method is based on the Penman-Monteith function (Monteith 1965), and it has been recommended as a standard method to estimate evapotranspiration in different climatic conditions by an expert panel in the Food and Agriculture Organization of the United Nations (Allen et al. 1998). Although the method is widely adopted, it has not been comprehensively evaluated in the northern con-

ditions. The evaluation of the method would be essential since the Penman-Monteith method has been reported to be inaccurate under specific weather conditions, such as cold air temperature (Widmoser 2009). Alternative methods to estimate evapotranspiration, such as eddy flux measurements (e.g. Gustafson et al. 2004) and water balance simulation studies (e.g. Knisel and Turtola 2000; Johnsson and Jansson 1991) have been applied in high-latitude agricultural fields. However, these methods have also been reported to include uncertainties (e.g. Gustaffson et al. 2004) or to require calibration against discharge data (e.g. Jonsson and Jansson 1991). Moreover, as shown by Farkas et al. (2016), different simulation methods can lead to different estimates of evapotranspiration; and it is hypothesized here that exclusion of lateral preferential flow processes (e.g. Knisel and Turtola 2000) may lead to biased estimates of evapotranspiration. Conducting water balance studies that simultaneously assess all the major water balance components in an integrated manner would potentially improve the knowledge of the evapotranspiration process as well as of the other water balance components.

1.3 Erosion and sediment transport

Detachment and mobilization of particulate soil material from agricultural land areas has harmful impacts, including eutrophication of surface waters and loss of topsoil (Quinton et al. 2010). The processes and factors causing erosion and transport of sediment are wide-ranging and complex (Vereecken et al. 2016). While local climatic conditions are one key controlling factor for erosion and sediment load generation (Vanmaercke et al. 2011), the processes are also impacted by other factors, such as land-use, catchment characteristics and agricultural management practices (e.g. García-Ruiz et al. 2015; Bechmann et al. 2008; Puustinen et al. 2007). Although the loads and load generation processes have been assessed in several previous studies in high-latitude clayey fields (e.g. Turtola et al. 2007; Puustinen et al. 2007; Jarvis et al. 1999; Øygarden et al. 1997), the understanding of erosion processes and transport pathways of particulate soil material remains incomplete (King et al. 2015; Sharpley et al. 2015; Ulén et al. 2012; Jarvis et al. 1999).

Field-scale assessments can be particularly important when assessing loads and transport pathways, since plot-scale studies often result in biased estimates of sediment loads (García-Ruiz et al. 2015) and catchment outlet data provide aggregated information on the catchment processes (Wellen et al. 2014). Previous long-term monitoring studies in high-latitude clayey fields have quantified sediment loads in different conditions (e.g. Bechmann 2012; Ulén et al. 2012; Puustinen et al. 2010; Turtola et al. 2007; Øygarden et al. 1997). Even though some studies assumed sediment load to occur mainly via surface runoff (e.g. Rankinen et al. 2010), field- and plot-scale studies demonstrated that a major part of the loads can occur via subsurface drains (e.g. Warsta et al. 2014; Warsta et al. 2013b; Bechmann 2012; Turtola et al. 2007; Øygarden et al. 1997). Based on these studies, sediment load via subsurface drains appears to be a distinct feature of structured soils, even though subsurface drainage is considered to decrease total

sediment loads when compared to poor drainage conditions (Istok et al. 1985; Skaggs et al. 1982). Previous studies (e.g. Ulén et al. 2012) also showed a high variability of transport pathways and sediment loads with time and between experimental sites. Sharpley et al. (2015) and Ulén et al. (2012) pointed out that knowledge of the impacts of different factors on transport pathways of sediment and other substances are not well known. King et al. (2015) reviewed studies concerning phosphorus transport to subsurface drains and claimed that year-round studies which concern hydrology and transport of substances are lacking, particularly in cold conditions. Furthermore, as pointed out by Allaire et al. (2009), lateral transport of suspended solids has been little studied compared to the vertical transport processes, and it is not known if lateral preferential flow pathways contribute to the sediment loads from fields to surface waters. These previous studies highlight the need to distinguish the main pathways that transport suspended sediment from the fields in varying conditions.

Knowledge of the processes that influence detachment of soil particles and transport of suspended particles could also benefit water protection measures. Many empirical studies indicate the majority of the eroded soil material originates from the soil surfaces (Uusitalo et al. 2001; Laubel et al. 1999), even though occurrence of subsurface erosion in soil macropores may also be possible (Nieber and Sidle 2010). The particle detachment on the field surfaces is likely mainly induced by the erosive forces of raindrops and surface runoff (e.g. Warsta et al. 2013b; Wicks and Bathurst 1996; Bissonnais and Singer 1992). The eroded particles are laterally transported on the soil surface by overland flow (e.g. Taskinen and Bruen 2007), deposited on the field surface (e.g. Warsta 2011) or transported to the soil profile or subsurface drains by water flow via continuous macropore pathways (e.g. Nielsen et al. 2015; Nielsen et al. 2010; Øygarden et al. 1997). The transport of sediment in soil profiles is further affected by processes such as sieving (Turtola et al. 2007; Jarvis et al. 1999). However, the contribution of these different processes to the sediment balance of clayey fields is not well understood.

Previous research has demonstrated that erodibility of structured soils is a complex and dynamic property which is influenced by factors such as soil water content, soil frost action, microbiological activity, land-use and tillage practices (Soinne et al. 2016; Kuhn and Bryan 2004; Bryan 2000; Muukkonen et al. 2009; Pietola et al. 2005). In clayey soils raindrop erosion may not be solely induced by the kinetic force of raindrops, but the raindrops may cause other erosive processes related to aggregate breakdown (Bissonnais and Singer 1992), such as slaking and dispersion (Aura et al. 2006; Amézketa 1999). However, since hydraulic erosion, erosion by the kinetic force of raindrops and aggregate breakdown by slaking and dispersion can occur simultaneously, separating the impact of each of the processes is challenging, and the contribution of each process in different conditions remains unknown. It can be hypothesized that, for example, the kinetic force of raindrops and rainfall-induced slaking have different impacts on particle detachment under cover crops (which are common means to mitigate erosion). Thus, in order to design effective water protection measures, it would be potentially beneficial to identify the dominating erosion processes and the major sediment balance components.

1.4 Modelling water flow, erosion and sediment transport

Hydrological models are simplified mathematical representations of physical reality (e.g. Refsgaard and Henriksen 2004). The models can include descriptions of the dominant processes of the studied systems, and thus they are useful in deciphering and quantifying the behaviour of the systems, although they fundamentally require empirical data for parameterization, calibration and validation purposes (Silberstein 2006). Different types of models have been developed; the models are typically classified as empirical, conceptual and process-based models (Devia et al. 2015). Empirical and conceptual models apply mostly empirically based functions and are also called black or grey box models. Process-based models aim to include physically based equations of the dominating processes, and therefore they provide the most detailed computational method to describe the studied hydrological processes and systems. Moreover, distributed and dynamic process-based models are essentially needed when the hydrological processes and impacts of spatially as well as temporally varying features are of interest. The drawback of process-based models is the involved complexity and high number of parameters, which can lead to a non-uniqueness problem where different parameter combinations and model structures lead to a similar correspondence between the simulations and the data (e.g. Schoups et al. 2008; Refsgaard and Henriksen 2004). However, when the amount of available data increases, the number of acceptable model setups typically decreases (e.g. Rozemeijer et al. 2010b), which potentially leads to an improved representation of the studied system. Since process-based models can simultaneously describe numerous processes and combine different types of data (e.g. soil, hydrometeorological and outflow data), combining data with the computational models provides the best method to analyse water flow, erosion and sediment transport processes in an integrated manner.

Numerous process-based modelling techniques have been developed to describe preferential water flow in structured soils (Gerke 2006; Simunek et al. 2003). Typically computational models divide the soil domain into micropores and macropores, which facilitate fast flow in preferential flow paths compared to slow or stagnant flow in the soil matrix (Beven and German 2013; Gerke 2006). Many studies have shown that such a division can satisfactorily describe the dominant processes of water flow and transport of substances (e.g. Warsta et al. 2013a; Warsta et al. 2013b; Gärdenäs et al. 2006; Gerke and Köhne 2004), even though complete process description and parameter estimation still remain a challenge (Beven and German 2013; Gerke 2006; Simunek et al. 2003). Most hydrological modelling studies in structured soils have been conducted with one-dimensional (1D) models that exclude or simplify the lateral flow processes (e.g. Hintikka et al. 2008; Larsson and Jarvis 1999). Only a few studies have investigated the topographic controls on macropore flow (Jarvis 2007). Gärdenäs et al. (2006) demonstrated that simulating hydrological processes satisfactorily requires two-dimensional (2D) models in sloping clayey field areas, and Warsta et al. (2013a) and Mohtanty et al. (1998) suggested that three-dimensional (3D) models are required in undulating regions. 3D models have the most advanced capability to describe the spatially varying features (such as drainage systems and soil proper-

ties) in the studied fields. In addition to the multidimensional models, a comprehensive assessment of hydrological processes in high-latitude conditions further requires descriptions of the snow and frost processes (e.g. Deelstra et al. 2009). However, only rare model codes include descriptions of the lateral preferential flow as well as the wintertime processes.

Since hydrological processes control erosion and transport of substances, process-based erosion and sediment transport models are built on top of water flow models (e.g. Warsta 2011; Taskinen and Bruen 2007; Wicks and Bathurst 1996). Typically models describe particle detachment as a result of the erosive forces of raindrops and overland flow (Merritt et al. 2003) and soil erodibility is often treated as a constant value in model applications and also in clayey soils (e.g. Rankinen et al. 2010; Jarritt and Lawrence 2007; Lundekvam 2007; Tattari et al. 2001; Wicks and Bathurst 1996). Such modelling approaches have been reported to satisfactorily reproduce measured sediment loads in clayey areas on different scales (e.g. Rankinen et al. 2010; Lundekvam 2007; Tattari et al. 2001) although the studies rarely assess the capability of the models to reproduce observed concentration dynamics. However, Rankinen et al. (2010), who simulated erosion and sediment transport in four small Finnish catchments with the INCA-Sed model, noted that their model was able to reproduce the measured concentration dynamics in other catchments except in a catchment dominated by clayey soils. This suggests that models need to take into account some distinct features of structured soils when applied to clayey areas. Based on the previous empirical studies (e.g. Turtola et al. 2007; Bryan 2000), describing erosion and sediment transport comprehensively in structured soils may also require computational schemes for the aggregate stability processes and preferential transport of suspended solids from soil surface to the subsurface drains. However, only rare models include descriptions of these processes.

The recently developed FLUSH model (Warsta et al. 2013a; Warsta et al. 2012; Warsta 2011) is among the few models that include descriptions of 3D water flow in soil micropores and macropores. It also includes descriptions of erosion processes and sediment transport in the preferential flow paths. The model has been recently benchmarked against short-term field-scale monitoring data recorded during summer and autumn periods (Warsta et al. 2013a; Warsta et al. 2013b; Warsta et al. 2014). However, 3D models with erosion, sediment transport and preferential flow path descriptions have not been comprehensively evaluated against long-term concentration, load, and water flow data from various outflow pathways during different seasons. Such analysis could reveal development needs in the models and in the underlying theories of erosion and sediment transport processes in clayey subdrained soils.

Assessing water and sediment balances as well as erosion processes critically with increasingly detailed process descriptions and data is hypothesized to be beneficial for the development of hydrological models. Simple models may include a considerable amount of structural uncertainty (assumptions due to the incomplete knowledge of the studied processes and choice of processes included in the model, e.g. Rersgaard et al. 2006) if they exclude some of the dominating processes. For example, an incomplete model structure (a model which excludes

some of the major processes) can occasionally be compensated by biased parameter values, and due to the model complexity it can thus be difficult to discern whether the model gives the right answers for the right reasons (Kirchner 2006; Refsgaard and Henriksen 2004). In addition to the inadequate process representations, structural uncertainty can also impact model predictions (Refsgaard et al. 2006). As pointed out by Refsgaard et al. (2006), sensitivity analyses are often applied to assess parametric uncertainty, but structural uncertainties are rarely evaluated. The importance of assessing structural uncertainty has been exemplified for example by Butts et al. (2004), who demonstrated that model structure choice can have as high impact on the simulation results as parametric uncertainty. Structural uncertainties have been rarely assessed in process-based erosion and sediment transport studies, even though such analysis would be beneficial in reducing uncertainty in the models.

1.5 Objectives and hypotheses

The literature review in Sections 1.2–1.4 indicated gaps in the current knowledge of water and sediment balances as well as erosion processes in clayey high-latitude agricultural fields. The gaps concerned the magnitude and distribution of water and sediment balance components in different topographic, drainage, soil property, agricultural land use and hydrometeorological conditions in high-latitude regions. Especially the role of groundwater outflow and associated lateral transport of suspended solids has been understudied in clayey soils. The contribution of different erosion processes also remains unknown. Furthermore, the ability of the 3D dual-permeability models to quantify the water balance and sediment load components and contribution of different erosion processes has been rarely assessed against intensive long-term data. Structural uncertainties in erosion and sediment transport models have been rarely studied. The research gaps in the literature led to the following specific objectives:

1) to produce a closure of the water balance in subdrained clayey fields and to quantify their annual and seasonal major water balance components (Papers I–III),
2) to quantify the impacts of different subdrainage design parameters (installation methods, drain spacing, drain depth and envelope material), terrain topography and hydrometeorological conditions on the water balance components (Papers I–III),
3) to assess the role of groundwater outflow and its impact on water balances in clayey fields (Papers I–III),
4) to evaluate the capability of standard methods to estimate evapotranspiration in cropped high-latitude clayey soils (Paper II),
5) to quantify sediment transport pathways and sediment balance components in different topographic conditions (Paper IV),
6) to identify the dominant erosion processes (Paper IV), and
7) to evaluate the capability of an advanced 3D distributed computational model to assess the preceding problems and to describe the spatially varying drainage and hydrological features of the fields (Papers I–IV).

This thesis approached these objectives by applying the recent 3D FLUSH model

(Warsta et al. 2013a; Warsta et al. 2013b; Warsta 2011) with long-term datasets of Äijö et al. (2014) to produce comprehensive field-scale analyses. The datasets included intensive hydrological and water quality measurements from three experimental fields in southern Finland. The combination of field-scale data and 3D simulations provided a method to study the processes in an integrated manner.

Based on the literature review, it was hypothesized that lateral preferential flow was active on the fields, and that the application of the 3D model approach with the field-scale data could produce a closure of the water and sediment balance, quantify the amount of lateral flow, and discern the impacts of the different factors on the water balance components and sediment loads. Since the literature review suggested that structural uncertainties have previously been relatively little studied, regarding uncertainty analyses, this thesis focused on assessing the impact of different model structures on simulation results.

2. Methodology

The research approach of this thesis is based on mathematical model applications with empirical field-scale hydrological data. More specifically the adopted approach can be considered to follow the earth science directed method where research does not focus on verifying hypotheses but on deriving general theories based on new evidence in open systems (Refsgaard and Henriksen 2004). The study is composed of four process-based model applications in two different experimental sites, and the results are presented in four distinct publications (Papers I–IV) (Figure 1). The data, the model, the simulation strategy and model setups are introduced in more detail in the following sections (2.1-2.4).

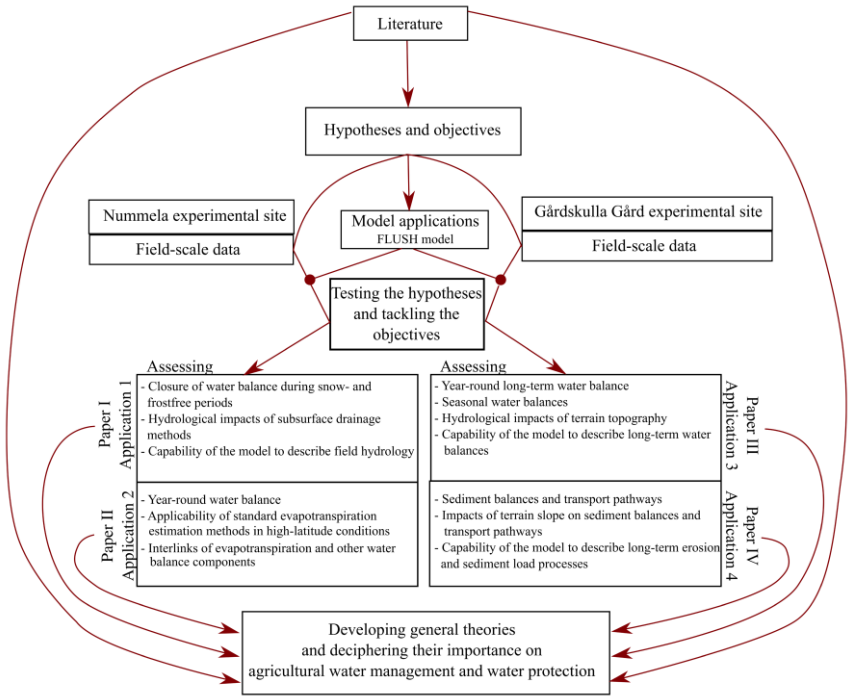

Figure 1. Main steps and methods adopted in the thesis to assess water and sediment balances as well as erosion processes in clayey subdrained high-latitude agricultural fields.

2.1 Experimental sites and measurements

Two intensively monitored experimental sites were chosen for the study to cover a range of experimental conditions regarding terrain topographies, drainage design methods, soil properties and other catchment features (Figure 2). The Nummela experimental site consisted of four monitored field sections with heavy clayey soils and relatively flat topographies (Papers I-II, Table 1). Different subsurface drainage methods were tested experimentally in the field. The Gårdskulla Gård experimental site consisted of two clayey fields that which had similar subsurface drainage systems but different terrain slopes (Papers III-IV, Table 1). The slopes of the studied fields (Table 1) can be considered to be representative of typical agricultural fields in Finland, which have a mean slope of approximately 1.3% and only rarely exceed a slope of 5% (Rekolainen 1993). The studied drainage systems (drain spacing 6–32 m and depth 0.9–1m) cover the range of typical Finnish drainage system design parameters (drain spacing 10–16 m and depth 1 m (Saavalainen 1984; Paasonen-Kivekäs et al. 2009)) as well as relatively intensively and poorly drained conditions. The closely located sites have similar climatic conditions prevalent in the climatic conditions of southern Finland (Figure 2).

Table 1. Key features of the Nummela and Gårdskulla Gård experimental sites.

Nummela experimental site	Gårdskulla Gård experimental site
Four adjacent monitored field sections.	Two monitored fields separated by a stream.
Different experimentally tested subdrainage methods.	Similar subdrainage systems in both fields.
The sections have slightly different terrain topographies.	The fields have different terrain slopes (1 and 5%).
Flat field (slope <1%) with a steep slope adjacent to the monitored area.	Steep sloping hill located adjacent to one of the monitored fields.
Heavy clay soils (average clay content 73%).	Clay soils (average clay content 52%).

Figure 2. Location of the Nummela and Gårdskulla Gård experimental sites as well as the other sites, weather stations and observatories from which data were adopted.

2.1.1 Nummela experimental site

The Nummela experimental site is located in Jokioinen (Figure 2), southern Finland, and it is administrated by the Natural Resources Institute Finland. The soil is classified as a Vertic Cambisol (FAO 2007). It had the mean clay (particle size ≤0.002 mm) content of 67% in the topsoil layer of 0–0.35 m and 75% in the subsoil layer of 0.35–1 m (Vakkilainen et al. 2010). Crops were cultivated in the field over decades, and spring barley (*Hordeum vulgare*) and oats (*Avena sativa*) were cultivated in the field during the studied periods (2007–2011).

The area of the monitored field was 9.3 ha and it consisted of four field sections (A–D, Figure 3) which had an average slope of <1%. Initially, Sections A (2.9 ha), B (1.3 ha) and C (1.7 ha) had a drain spacing of 16 m. Section D (3.4 ha) had a drain spacing of 32 m. The drain tiles were installed in 1952 with an average depth of 1 m and an inner diameter of 0.05 m. No envelope material was used, but small amounts of coarse gravel may have been deposited around the gaps between the drain tiles. An unmonitored area (4.8 ha) between the monitored field sections with a steep northward facing slope (Section E in Figure 3) was included in the simulation to facilitate the modelling of the entire field area. The nearby areas outside the studied field area consisted mainly of flat arable lands. In addition to the subsurface drainage systems, open ditches surrounded the field at the field boundaries (Figure 3).

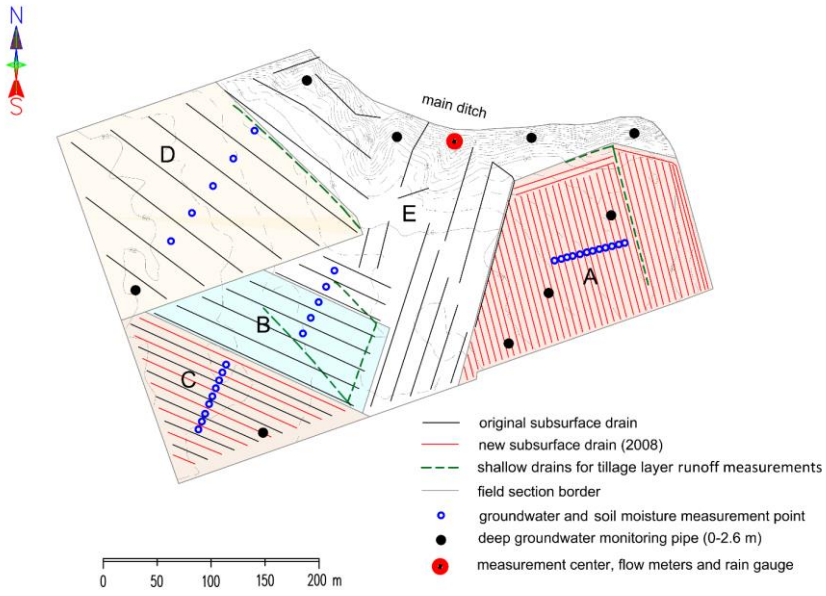

Figure 3. The layout of the experimental setup of the Nummela experimental site after the drainage installations in 2008. A: drain spacing 6 m (trenchless installation method, Fibrella fibre as envelope material), B: drain spacing 16 m (control section, no envelope material), C: drain spacing 8 m (trench installation method, gravel as envelope material), D: drain spacing 32 m (control section, no envelope material); E: unmonitored area (included in the simulations). (Paper I)

Precipitation, snow water equivalent (SWE), TLR, drain discharge, soil water content and level of the groundwater table (LGT) were continuously measured on site from May 2007 onwards. Hydrometeorological data were available from the nearby weather stations, and data of soil hydraulic properties were available from each of the monitored field sections. The mean long-term precipitation in the area was 627 mm a^{-1} (Pirinen et al. 2012).

Hydrology of the field sections was monitored from May 2007 to May 2008 under the initial drainage design. New drains were installed in Sections A and C on Jun 9, 2008 (Figure 3). In Section A, the new drains were installed with the trenchless installation method and a spacing of 6 m. "Fibrella 2160" fibre (60% polyester and 40% rayon) was used as the envelope material. The installation machinery was used to break the old tile drains before the installation of the new drains. In Section C, supplementary drains were installed between the old tile drains with the trench installation method (trench width 0.24 m). Thus, the new and old drains formed a drain spacing of 8 m in Section C. Coarse gravel was used as an envelope material, and gravel deposits were installed every 7 m along the drain trench. On 28 Sep – 1 Oct 2009, Section A was subsoiled to a depth of 0.45 m with the tine space of 0.6 m. While drainage installations were conducted in Section A and C, Sections B and D functioned as control sections.

Precipitation was measured on site with a RAINEW 111 tipping bucket rain gauge (RainWise Inc., Bar Harbor, ME, USA) with a time resolution of 15 min. The observed rainfall and snowfall values were corrected with coefficients of 1.05 and 1.3, respectively (Førland et al. 1996). Snowfall was manually measured weekly or bi-weekly and the daily observations were disaggregated to hourly data based on the snowfall observations by the Finnish Meteorological Institute at the Jokioinen Observatory (located approximately 7 km from the experimental site). Other meteorological data adopted from the Jokioinen Observatory are listed in Table 2. Daily Class A evaporation pan (e.g. McMahon et al. 2013) measurements were conducted at the Jokioinen observatory by the Natural Resources Institute Finland.

SWE was measured weekly or bi-weekly during field visits. In 2008–2009 only snow depth was measured, but during the other time periods SWE observations were based on weighed snow samples. In 2008–2009 SWE was estimated as a function of snow depth and long-term average snow density.

TLR was measured with shallow subsurface drains (depth 0.4 m) which had coarse gravel as trench backfill. In addition to the subsurface flow in the topsoil layer of 0–0.4 m, embankments on the soil surface beside the drains and the highly permeable backfill material also directed surface runoff to the drains. Due to the farming operations the embankments were occasionally levelled, which caused uncertainty in the TLR measurements. In Section B, a malfunction afflicted the TLR measurements during the autumn 2008, and thus TLR was not measured during that autumn in the field section. Furthermore, field observations suggested that during spring snowmelt periods, the TLR measurement devices in Section B received an influx of water outside the section. Therefore, TLR was overestimated in Section B during spring snowmelt periods. Also, it is possible that overland flow occasionally bypassed the TLR measurement devices in Sections A–

D due to occurrence of soil frost and an ice layer on top of the trench of the measurement devices during the winter and spring seasons.

Table 2. Summary of the applied empirical data from the Nummela experimental site, nearby experimental fields and meteorological observatory of the Finnish Meteorological Institute. (Modified from Paper I)

	Measurement frequency	Measurement location
Precipitation	15 min	Nummela field
Subsurface drain discharge	15 min	Nummela field
Tillage layer runoff	15 min	Nummela field
Incoming solar radiation	Hourly	Jokioinen Observatory
Reflected solar radiation	Hourly	Jokioinen Observatory
Relative humidity of air	Hourly	Jokioinen Observatory
Sun hours	Hourly	Jokioinen Observatory
Air temperature	Hourly	Jokioinen Observatory
Wind-speed	Hourly	Jokioinen Observatory
Evaporation (Class A)	Daily	Jokioinen Observatory
Precipitation	Daily	Jokioinen Observatory
Level of the groundwater table	Weekly or biweekly	Nummela field
Snow depth	Weekly or biweekly	Nummela field
Snow water equivalent	Weekly or biweekly	Nummela field
Soil water content	Weekly or biweekly	Nummela field
Macropores	Once	Nummela field
Water retention curves	Once	Nummela and Hovi fields
Saturated hydraulic conductivity	Once	Nummela field
Soil shrinkage characteristic curve	Once	Sjökulla field
Terrain topography (manual leveling)	Once	Nummela field
Terrain topography (airborne laser scanning)	Once	Nummela field

Drain discharge and TLR were measured with an automated Datawater WS vertical helix water meter (Maddalena, Povoletto, Italy) with a time resolution of 15 min. Cumulative volumes were also manually checked from the mechanical water flow meters. The measurement range of the devices was 0.2–50 $m^3\ h^{-1}$ and the data were aggregated to hourly values. From 27 Jul to 3 Aug 2007, a malfunction afflicted the drain discharge data loggers in Sections B and D, and only the total amount of drain discharge was recorded during this time period. The data were evenly disaggregated for the time period.

The soil water content was measured with the TRASE system I moisture meter using time domain reflectometry (TDR) (Soil Moisture Equipment Corp., Goleta, CA, USA) at the depth of 0.0–0.3 m. LGT was observed with observation tubes (plastic, bottom close, perforated) with a depth of 1.6 m. Similar tubes, but with a depth of 2.6 m, were installed on 5 Nov 2009 to monitor deeper groundwater levels. LGTs were manually measured weekly or bi-weekly during field visits. Though it is not clear whether the LGT observations with the tubes in heavy clay soils describe the water table level in soil macropores or matrix (Bouma 1980), it was hypothesized that that the observations describe either one of them, or their combination, depending on the location of the tube in relation to the macropore system.

Soil hydraulic properties were measured on site to the depth of 0.6 m in autumn 2006. Thus, the measurements represent the soil properties prior to the installation of the new drains. Undisturbed soil samples with the diameter of 0.15 m and length 0.6 m were taken with a tractor auger from five different locations in each of the four field sections (see Figure 3). These samples were cut into three layers (0.0–0.2 m, 0.2–0.4 m, and 0.4–0.6 m) for laboratory analysis. From these samples, water retention curves (WRC) were measured up to the suction pressure of 1 m as a drying curve (Aura 1990). Later, soil water content at the wilting point (pressure -150 m) was measured. However, water contents at the wilting points were not available for the parameterization in Paper I, and the measurements from -1 m to -150 m pressure were adopted from the data of the Hovi experimental field (Warsta 2011), which is another subdrained clayey agricultural experimental site in southern Finland. Soil macropores were defined as pores that release water at the suction 0.1 m (e.g. Jarvis 2007).

Saturated hydraulic conductivities (K_{sat}) were measured with the method of Youngs (1991). The soil shrinkage characteristic curve (SSCC) was adopted from Kankaanranta (1996), who measured soil shrinkage characteristics in a clayey Sjökulla experimental field in southern Finland, and fitted the parametric SSCC of Kim et al. (1992) to the data.

Terrain topography was measured on site by levelling, with the average distance of 19 m between the measurement points (Paper I, Table 2). Later, digital elevation data with a resolution of 2×2 m² were derived from the laser scanning data of the National Land Survey of Finland (Paper II, Table 2). The data and the site are described in more detail in Äijö et al. (2014) and Vakkilainen et al. (2008; 2010).

2.1.2 Gårdskulla Gård experimental site

The Gårdskulla Gård experimental site was located in the Kirkkojoki stream catchment area in southern Finland (Figure 2). The site consisted of two intensively monitored and subsurface drained experimental fields. The Kirkkojoki stream was located between the studied fields (Figure 4). The north facing Section 1 and south-facing Section 2 had mean slopes of 1% and 5%, respectively. The drain tiles were installed in the 1940s at both sections with a drain spacing of 16 m, an average depth of 1 m and an inner diameter of 0.05 m. Bedrock reached the

soil surface in the vicinity of the sections, which indicated that the bedrock was likely close to the soil surface in the monitored areas. Clayey soils were dominant in the region. A forested hill was located at the south side of Section 1 (Figure 4), and it was hypothesized that the upslope area may contribute to the water balance of the monitored area. This hypothesis was further studied in a simulation scenario (see Section 2.4.2.1 for details).

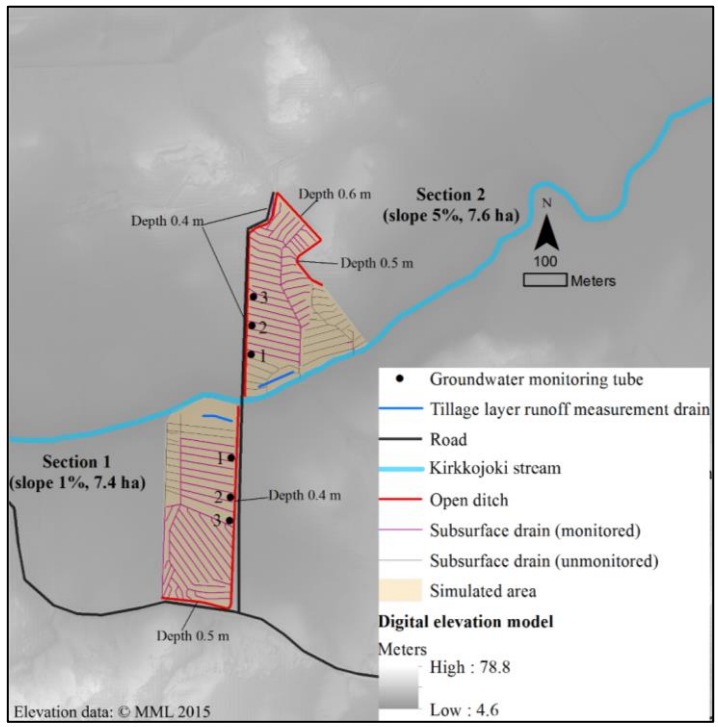

Figure 4. Layout of the two monitored fields of the Gårdskulla Gård experimental site. (Paper III)

The fields were under conventional agricultural land-use during the studied period (2008–2012), and the land-use varied among the years as listed in Table 3. Winter wheat and spring barley were sown until land-use changed to perennial grassland in 2012 in Section 1 and to pastureland in 2011 in Section 2. In Section 1, grass was harvested in July and October each year, except in 2012 when it was harvested only in July. The annual crops were harvested during the autumns (11-21 Aug).

Precipitation, SWE, TLR, drain discharge, and LGT were continuously monitored on site similarly as at the Nummela experimental site (see Section 2.1.1), with the following exceptions. Firstly, the data were available from Jan 2008 onwards. The depth of the LGT monitoring tubes was 2 m and the SWE observations were based on weighed snow samples during each of the studied years. During the autumn 2009, impermeable plastic sheets were installed at the downslope side of

the trenches of the TLR measurement devices (Figure 5). The installation was conducted to prevent water flow through the trenches. The TLR devices collected runoff from areas of 3.3 ha and 3.0 ha in Sections 1 and 2, respectively. Due to the frozen soil conditions, an unquantified share of surface runoff was observed to bypass the TLR measurement systems during spring snowmelt periods in 2009–2011. However, in 2008 and 2012 the TLR measurement devices were observed to function adequately. The areas of the monitored subsurface drains were 5.7 ha in Section 1 and 4.7 ha in Section 2. Also, the soil frost depth and water level in the Kirkkojoki stream were manually measured on site weekly or bi-weekly. The location of the measurement devices is shown in Figure 4.

Table 3. Land use and tillage methods in Sections 1 and 2 of the Gårdskulla Gård experimental site in 2008–2012. The depths of autumn mouldboard ploughing and harrowing were approximately 0.23 m and 0.05 m, respectively. (Modified from Paper III)

Year	Section 1		Section 2	
2008	Winter wheat (*Triticum aestivum)*	Autumn ploughing	Winter wheat (*Triticum aestivum)*	Autumn ploughing
2009	Spring barley (*Hordeum vulgare)*	Spring harrowing, autumn disc harrowing	Winter wheat (*Triticum aestivum)*	Autumn ploughing
2010	Winter wheat (*Triticum aestivum)*	Autumn disc harrowing	Spring barley (*Hordeum vulgare)* and grass	Spring harrowing
2011	Spring wheat (*Triticum aestivum)* and grass	No soil tillage	Pasture (30 cows and a bull)	No soil tillage
2012	Grass	No soil tillage	Pasture (30 cows and a bull)	No soil tillage

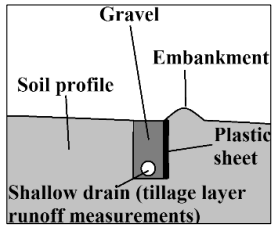

Figure 5. Schematic illustration of the tillage layer runoff measurement system in Gårdskulla Gård. (Paper III)

Meteorological data were available from the nearby weather stations of the Finnish Meteorological Institute. Hourly temperature and relative humidity were obtained from the Porla Station (10 km from the Gårdskulla Gård site), hourly wind speed from the Sepänkylä station (32 km from the Gårdskulla Gård site), and hourly shortwave radiation from the Helsinki-Vantaa airport station (47 km from the Gårdskulla Gård site).

Soil particle size distributions (sieve analysis) and organic carbon contents (dry combustion) were measured in the autumn 2007 from four soil layers and three different locations in both field sections. The particle size distributions and organic carbon contents are listed in Table 4. Section 1 had a higher average clay content in the topsoil layer (Table 4). However, the average clay content was higher in Section 2 than in Section 1 1 in the deepest measured layers (0.8–1.0 m).

WRCs were measured from four parallel undisturbed soil samples at three different depths (0.10–0.15 m, 0.30–0.35 m and 0.50–0.55 m) in the autumn 2012. The samples had a size of 0.072 m and height 0.048 m. WRCs were determined in the suction pressures of 0 m, 0.1 m, 0.3 m, 1.0 m and 10.0 m as a drying curve.

Total suspended sediment (TSS) concentrations were measured from drain discharge and TLR in both field sections. A composite sampling strategy was adopted, where an automated system collected a subsample of approximately 1.5×10^{-4} m^3 per each 50 m^3 (Section 1) or 20 m^3 (Section 2) of water flowing through the system. Thus, the sampler produced more samples during time periods of intense outflow. The water volume which triggered the collection of a subsample was higher in Section 1 (50 m^3) than in Section 2 (20 m^3) since more outflow occurred in Section 1. Hypothetically, water outflow was higher in Section 1 than in Section 2 due to the flat terrain topography and an influx of water of water from the adjacent hill area (Figure 4). The composite samples were composed of the subsamples, and the composite samples were collected from the field weekly or bi-weekly during field visits. In the laboratory, the composite samples were analysed for TSS according to the standard SFS 3008: 1990 (evaporation residual weighing). The sediment load for the composite sampling intervals was calculated as the product of the TSS concentrations and the measured discharge.

Table 4. Average content of organic carbon, clay (≤0.002 mm), silt (0.002−0.02 mm), fine sand (0.02−0.2 mm), coarse sand (0.2−2 mm) and gravel (2−20 mm) in Sections 1 and 2 of the Gårdskulla Gård experimental site. (Paper III)

	Section 1, content [%]					
Depth [m]	Organic carbon	Clay	Silt	Fine sand	Coarse sand	Gravel
0-0.2	3.1	49.2	31.1	12.7	7.0	0.0
0.2-0.4	2.3	51.1	33.6	13.2	2.1	0.0
0.4-0.8	0.9	53.6	31.2	13.3	1.8	0.0
0.8-1.0	0.7	56.7	33.1	13.2	0.3	0.0
	Section 2, content [%]					
Depth [m]	Organic carbon	Clay	Silt	Fine sand	Coarse sand	Gravel
0-0.2	2.3	41.1	35.6	19.6	3.7	0.0
0.2-0.4	1.3	42.7	33.7	20.6	3.0	0.0
0.4-0.8	0.5	56.4	29.5	13.2	0.9	0.0
0.8-1.0	0.3	68.7	21.4	8.7	0.4	0.0

A digital elevation model with a spatial resolution of 2 × 2 m² was derived from the laser scanning data of the National Land Survey of Finland. The applied measurements from the Gårdskulla Gård experimental site are listed in Table 5. The data and the site are presented in more detail in Äijö et al. (2014) and Vakkilainen et al. (2008; 2010).

Table 5. Summary of the applied empirical data from the Gårdskulla Gård experimental site and the nearby experimental fields and meteorological weather stations of the Finnish Meteorological Institute.

	Measurement frequency	Measurement location
Precipitation	15 min	Gårdskulla Gård site
Subsurface drain discharge	15 min	Gårdskulla Gård site
Tillage layer runoff	15 min	Gårdskulla Gård site
Incoming solar radiation	Hourly	Helsinki-Vantaa airport station
Relative humidity of air	Hourly	Porla station
Air temperature	Hourly	Porla station
Wind speed	Hourly	Sepänkylä station
Precipitation	Daily	Porla station
Level of the groundwater table	Weekly or biweekly	Gårdskulla Gård site
Snow water equivalent	Weekly or biweekly	Gårdskulla Gård site
Total suspended sediment concentration	Weekly or biweekly	Gårdskulla Gård site
Water level of the Kirkkojoki river	Weekly or biweekly	Gårdskulla Gård site
Macropores	Once	Gårdskulla Gård site
Water retention curves	Once	Gårdskulla Gård site
Soil shrinkage characteristic curve	Once	Sjökulla field
Terrain topography	Once	Gårdskulla Gård site

2.2 FLUSH model

FLUSH is a process-based, dynamic and spatially 3D distributed numerical hydrological model which is tailored for simulating water flow, erosion and transport of substances in structured soils (Warsta et al. 2013a; b; Warsta 2011). The model was chosen for the study due to its unique ability to simulate erosion as well as 3D preferential flow and transport with subdiurnal time steps in cold conditions. The applied dual-permeability approach supports simulation of water flow in both micro- and macropores of the clayey soils. Warsta et al. (2012) added description of snow and frost processes (Koivusalo et al. 2001) to the model and

it is thus suitable for simulating hydrological processes in high-latitude conditions. The model supports simulation with subdiurnal time steps which allows it to take into account the temporally varying hydrological processes within each day. Numerical solutions of flow and transport functions were derived with implicit volume based methods (Warsta 2011). The governing equations and the main principles of the water flow and heat convection-diffusion models are presented in Section 2.2.1 and the erosion and sediment transport model in Section 2.2.2.

2.2.1 Water flow and heat convection-diffusion models

FLUSH divides the simulated area into 2D overland and 3D subsurface domains (Warsta et al. 2013a; Warsta 2011). A conceptual representation of the dominating water flow and heat convection-diffusion processes is given in Figure 6.

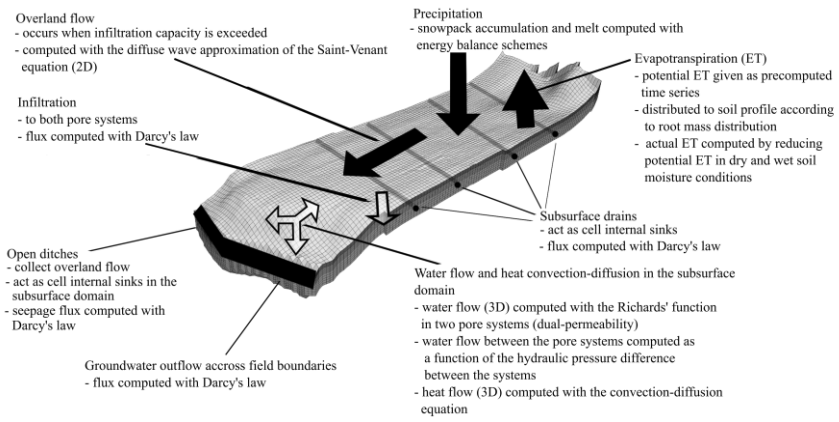

Figure 6. Schematic presentation of the main components of the water and heat flow processes in the FLUSH model.

In the model, precipitation is deposited on the field surface and the water flow in the overland domain is calculated. Overland flow is generated in those locations on the field surface where the water level exceeds the soil surface depression storage capacity. Typically, the soil surface storage capacity can be exceeded during high precipitation intensities or during saturated soil moisture conditions in the soil profile. The flow of water on the field surface is described by the diffuse wave approximation of the Saint-Venant equations (Warsta et al. 2013a). Infiltration of water to the micro- and macropores of the subsurface domain is explicitly calculated with Darcy's law. Infiltration is treated as a cell internal source term in the uppermost grid cells of the subsurface domain. Total soil pore space is divided into soil matrix and macropore systems, following the dual-permeability approach (e.g. Beven and Germann 2013). Water can infiltrate from the overland domain to both pore systems. The movement of water in the pore systems of the subsurface domain is computed with the Richards' equation, and water retention properties are calculated with the van Genuchten approach (van Genuchten 1980):

$$\theta = \theta_r + \frac{\theta_s - \theta_r}{[1+(a|\psi|)^c]^{1-1/c}} \quad (1)$$

where θ [m^3 m^{-3}] is the soil water content, θ_s [m^3 m^{-3}] is the saturated water content, θ_r [m^3 m^{-3}] is the residual water content, ψ [m] is the suction pressure, and α [m^{-1}] and c [-] are empirical parameters estimated on the basis of the measured soil water retention properties.

Unsaturated hydraulic conductivities are simulated with the Mualem-van Genuchten schemes (van Genuchten 1980). Saturated and unsaturated flow is supported in both pore systems and all macropores are considered continuous. In the macropore system, saturated hydraulic conductivity is calculated as the product of the volumetric fraction of soil macropores and K_{sat} multiplier of the macropores (Warsta et al. 2013a; Jarvis 2008). Soil macropores are composed of static (permanent preferential flow paths) and dynamic (shrinkage cracks) portions in the model. Soil shrinkage and swelling description were adopted from the SWAP model (van Dam et al. 2008) and SSCC from Kim et al. (1992). Soil shrinkage increases the fraction of macropores from the total porosity whereas swelling decreases the dynamic macroporosity. Water exchange between the micro- and macropores is calculated as a function of hydraulic pressure difference between the pore systems (Gerke and van Genucthen 1993), as follows:

$$\tau = \alpha_w(h_f - h_m) \quad (2)$$

where τ [h^{-1}] is the water exchange rate between the pore systems, α_w [m^{-1} h^{-1}] is the water exchange coefficient, and h_f and h_m [m] are the hydraulic pressure heads in the soil macropore and matrix systems, respectively. α_w is estimated with the following function:

$$\alpha_w = \frac{\beta}{d^2}(K_A\gamma) \quad (3)$$

where β [-] is the geometry coefficient, d [m] is the half-width of the matrix structure or the characteristic radius, K_A [m h^{-1}] is the hydraulic conductivity of the interface between the matrix and macropore systems, and γ [-] is a scaling coefficient.

In FLUSH, water can be removed from the simulated domain by cell internal sink terms. All of the sink terms can remove water from both macro- and micropores. Drainage networks in the simulated area are discretized into segments within the computational grid, and the parameterizations and lengths of the segments are embedded in the grid cells. Currently, water flow in the drain pipes and open ditch channels are not described separately in the model, but the sink terms remove water from the simulated domain. Flow to drains and seepage to ditches are calculated based on Darcy's law as follows:

$$q = K_{sat} A_s \frac{H_c - H_s}{\lambda} \quad (4)$$

where q [m^3 h^{-1}] is the volumetric flux to the sink, A_s [m^2] is the surface area of the sink, H_c [m] is the hydraulic head in the subsurface grid cell containing the sink, H_s [m] is the hydraulic head in the sink and λ [m] is the calibrated entrance parameter which can be interpreted as an equivalent length for flow path.

Potential evapotranspiration (PET) is given as a precalculated time series for the model. PET is distributed into the soil profile according to the crop root mass distribution. The root mass distribution can vary temporally and the mass decreases linearly from the maximum close to the soil surface to the minimum at the maximum root depth. Actual evapotranspiration is calculated by reducing PET in dry and wet soil moisture conditions using the model of Feddes et al. (1978).

Lateral groundwater outflow across the field boundaries is computed with Darcy's law and it removes water from the horizontally outermost cells of the computational domain. The hydraulic head gradient is calculated based on the surface slope between the middle point of each outermost grid cell and the corresponding cell outside the field boundary.

The accumulation and melt of snow are computed with the energy balance approach of Koivusalo et al. (2001), where snowpack is subdivided into two layers. The energy exchange between the atmosphere and the snowpack is limited to the top snow layer. The surface temperature of the snowpack is calculated iteratively by balancing the surface energy fluxes (radiative and turbulent fluxes and heat advected with precipitation) with heat conduction into the snowpack. The bottom layer of the snowpack exchanges energy with the top snow layer and the underlying soil profile through heat conduction. In the soil profile, heat flow as well as freezing and thawing processes are computed with a modified convection-diffusion equation (Warsta et al. 2012; Karvonen 1988). Both convection and conduction transport heat in the model, and phase transitions of water release or consume energy. Currently, soil freezing processes are not coupled with the water flow model.

2.2.2 Erosion and sediment transport

The erosion and sediment transport scheme of FLUSH (Figure 7) is composed of different processes related to particle detachment on the soil surface and transport of suspended solids in the surface and subsurface domains (Warsta 2013b; Warsta 2011). In the subsurface domain, the transport of sediment is allowed only in soil macropores and no transport occurs in the soil matrix; i.e., pore pathways in the soil matrix are assumed to be too small for the transport of suspended solids. In FLUSH, particle detachment is described as raindrop splash erosion and hydraulic sheet erosion. Erosion processes occur solely in the surface domain of the model, and thus subsurface erosion is assumed to be negligible compared to the surface erosion. Eroded solids can be advectively transported in

the surface domain with overland flow and be removed from the domain by deposition on the soil surface, by flow to open ditches, or infiltration to the subsurface soil macropore domain. Transport of sediment in the subsurface domain is calculated with the 3D advection-dispersion equation (Warsta et al. 2013b; Warsta 2011). Sediment in the subsurface domain is transported forward by the advection and dispersion processes or removed from the domain by open ditches, subsurface drains or retention.

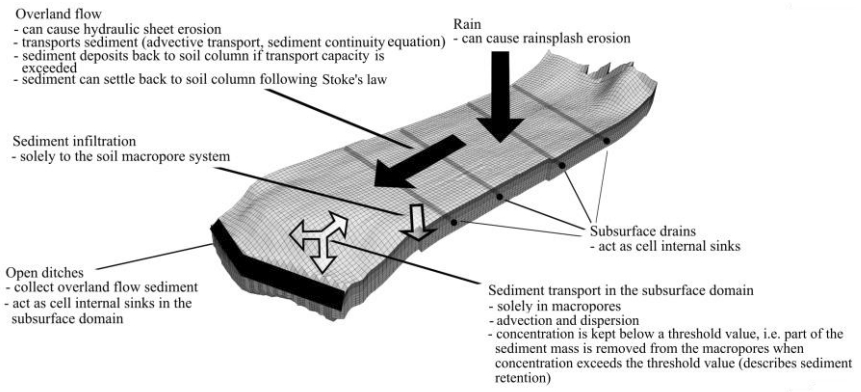

Figure 7. Schematic presentation of the main components of the erosion and sediment transport processes of FLUSH model. (Paper IV)

Raindrop splash erosion r_e [kg m^{-2} h^{-1}] is calculated in the model with a simplified version of the raindrop splash scheme of the SHE model (Wicks and Bathurst 1996), as follows:

$$r_e = k_r F_w (1 - C_C) M_r \quad (5)$$

where k_r [h^2 kg^{-1} m^{-2}] is the raindrop splash soil erodibility coefficient, F_w [-] is the overland water depth correction factor, C_c [-] is the proportion of soil covered by canopy cover, and M_r [kg^2 h^{-3}] is the momentum squared for rainfall. M_r is computed with the empirical approach of Wicks and Bathurst (1996) and F_w is computed with the following approach:

$$F_w = \begin{cases} \exp(1 - \frac{h_w}{D_r}), & h_w > D_r \\ 1, & h_w \leq D_r \end{cases} \quad (6)$$

where h_w [m] is the overland water depth and D_r [m] is the median raindrop diameter. D_r is calculated as follows:

$$D_r = k_i I^{0.182} \quad (7)$$

where k_i [-] is an empirical constant and I [mm h^{-1}] is the rainfall intensity.

In the model, hydraulic erosion occurs during those overland flow events when the shear stress of the flow exceeds the critical shear stress value. Shear stress caused by the overland flow in a computational cell is calculated as a function of field surface slope and water depth in the cell (Warsta et al. 2013b; Taskinen and Bruen 2007). The critical shear stress value is computed with the modified Shields method for small soil particle sizes, following Yalin (1977). Soil erodibility coefficients for raindrop splash and hydraulic erosion are given as time series for the model, i.e., the erodibilities are not coupled with the state variables of the water flow model.

When TSS concentration in the overland flow exceeds the transport capacity of the flow, the excess sediment mass deposits on the soil surface and is removed from the domain. The overland flow transport capacity is calculated with the approach of Yalin (1963). Sediment mass can deposit on the field surface also due to the settling of the suspended soil particles. The settling is computed with Stoke's law.

In previous FLUSH applications (Warsta et al. 2014; Warsta et al. 2013b), the transport of sediment was restricted to the soil domain from the soil surface to the subsurface drain depth (0–1.0 m), and sediment mass was allowed to deposit in a computational cell when the cell dried up due to evapotranspiration or infiltration of water in the surrounding soil matrix. In the current study, sediment mass transport was also allowed in the soil macropores below the subsurface drain depth. Furthermore, TSS concentrations were not allowed to exceed the threshold value C_T [g m^{-3}]. During those time periods when the concentration exceeded C_T in a computational cell, the excess sediment mass was removed from the cell. It was assumed that soil pore sizes set restrictions on the transport and accumulation of a high amount of sediment mass in the macropores and the process described the sediment retention in the model. The sink term describing the retention process was added to avoid long-term accumulation of sediment mass to the subsurface drain depth in the simulations. Even though the description is not physically as detailed as the other processes in the model, preliminary simulations showed that it was necessary to add a retention process to the model to avoid accumulation of unrealistically high amount of TSS concentrations in the soil profile.

2.3 Estimation of potential evapotranspiration and longwave radiation

Three different methods were applied to simulate potential evapotranspiration at the experimental sites (Figure 8). Two of the methods were based on the FAO-56 approach of Allen et al. (1998). Furthermore, the capability of a Class A evaporation pan to estimate the potential evapotranspiration in cropped agricultural fields was evaluated (Paper II). Since the Penman-Monteith approach and the energy balance based snow model scheme require an estimate of the hourly longwave radiation, longwave radiation was also computationally approximated.

For reference, PET was computed with the MACRO model (e.g. Larsson and Jarvis 1999), with daily time step and model default values and sowing and harvest dates were used as the input values.

Firstly (Paper I), hourly PET for reference surface (PET_0) was computed with the Penman-Monteith function, following Allen et al. (1998). PET_0 describes PET in a grass reference surface which has specific characteristics. Net incoming radiation for the Penman-Monteith equation was derived from the observed solar radiation and computed incoming and outgoing longwave radiation fluxes. Incoming longwave radiation was calculated based on the Stefan-Boltzmann law, the observed air temperature and emissivity of the sky. To estimate the emissivity of the sky, the cloudiness index was estimated as a function of the observed daylight duration and a computed maximum possible daylight duration. The maximum daylight duration was computed with the method of Allen et al. (1998). Furthermore, the emissivity during maximum cloudiness was set to 1.0, and the emissivity of a cloudless sky was estimated with the method of Satterlund (1979). Outgoing longwave radiation was also calculated based on the Stefan-Boltzmann law. The emissivity of the soil surface was set to 1.0 and the soil surface temperature was assumed to be equivalent to the observed air temperature. In Paper I, the potential evapotranspiration of a cropped surface (PET_{07}) was estimated by multiplying the hourly PET_0 values with a constant crop coefficient. Since crop coefficients have not been empirically estimated in the local conditions of the experimental sites, the applied crop coefficient was calibrated and set constant throughout the studied periods.

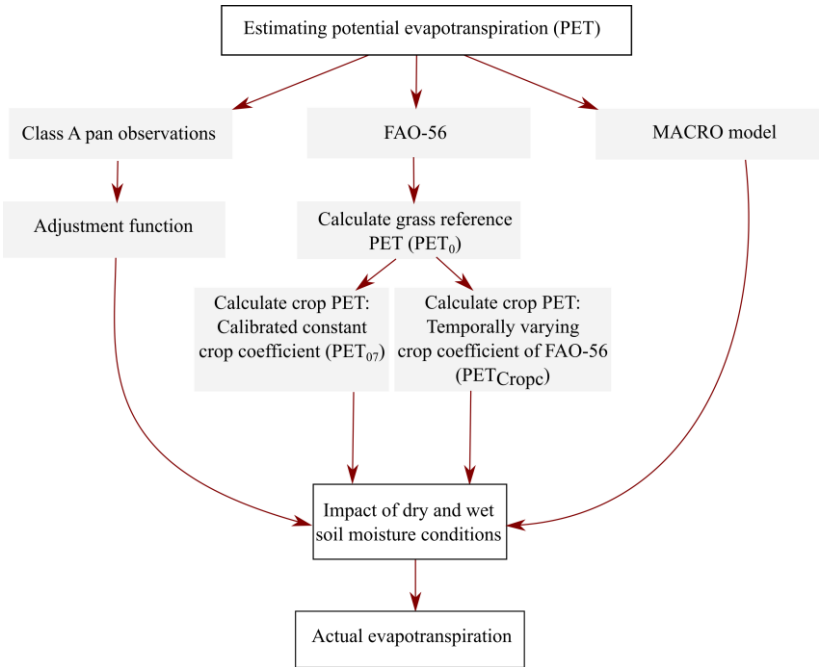

Figure 8. Main steps and methods adopted in the thesis to estimate evapotranspiration in clayey subdrained high-latitude agricultural fields. Steps related to potential evapotranspiration calculation are denoted with a grey background.

In Paper II, the PET model was modified to include a description of temporally changing crop growth phases (PET_{Cropc}). The approach was similar as in Paper I, but the cloudiness index was calculated as a function of measured solar radiation and clear-sky solar radiation, which was estimated using the method of Allen et al. (1998). Since the estimate was conducted also for winter periods, PET_o was set to 0 mm h^{-1} when the air temperature was below the freezing point. Temporal variation in the growing phases of annual crops was estimated by first dividing the growing seasons into initial, development, mid-season and late-season phases with corresponding crop coefficients, following Allen et al. (1998). The growing phase durations were estimated on the basis of cumulative effective degree days (CDD), following Peltonen-Sainio and Rajala (2008), who presented estimates of CDD needed for different growing phases of spring crops. The initial phase was set from sowing to CDD of 150, the development phase from the end of the initial phase to CDD of 500, the mid-season phase from the end of the development phase to 950 CDD, and the late-season phase from the end of mid-season phase to the harvest date.

Crop coefficients for the initial phases were computed as a function of daily meteorological data and soil properties, following Allen et al. (1998). Since Allen et al. (1998) also recommended the same method for bare soil conditions and since the method has been reported to perform well in bare soil conditions in different climates (Mutziger et al. 2005), one crop coefficient was calculated annually to describe the bare soil and initial phase conditions before the crop development phase. All parameters were set as recommended by Allen et al. (1998), but the maximum amount of water that can evaporate from bare soil with a potential evaporation rate was set to 6 mm, following the observations of Ritchie (1972). As recommended by Allen et al. (1998), the crop development phase coefficient was set to linearly increase from the crop coefficient of the initial phase to the mid-season phase coefficient. Mid-season phase crop coefficients were first set to 1.15 and then adjusted to local conditions as a function of crop height and meteorological observations (Allen et al. 1998). Plant height was set to 0.8 m, based on the observations of Kangas et al. (2012). As recommended by Allen et al. (1998), the mid-season phase coefficient was set to decrease linearly to the end-phase stage. Furthermore, the end-phase crop coefficient was calculated with the same method as the initial phase coefficient but with the meteorological data of the autumn period.

Potential evapotranspiration (PET_{ClassA}) was estimated also based on the Class A pan observations and a local adjustment function of Vakkilainen (1982):

$$C = 0.05 + 0.18 \ln(J - d_l) \qquad (8)$$

where C [-] is the correction coefficient (from 1 May), J [-] is the Julian day and d_l [-] is 121 in leap years and 120 in regular years. The function was derived by fitting Class A data against the evapotranspiration measurement from well-watered grassed lysimeters (Vakkilainen 1982) and it thus represents PET_o. Vakkilainen (1982) also reported a bi-hourly distribution of energy consumed by evapotranspiration within a day during different growing season phases. In the current

study, the daily Class A evapotranspiration estimate was disaggregated to hourly values based on the energy distribution represented by Vakkilainen (1982) (Table 6).

Table 6. Bi-hourly distribution of the energy consumed by evapotranspiration within a day during different months of the growing season. Data adopted from Vakkilainen (1982).

Time	Apr	May	Jun	Jul	Aug	Sep	Oct
0:00–2:00	0.00	0.00	0.00	0.01	0.00	0.02	0.01
2:00–4:00	0.00	0.00	0.00	0.01	0.00	0.00	0.01
4:00–6:00	0.03	0.04	0.03	0.04	0.01	0.01	0.04
6:00–8:00	0.10	0.11	0.16	0.08	0.07	0.05	0.05
8:00–10:00	0.17	0.18	0.16	0.14	0.15	0.15	0.14
10:00–12:00	0.18	0.19	0.20	0.19	0.21	0.23	0.21
12:00–14:00	0.19	0.18	0.16	0.18	0.22	0.22	0.23
14:00–16:00	0.16	0.15	0.13	0.15	0.17	0.18	0.15
16:00–18:00	0.08	0.09	0.09	0.10	0.10	0.09	0.07
18:00–20:00	0.08	0.05	0.05	0.06	0.05	0.02	0.05
20:00–22:00	0.01	0.01	0.02	0.03	0.01	0.00	0.02
22:00–24:00	0.00	0.00	0.00	0.01	0.00	0.02	0.01

2.4 Simulation strategies and model setups

The simulations in this thesis consist of four different model applications, of which two were conducted at the Nummela site (Papers I–II) and two at the Gårdskulla Gård site (Papers III–IV). The main simulation strategy was to calibrate FLUSH against the field-scale data by the manual inverse modelling approach and to validate the model against the data by the split sample approach. The calibrated and validated models were further applied to conduct simulation scenarios to decipher the impacts of different factors on the hydrology of the studied fields (Figure 9).

In this thesis, a model is considered to be valid when it can reproduce the magnitude and temporal variation of the site-specific hydrological observations during calibration and validation periods (e.g. Refsgaard and Henriksen 2004). Due to the relatively large number of parameters and possible model structures, the models may be subject to non-uniqueness, i.e. several model parameterizations and structures can lead to similar results, and thus simulation scenarios can include predictive uncertainty (e.g. Højberg and Refsgaard 2005). In case the simulations did not result in an acceptable correspondence with the observation during validation, the model structure was revisited and the calibration was conducted again (Figure 9, e.g. Thacker et al. 2004). It is recognized that in agricultural fields and other open systems, a model can be valid against the given data, but may not provide a comprehensive description of all hydrological processes within the field (Refsgaard and Henriksen 2004; Oreskes et al. 1994). However,

the available data are considered to contain information of the dominating water balance components; and thus a valid model is considered to describe the field water balance adequately. Thus, model scenarios conducted with a valid model are considered to conceptually provide an adequate description of the response of the system to the studied changes. Regarding erosion and sediment transport simulations, different model structures were tested and a sensitivity analysis was conducted to assess the impact of different factors on erosion processes and sediment balances (see Section 2.4.2.2).

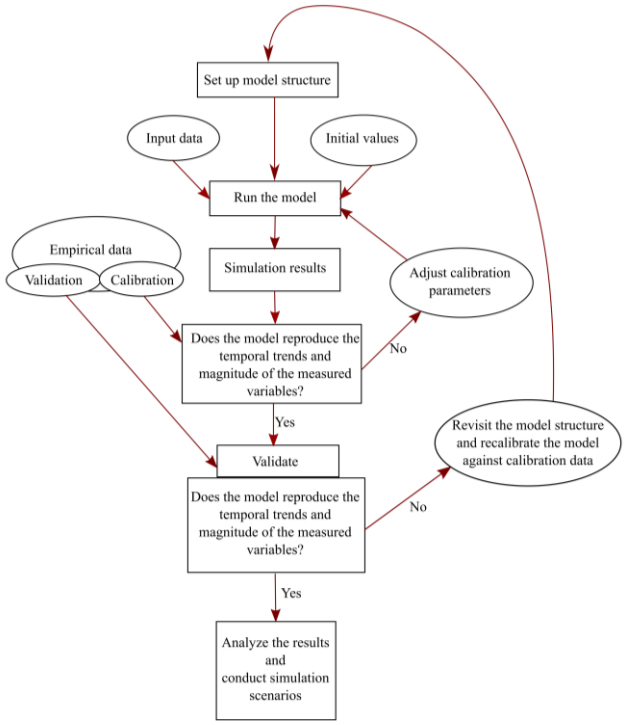

Figure 9. Flowchart of the different steps of the applied modelling procedure.

2.4.1 Nummela experimental site

Two different model applications were conducted at the Nummela experimental site. In Paper I, the model was applied to the snow- and frost-free periods in the years 2007–2009 to assess the water balance of the field and to quantify the effects of the recent subsurface drain installations on the hydrology of the field sections. All field sections were simulated simultaneously to facilitate a comprehensive assessment of the water balance and hydrological impacts of the drainage procedures. In Paper II, the model was extended with the winter-time processes and applied in 2008–2009 and 2011 to assess year-round water balances and to study different evapotranspiration estimation methods. The connection between

evapotranspiration and other components of the water balance was also studied in Paper II. The common parameters between the first and second application are presented in Section 2.4.1.1. Sections 2.4.1.2 and 2.4.1.3 present those parameters that are applied solely in Paper I or II, respectively.

2.4.1.1 Field geometry, boundary conditions and common parameters

In both Paper I and Paper II, the depth of the soil profile was set to 2.4 m and the profile was vertically divided into 16 layers, with the cell depth increasing gradually from 0.02 to 0.5 m from the soil surface. Horizontally, the area of each computational cell was 5 x 5 m^2. The topography of the grid bottom was set similar to the measured topography of the field surface. The LGT data suggested that the depth of the groundwater table fluctuated typically between 0–2 m. It was assumed that the dominating hydrological processes below the subsurface drain depth occurred in the depth of 1.0–2.4 m and that the hydrological processes could be described with the chosen profile depth. The bottom of the computational grid was treated as an impermeable no-flow boundary in the simulations. Field borders were treated as open boundaries, where horizontal water outflux across the field borders could occur as groundwater outflow. Influx of water to the field across the field boundaries were neglected in the simulations, as the surrounding upslope areas were relatively flat.

The drain diameters were set to 0.05 m in all of the field sections, except in Section C, where the diameter of the new drains (installed in 2008; see Section 2.1.1) was set to 0.07 m due to the envelope material (coarse gravel), which was assumed to increase the effective diameter of the drains, following Stuyt et al. (2005). The impacts of the vertical gravel deposits in Section C were neglected because Aura (1990), who empirically studied the hydrological impacts of gravel deposits, suggested that the deposits have only a minor impact on field hydrology. The depths of the ditches that surrounded the field area were set to 0.8–1.0 m. The initial soil water content and hydraulic pressure head values were derived from the LGT data. The hydraulic pressure head values above the groundwater level were set corresponding to static steady state conditions.

K_{sat} of the soil matrix was set to the measured minimum values of the soil samples (0.0032 m h^{-1} for the topsoil layer of 0–0.25 m and 1×10^{-4} m h^{-1} for the soil layers of 0.25–2.4 m). The volumetric fraction of soil macropores was set to the measured values in the soil layers from 0 to 0.6 m. Manning's roughness coefficient for the soil surface was set to 0.1 (Warsta et al. 2013a). Soil surface depression storage was set to 1 mm (Warsta et al. 2013a).

Maximum root depth was set to 0.8 m, following the observations of Ilola et al. (1988) in Finnish clay soils. Root depths were given as an input time series for the model. During the time periods from the sowing until 3 Jun, the root depth was set to linearly increase from the minimum (0.05 m) to the maximum depth. Before the sowing and after the harvest, the root depth was set to the minimum value, which described the evaporation from the soil surface during non-vegetated soil surface conditions.

2.4.1.2 Paper I: Water balance during snow- and frost-free periods and hydrological impacts of drainage methods

In the first application (Paper I), the model was calibrated against drain discharge, TLR and soil moisture data. The calibrated parameters were the constant crop coefficient, the fraction of static macropores beneath the measurement depth of 0.6 m, dry ends of the WRCs (Eq. 1, parameters α and c), K_{sat} multiplier of the macropores, λ values (Eq. 4) of the drains and TLR measurement drains (in each field section) and annual water level in the surrounding ditches. The model was first calibrated in all field sections against the data from 6 May 2007 to 31 Dec 2007 (Figure 10). Secondly, due to the drain installations in Sections A and C (Fig. 3), the λ values of the new drains (Eq. 4) were recalibrated due to the changing drain properties against the data from 6 May 2008 to 28 Nov 2008. The simulation results of Sections B and D were validated against the data of the periods 6 May 2008 – 28 Nov 2008 and 6 May 2009 – 10 Dec 2009. The simulation results from Section A and C were validated against the data from 6 May 2009 – 10 Dec 2009.

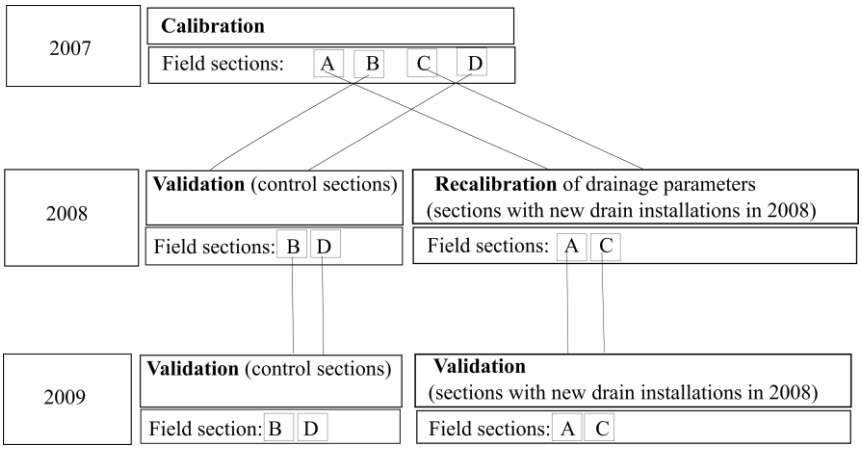

Figure 10. Flowchart of the calibration and validation procedure in Paper I.

WRCs for the soil matrix were initially derived by fitting Eq. 1 to the measured WRCs from the Nummela and Hovi sites. Because the dry end of the measured curves was adopted from the Hovi site, the parameters α and c (Eq. 1) were calibrated. For the soil macropore system, the parameters α, c, and θ_r of Eq. 1 were set to the values of 7.0, 2.0 and 0.01 $m^3\ m^{-3}$, respectively, following Warsta et al. (2013a). The parameterization of Section E was set similar to Section A, except that the macroporosity beneath the measurement depth of 0.6 m was set to the lowest measured value in Section A. Other soil parameters were set as in Warsta et al. (2013a). The values of the calibrated parameters are presented in Paper I.

Simulation scenarios were conducted with the calibrated and validated model to analyse the impacts of drain installations (Sections A and C), the terrain topography (Section A–D) and the trenchless drain installation method (Section A) on

drain discharge generation. The impacts of the trenchless installation method were analysed by identifying plausible soil disturbance effects on soil hydraulic parameters from the literature and testing their hydrological impacts with the calibrated model. Based on the observations of Spoor and Fry (1983), it was assumed that the trenchless drain installation causes a decrease in soil macroporosity and loosening of the soil structure. These changes were described in the model by adjusting the macroporosity and γ above the drain depth. Also, the impacts of terrain topography on drain discharge were assessed by changing the topography of the simulated domain to a completely flat domain with a slope of zero.

2.4.1.3 Paper II: Year-round water balances and evapotranspiration estimation

In Paper II, the parameterization of Paper I was revisited. For the second application, the soil water content measurements at the wilting point (-150 m) were available from the Nummela site, and thus WRCs were recalculated with the completed WRC data. Furthermore, since Berisso et al. (2013) noticed that air permeability appeared to be anisotropic in a clayey soil in Jokioinen, it was assumed that hydraulic conductivity was anisotropic in the studied site. Following Berisso et al. (2013), the ratio of lateral to vertical K_{sat} in the soil macropore system was set to 0.02, 0.83 and 1.0 in the soil layers at the depths of 0–0.425 m, 0.425–1.05 m and 1.05–2.4 m, respectively. K_{sat} of the soil matrix was set to be isotropic in all soil layers. In the current application, a single value was calibrated to describe the volumetric fraction of macropores in the subsoil layers (depth >1.05 m) (w_{fs}) in the entire field area. Due to the availability of the new information and the extended calibration period (Jan–Dec 2011), λ values (Eq. 4) of the subsurface drains were recalibrated. Model calibration was conducted against drain discharge, TLR and LGT data.

The bottom boundary condition of the heat flow model was set to a fixed value of 5.9 °C, which is within the range of observed values presented by Lemmelä et al. (1981) in southern Finland. Parameters for the heat and snow model were derived from Warsta et al. (2012) and Koivusalo et al. (2001).

PET was estimated using the three different approaches introduced in Section 2.3, including the FAO-56 method with a constant crop coefficient (PET_{07}), the FAO-56 method with the dynamic crop coefficients (PET_{Cropc}) and the Class A approach (PET_{ClassA}). The parameters of this model application are shown in more detail in Paper II.

2.4.2 Gårdskulla Gård experimental site

Two different model applications were conducted at the Gårdskulla Gård site. In Paper III, water balances in the two fields of the experimental site were simulated throughout five years to assess long-term and seasonal water balance components and to assess the impacts of terrain slope on the water balance of the fields. In Paper IV, the erosion and sediment transport model was applied in the fields on

top of a water flow model derived from Paper III. The aim of Paper IV was to assess sediment balances and erosion processes in the two fields with different slopes.

2.4.2.1 Paper III: Effects of terrain slope on long-term and seasonal water balances

In the Gårdskulla Gård applications, the depth of the soil profile was set to 2.4 m. In the model calibration and validation, the soil profile was divided into 21 soil layers, and the thicknesses of the layers were set to increase gradually from 0.025 m to 0.25 m from the soil surface. The horizontal area of the computational cells was 4×4 m². Similarly to the model applications in the Nummela field, the topography of the grid bottom was set identical to the measured topography of the field surface. The impacts of this assumption on the simulation results were further tested with a simulation scenario (Scenario 1, Figure 11). Horizontal boundaries of the simulated fields were set to include the monitored subsurface drain networks, delineated downslope side by the Kirkkojoki stream and extended west in Section 1 and east in Section 2 to avoid angular boundary conditions in the slope direction (Figure 4). All of the horizontal borders of the simulated area, except the downslope side border delineated by the Kirkkojoki stream, were treated as no-flux boundaries. A head- and state-dependent flux boundary was applied on the soil surface (e.g. Warsta et al. 2013a). On the downslope side of the fields, the simulated areas were delimited by the Kirkkojoki stream (Figure 4), which was described as a 1 m deep open ditch in the simulations. The measured water levels in the stream were linearly interpolated from the weekly/bi-weekly data to hourly levels, and used as a boundary condition in the downslope side of the grids. However, the water level in the stream was set to have the maximum depth of 1 m, as the model currently does not include description of water flooding to the stream banks. In this application, groundwater outflow was defined as the water seepage into the Kirkkojoki stream. It was hypothesized that the influx of groundwater across the field boundaries occurred especially in Section 1 (due to the adjacent hill area; see Fig. 4) and thus the impact of the upslope water inflow on the field water balance was assessed with an additional simulation scenario (Scenario 2, Figure 11). The simulation scenarios are presented in more detail below.

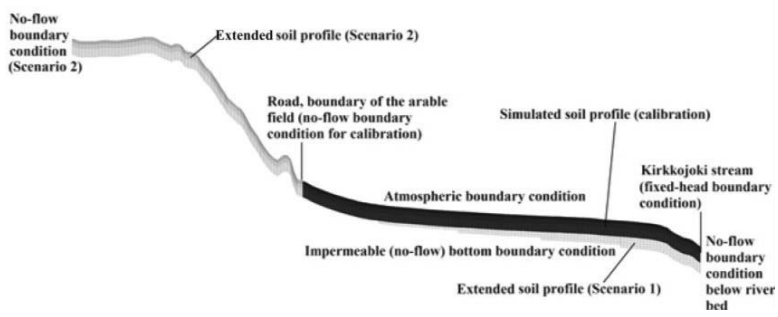

Figure 11. Schematic illustration of the boundary conditions and hydrogeological model structures of the simulated area during model calibration and validation as well as in Scenarios 1 and 2. (Modified from Paper III)

The hydraulic properties of the soil profiles were parameterized using the field measurements, pedotransfer functions and literature values. The parametric WRCs were derived from the measured WRCs. Since water content data at wilting point (θ_w) were not available, a pedotransfer function of Rawls et al. (2003) was applied to estimate θ_w in Section 1 (clay content 47–60%) and soil layers 0–0.224 and 0.225–0.425 m (clay content 39–47%) in Section 2, following Kätterer et al. (2006). The authors evaluated the performance of different pedotransfer functions against a large dataset in Sweden and recommended the function of Rawls et al. (2003) for soils with clay contents <60%. The subsoil of Section 2 had a higher clay content (55–86%) and therefore θ_w in this soil was estimated with Model 6 of Kätterer et al. (2006). WRC parameters for the soil macropore system were adopted from Gärdenäs et al. (2006). The parametric SSCC was derived from Kankaanranta (1996). K_{sat} of the soil matrix in the depth of 0–0.225 m was set to 10.0 mm h^{-1}, following Warsta et al. (2013a). K_{sat} of the deep soil layers (0.225–2.4 m) in both sections was calibrated due to the clearly different subsoil particle size distribution at the Gårdskulla Gård site compared to the study of Warsta et al. (2013a). The ratio of horizontal to vertical K_{sat} of the macropore system was set anisotropic, following the findings of Berisso et al. (2013) (see Section 2.4.1.3 for details). The Manning's roughness coefficient on the field surface was set to a value of 0.1 (Warsta et al. 2013a). During those time periods when high amounts of snowmelt occurred in the simulations (January 2008 and springs 2010–2012), the roughness coefficient was increased to 20.0 to describe the impact of the snowpack on the overland flow. A similar approach has been previously applied by Bathurst and Cooley (1996), who simulated snowmelt runoff with the SHE model.

The snow model and the water flow model were calibrated separately. First, the snow model was independently calibrated against SWE data from the year 2012 by adjusting the surface roughness height in the range 3–7 mm. Secondly, the snow model was validated against the SWE data of the remaining years 2008–2011.

The water flow model was calibrated against drain discharge, TLR and LGT data from the years 2008–2010 and validated against the data from the years 2011–2012. Parameters that had clear physical site-specific differences as well as an impact on the field water balance (Warsta et al. 2013a; Nousiainen et al. 2015; Turtola et al. 2007; Schulze-Makuch et al. 1999) were calibrated to the local conditions. The calibrated parameters of the flow model were w_{fs}, λ values of the subsurface and TLR measurement drains, K_{sat} of soil matrix at the depth 0.225–2.4 m and the soil surface depression storage. The calibration procedure is presented in more detail in Paper III.

The crop root depths were calculated based on the crop growing phases (see Section 2.3). The spring crop minimum root depth was set to 0.05 m (Warsta et al. 2013a) and maximum root depth to 0.75 m (Ilola et al. 1988). The root depth of spring crops was set to the minimum value before sowing in spring. Winter wheat and overwintering grasses were set to have a root depth of 0.5 m in the beginning of spring, and winter wheat was set to have a maximum root depth of 1.1 m (Alakukku, personal communication, 4 Feb, 2014). For spring crops, the

root depth was set to increase linearly as a function of time from the initial value to the maximum depth. Winter wheat and grasses were set to start growing on 1 May. Root depths of the annual crops were set to reach their maximum value at the beginning of the mid-season stage (Pietola and Alakukku 2005). Grasses were set to reach their maximum root depth on 1 Jun each year. Root depths were set back to the minimum value (0.05 m) after harvest. If the vegetation was not harvested, root depths were set back to the minimum value on 15 Sep.

The hydrological impacts of soil profile depth and upslope boundary conditions were assessed with Scenarios 1 and 2 (Figure 11). In Scenario 1, the impermeable bottom boundary was set to gradually increase from 2.4 m at the uphill to 4 m at the stream location (Figure 11), and the hydrological effects of the depth changes were assessed against the calibration and validation results. In Scenario 2, it was presumed that the hill adjacent to Section 1 (Figure 4) induced an influx of water to the monitored field area, and the upslope boundary condition was extended south to the top of the forested hill area (Figure 11). The extended area of the simulated domain was set to have the same soil and crop parameters as in the model calibration, and the extended domain was 60% larger than the domain during calibration. The road structure between the forested hill and the monitored area (Figure 4 and Figure 11) was described as a ditch with a depth of 1 m in the simulations. Other parameters and boundary conditions in the simulation scenarios were set similarly as in the model calibration.

2.4.2.2 Paper IV: Sediment balances and structural uncertainties in sediment transport models

The erosion and sediment transport application was built on top of the extended water model application (Koivusalo et al. 2015), which was based on Paper III. In the application, the simulated area of Section 1 was extended to include the uphill area (Scenario 2 in Figure 11) and the w_{fs} was set to the same value (0.08) as in Section 2, since the results of Paper III suggested that the uphill area contributed to the water balance of Section 1 and the calibrated w_{fs} value was likely too small in Section 1 due to the exclusion of the uphill contributing area. The main simulation strategy was to form three model structures (Models A–C in Figure 12) which encompassed different assumptions of the capability of soil preferential flow pathways to transport sediment. It was assumed that lateral macropores may be partly discontinuous and may thus allow the preferential water flow but may prevent preferential transport of sediment. The different structures were calibrated and validated against sediment load and concentration data. In Model A, all soil layers in the subsurface domain were able to transport sediment in 3D. In Model B, transport was enabled in 3D, but only the soil layers above the subsurface drain depth (1 m) were allowed to transport suspended sediment. In Model C, solely vertical transport was allowed and transport was possible only above the subsurface drain depth.

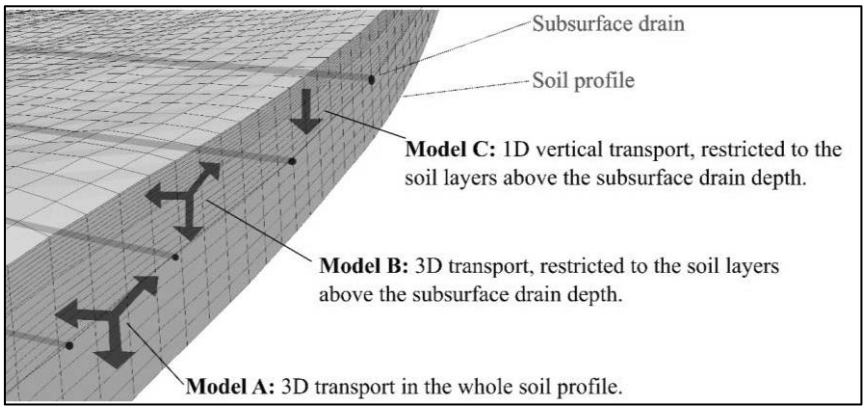

Figure 12. Conceptual representation of the three different applied model structures (Models A–C) of the erosion and sediment transport model of FLUSH. (Paper IV)

The model was calibrated against the sediment load and concentration data collected from drain discharge and TLR. Data from Jan–Dec 2008 and Jan–Dec 2009 were used for calibration and validation, respectively. Warsta et al. (2013b) demonstrated that the key parameters of the erosion and sediment transport model in FLUSH were those that affected the erosion rates rather than those describing sediment transport. Furthermore, at the Gårdskulla Gård site, the amount of overland flow was small and overland flow events occurred sporadically. Thus, it was assumed that hydraulic erosion could only have an intermittent impact on erosion rates, and it was assumed that raindrop erosion was the major force causing erosion on the fields. Therefore, the empirical coefficient k_r (Eq. 5) and k_i (Eq. 7), which control raindrop erosion in the model, were chosen as the calibrated parameters. The calibrated parameters were set temporally constant and spatially uniform. Similar parametrization was applied for both of the field sections, since the sections had relatively similar soil properties (Table 4). During time periods when a vegetation cover prevailed on the soil surface, C_C (Eq. 5) was set to 1. During the other time periods, C_c was set to 0. The threshold value C_T was set to the maximum measured concentration value of 1 489 g m^{-3}, which is in the range of the maximum concentrations measured by Turtola et al. (2007) and Warsta et al. (2014). The erodibility of the forest area adjacent to the monitored area of Section 1 was set to zero. Other parameter values were adopted from Warsta et al. (2013b). The calibrated values and the model setup are presented in more detail in Paper IV.

The sensitivity of the model parameters was addressed with a sensitivity analysis, where the calibrated parameter values were altered by ±20%. The sensitivity of the model to changes in soil hydraulic parameters was addressed by simulating Section 1 with the soil hydraulic parameters of Section 2 and vice versa.

2.4.3 Model evaluation criteria

The goal of the model applications was to reproduce the timing and magnitude of the observed hydrological variables. In Paper I, the performance of the model was numerically evaluated with the Nash-Sutcliffe coefficient (N-S) (Nash and Sutcliffe 1970), the mean absolute error (MAE) and the difference between simulated and measured annual accumulations (D). The MAE values were compared against the standard deviation (SD) of the measured values. For TLR and drain discharge, the evaluation criteria were calculated for those periods when water outflow occurred in the field.

In Papers II-IV, the results were evaluated with the MAE, D, SD and the modified Nash-Sutcliffe coefficient (N-S_m), where the squared values of the original Nash-Sutcliffe equation are replaced with absolute values, following the suggestions of Legates and McCabe (1999).

3. Results

This section presents the main results in Papers I-IV. Sections 3.1 and 3.2 present the main findings in Paper I and II, respectively, from the Nummela experimental site. Section 3.3 presents the main findings in Paper III, and Section 3.4 in Paper IV from the Gårdskulla Gård experimental site.

3.1 Paper I: Water balance during snow- and frost-free periods and hydrological impacts of drainage methods

In this application, the water balances and hydrological impacts of drainage methods were analysed during the snow and frost-free periods of the years 2007–2009 at the Nummela experimental site (Section 2.4.1.2). All field sections were simulated simultaneously and model scenarios were conducted to quantify the impacts of terrain topography and drainage methods on the water balances of the field sections.

3.1.1 Calibration period 2007

During the calibration period 2007, the simulated hourly drain discharge results were comparable with the observations in terms of the model evaluation criteria (Table 7). The N-S values varied between 0.35 and 0.76 and the MAE values were low compared to the SD values. When the N-S values were computed for a daily time step, they showed better agreement with the observations (N-S values 0.72–0.85 for daily time series). The D values in 2007 varied from -14 mm to 3 mm between the field sections, which demonstrated a correspondence between the simulated and measured drain discharge accumulations. The correspondence of simulated and measured hourly TLR values was clearly inferior compared to the drain discharge, which was demonstrated by the negative N-S values of TLR. However, the D values of TLR (1–19 mm) were in the same order of magnitude as for the drain discharge, which suggested a relatively small error in the context of water balance, as the amount of precipitation during the calibration period was 486 mm. In addition to the outflow components, the model reproduced the observed soil moisture values, with the MAE values ranging from 2% to 4% between field sections.

Table 7. Model evaluation criteria values for hourly drain discharge in 2007. (Paper I)

	From 1 Oct to 31 Dec			
	Section A	Section B	Section C	Section D
N-S[a]	0.35	0.76	0.73	0.66
MAE[b]	0.028	0.021	0.025	0.013
SD[c]	0.069	0.083	0.081	0.034

[a] Nash-Sutcliffe model efficiency coefficient [-].

[b] Mean absolute error [mm h^{-1}].

[c] Standard deviation [mm h^{-1}].

Drain discharge and TLR accumulations during the calibration period 2007 (Figure 13) also demonstrated a correspondence between the simulated and observed timing and magnitude of these water balance components. Furthermore, there were apparent differences in the drain discharge amounts between field sections A–D (Figure 13). The observed drain discharge was the lowest in Section D (61 mm), which had the sparsest drain spacing (32 m). All other sections (A–C) had a drain spacing of 16 m, but their discharge amounts differed. In Sections B and C, the observed drain discharge values were 123 mm and 121 mm, respectively, whereas the observed drain discharge was lower in Section A (85 mm). As shown in Figure 13, the relatively low drain discharge in Section A was not explained by the differences in the amount of observed TLR. The location of Section A close to the steep slope (Figure 3) would likely explain the difference, and the impact of terrain topography on the field water balance was further assessed with an additional simulation scenario (see Section 3.1.3).

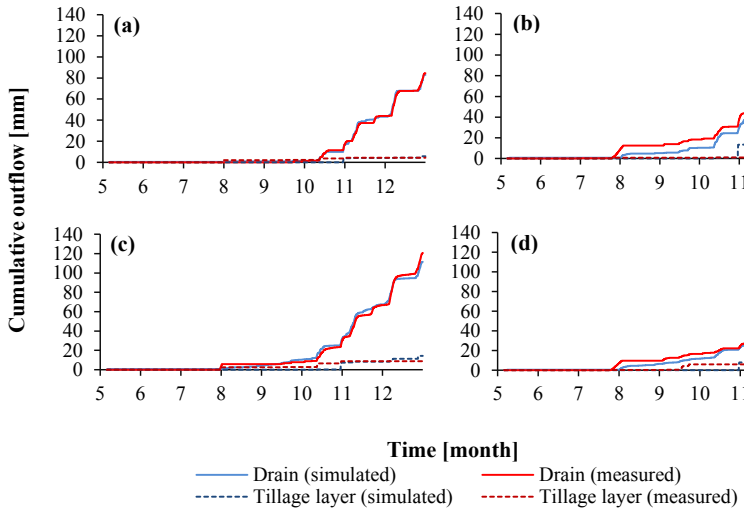

Figure 13. Simulated and measured cumulative outflows in 2007 (from 6 May to 31 Dec) in field sections (a) A, (b) B, (c) C and (d) D of the Nummela experimental site. (Paper I)

The analysis of all of the main water balance components in the whole field area during the calibration period 2007 (Table 8) showed that the groundwater outflow comprised a relatively high outflow component (74 mm, or 15% of precipitation). As listed in Table 8, drain discharge and groundwater outflow were the largest outflow components, whereas flow to open ditches (surface runoff and seepage of water from the soil matrix and macropores into the ditches) was the lowest outflow component. Evapotranspiration dominated the field water balance as the growing season covered a large portion of the simulation period.

Table 8. Components of the water balance in the whole field area in 2007 from 6 May to 31 Dec. (Paper I)

	Amount [mm]	Proportion of the precipitation [%]
Precipitation	486	100
Evapotranspiration	284	58
Flow to ditches	40	8
Drain discharge	75	16
Groundwater outflow	74	15
Change of storage	12	2
Mass balance error	3	1

3.1.2 Simulation periods 2008 and 2009

The model was validated against the data from 2008 and 2009 from the reference Sections B and D. However, since the drain installations were conducted in Section A and C in Jun 2008, the drainage parameters were recalibrated in these sections and then validated against the data from 2009 (see Section 2.4.1.2 and Figure 10).

During the model validation in 2008 and 2009, the model evaluation criteria for the hourly drain discharge and TLR in Sections B and D were comparable to the calibration period 2007 (Table 9). In 2008–2009, also the D values of drain discharge (from -20 mm to 8 mm) and TLR (from -15 mm to 4 mm) in these sections were close to the ranges obtained during the calibration period.

In the recalibration of the drainage parameters of Sections A and C in 2008 (Figure 10), the D values of drain discharge (7 to 23 mm) and TLR (-35 to -14 mm) were comparable to the 2007 calibration period. During the validation period 2009 the D values of drain discharge (-24 to -9 mm) and TLR (-4 to -2 mm) were relatively similar to the 2007 calibration period in these sections. However, the model evaluation criteria for the hourly drain discharge in these sections in 2008–2009 were inferior compared to the results of the calibration period 2007 (Table 9). The correspondence of the simulated and observed hourly drain discharge values in 2008–2009 was particularly poor in Section A, which is demonstrated by the negative N-S values in Table 9 and by the graphical comparison in Figure 14. The reason for the poor N-S values in Section A was likely the impact

of the trenchless installation method on soil hydraulic properties, and the impact could not be described by the drainage parameter recalibration in the model. The hydrological impacts of the drainage installations were further assessed with additional simulation scenarios (see Section 3.1.3).

Table 9. Results of the model evaluation criteria for hourly drain discharge in 2008 and 2009 with the new drain installation in Sections A and C. (Paper I)

	2008 (1 Oct to 28 Nov)			
Section	A	B	C	D
N-S[a]	-1.29	0.8	0.46	0.77
MAE[b]	0.061	0.02	0.05	0.011
SD[c]	0.081	0.082	0.138	0.032
	2009 (15 Nov to 10 Dec)			
Section	A	B	C	D
N-S[a]	-0.88	0.63	0.06	0.54
MAE[b]	0.033	0.029	0.054	0.03
SD[c]	0.05	0.102	0.115	0.072

[a] Nash-Sutcliffe model efficiency coefficient [-].

[b] Mean absolute error [mm h^{-1}].

[c] Standard deviation [mm h^{-1}].

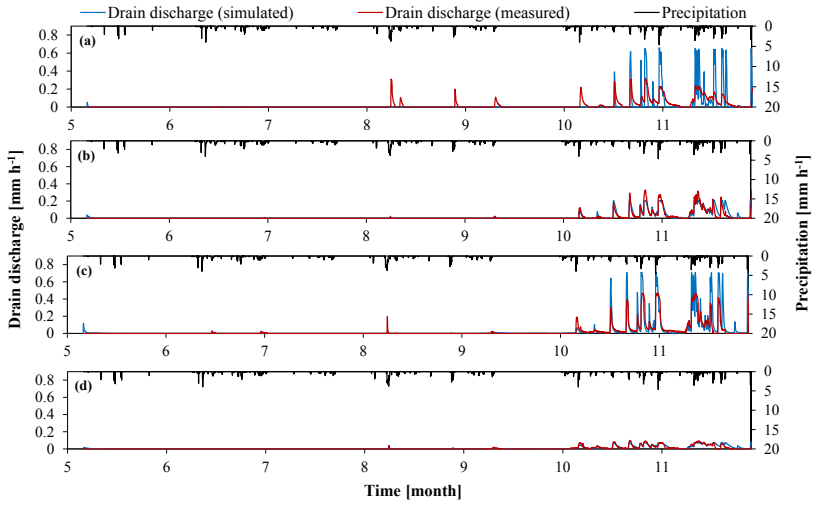

Figure 14. Simulated and measured hourly drain discharge in 2008 (6 May – 28 Nov) in field sections (a) A, (b) B, (c) C and (d) D of the Nummela experimental site. (Paper I)

As listed in Table 10, the distribution of the water balance components in 2008 was qualitatively similar to the calibration period 2007 as drain discharge and groundwater outflow were the dominant outflow components, whereas flow to ditches was the lowest outflow component. Evapotranspiration was the highest water balance component during the simulation period in 2008 (57% of precipitation) but formed even a higher share of the water balance in 2009 (80% of precipitation) due to the relatively low amount of precipitation. Due to the low amount of precipitation in 2009, the amount of water outflow in 2009 was also lower than in 2008 and 2007. Consequently, the amount of groundwater outflow exceeded drain discharge since groundwater outflow from the field occurred even when the LGT resided below the depth of the subsurface drains and open ditches.

Table 10. Simulated water balance components of the whole field area of the Nummela experimental site in 2008 (from 6 May to 28 Nov) and 2009 (6 May to 10 Dec) with the new drain installations. (Paper I)

	2008 (6 May to 28 Nov)		2009 (6 May to 10 Dec)	
	Amount [mm]	Proportion of precipitation [%]	Amount [mm]	Proportion of precipitation [%]
Precipitation	452	100	366	100
Evapotranspiration	256	57	292	80
Flow to ditches	52	11	6	2
Subsurface drains	71	16	17	5
Groundwater outflow	58	13	32	9
Change of storage	16	3	20	5
Mass balance error	2	<1	3	1

3.1.3 Simulation scenarios

Three simulation scenarios were conducted to analyse the hydrological impacts of the (1) new drain installations, (2) field topography and (3) trenchless installation method on drain discharge generation.

In the first scenario, simulations with and without the new drain installations provided a method to decipher the impacts of drain installations on drain discharge generation. As shown in Figure 15, the new drain installations did not increase the total amount of drain discharge in Section A (Figure 15a and e) as much as in Section C (Figure 15c and g). In 2009, the drain installations had practically no impact on the drain discharge of Section A (Figure 15e). As shown in Figure 15b and f, when the drain installation in Section C increased the drain discharge by 51%, the drain discharge in the control section B decreased by 11%. These simulation results indicate that the field sections shared a hydrological connection

and that the drain installation conducted in Section C also affected the hydrological processes in Section B. The field slope likely induced the hydrological connection between Sections B and C. Section C declines gently toward Section B (Figure 3) and in 2007 the LGT was higher in Section C than in Section B. Drain installations decreased the LGT in Section C and thus decreased the hydraulic gradient and also the groundwater flow from Section C to Section B. This further caused the decrease in the drain discharge in Section B.

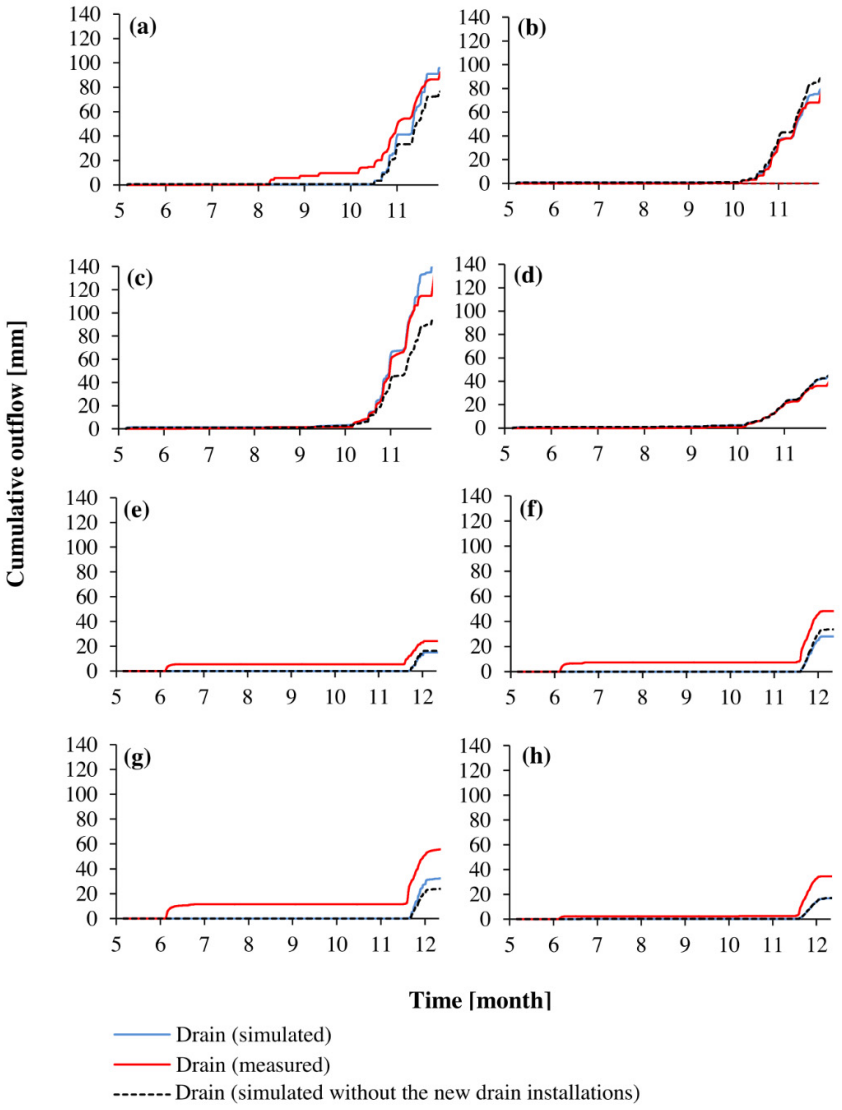

Figure 15. Simulated and measured accumulated drain discharges in 2008 (6 May – 28 Oct) in field sections (a) A, (b) B, (c) C, and (d) D and in 2009 (6 May – 10 Dec) in field sections (e) A, (f) B, (g) C and (h) D of the Nummela experimental site. The results of a simulation scenario where the model was run without the new drain installations in Section A and C are shown by a dashed line. (Paper I)

The drain discharge change appeared to be smaller in Section A than in Section C due to the steep slope in the vicinity of Section A (Figure 3). Additional simulations (not shown) suggested that the envelope material of Section C (coarse gravel) and the 0.1 m shallower drain depth in Section A compared to Section C (0.9 m vs 1.0 m) did not explain the difference in the simulated drain discharges in Sections A and C. Overall, the differences in the envelope material and drain depth had a minor impact on the drain discharge generation in the simulations when compared to the hydrological impact of changing the drain spacing.

In the second scenario, the impact of terrain topography was assessed by running the calibrated model during the simulation period 2008 with flat field topography (slope zero). The results indicated that the presence of steep topography in the northeast side of the field decreased drain discharge the most in Sections A (-40%) and D (-40%), which are located in the vicinity of the steep slope (Figure 3). The change had almost as high an impact in Section B (-37%), probably due to decreased groundwater flow from Section C and the relatively low calibrated volumetric fraction of macropores in the subsoil layers (see Table 4 in Paper I). The change in terrain slope had the lowest impact in Section C (-18%), which was located furthest from the steep slope. Also the LGT observations (Annex I) supported the simulation results of the occurrence of a relatively high amount of groundwater outflow in Sections A, B and D compared to Section C. During winter periods (Jan–Apr), when evapotranspiration was minimal and other outflow pathways remained inactive and LGT was lower than the depth of the subsurface drains and open ditches, groundwater depth was observed to decrease clearly below the drain depth in other field sections except in Section C. LGT decreased most rapidly and to the greatest depth in Section A (Annex I), which suggests that there was spatial variability in the amount of groundwater outflow and that groundwater outflow was the highest in Section A.

In the third simulation scenario, the impacts of the trenchless installation method on drain discharge generation were studied. Even though the drain installations had a higher impact on the accumulated drain discharge generation in Section C than in Section A, hourly drain discharges were affected more by the trenchless installation in Section A than by the trench installation method in Section C (Figure 14). To reproduce the impacts of the trenchless installation method on drain discharge generation in the model, the volumetric fraction of soil macropores and the water exchange coefficient γ (Eq. 3) above the drain depth were recalibrated against the discharge data of the simulation period 2008. Recalibration of the γ value described the impact of soil loosening due to the plough blade of the trenchless installation machine. The macroporosity was decreased by 25%, and γ was increased from 0.01 to 0.65. Due to the adjusted parameter values, the N-S value of drain discharge in 2008 increased from -1.29 to 0.21 and the MAE decreased from 0.061 mm h^{-1} to 0.037 mm h^{-1}. In 2009, the N-S increased from -0.88 to 0.27 and the MAE decreased from 0.033 mm h^{-1} to 0.020 mm h^{-1}. The impact of the parameter adjustment on hourly drain discharge is visualized in Figure 16 (see Figure 14a for reference). After the adjustment, the D value of drain discharge accumulations was 3 mm and -3 mm in 2008 and 2009, respec-

tively, which was relatively close to the D values of the simulations with the unadjusted soil parameters (7 mm in 2008 and -9 mm in 2009). The results suggested that soil disturbance had a clear impact on soil hydraulic properties and that these effects can be partly described by changes in the volumetric fraction of macropores and the water exchange coefficient γ (Eq. 3).

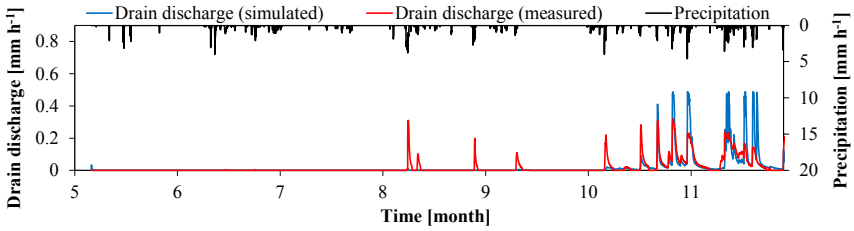

Figure 16. Simulated and measured hourly drain discharge in 2008 (6 May to 28 Oct) in Section A of the Nummela experimental site with adjusted soil hydraulic parameters (macropore multiplier 0.75 and water exchange coefficient multiplier 65.0 above the drain depth) after the trenchless drain installation. (Paper I)

3.2 Paper II: Year-round water balances and evapotranspiration estimation

In this application, the simulation at the Nummela experimental site was extended to also include winter and spring periods and the related hydrological processes (Section 2.4.1.3). Different standard evapotranspiration estimation methods were applied to study the interlinks of evapotranspiration and other water balance components and the applicability of the standard evapotranspiration estimation methods in high-latitude conditions.

3.2.1 Calibration and validation

During the calibration period (1 Jan – 31 Dec 2011), the simulated hourly drain discharge values corresponded with the observed values with the N-S_m values of 0.56 and 0.44 in Sections B and D, respectively. The N-S_m value of Section D was 0.62 when the spring snowmelt period was excluded, which demonstrated the higher correspondence of simulated and measured values during the seasons other than the spring period. Also the D values of drain discharge (22 mm in Section B and 24 mm in Section D) demonstrate a comparable magnitude of the simulated and measured drain discharge accumulations (Figure 17). For reference, the amount of cumulative precipitation during the calibration period was 676 mm.

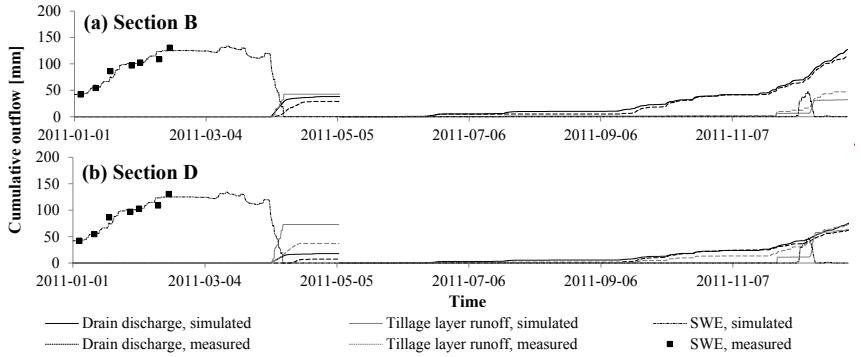

Figure 17. Simulated and measured snow water equivalent (SWE), and cumulative simulated and measured drain discharge and tillage layer runoff in field Sections (a) B and (b) D of the Nummela experimental site in the calibration period 1 Jan – 31 Dec 2011. (Paper II)

The simulated TLR values compared to the observations similarly as in Paper I, i.e. the hourly N-S_m values were negative. During the spring snowmelt in 2011, surface runoff was observed to enter Section B from the surrounding field areas, likely due to the impact of local soil frost conditions on water flow in a topographic depression adjacent to Section B, which was not taken into account by the model. However, the D values of -15 mm in Section B (Jun–Dec) and 27 mm in Section D (Jan-Dec) showed a comparable fit of simulated and measured amounts of accumulated TLR (Figure 17). Note that the TLR results in Section B during the snowmelt events of 2011 are not shown in Figure 17. The model was able to simulate SWE with the MAE value of 6 mm, and the timing of the snowmelt events corresponded with the outflow measurements as shown in Figure 17. Most of the drain discharge and TLR occurred in the autumn periods and during the spring snowmelt (Figure 17).

The simulated LGTs in the soil macropores or matrix resided between the observed minimum and maximum values during most of the simulation period (60% in Section D and 50% in Section B), even though in August and the beginning of September 2011 the simulated LGTs were high compared to the observations (Figure 18). Furthermore, in the autumn of 2011, the simulated LGTs rose more slowly to the field surface compared to the observed levels.

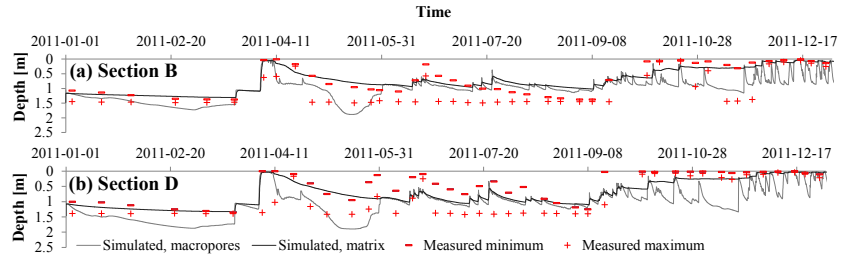

Figure 18. Average simulated groundwater depths in soil macropores and matrix, and measured minimum and maximum depths in field Sections (a) B and (b) D of the Nummela experimental site in the calibration period 1 Jan – 31 Dec 2011. (Paper II)

As in Paper II, evapotranspiration was the dominant water balance component (48% of precipitation) in the whole field area (Sections A–E, Figure 3) during the calibration period (1 Jan 2011 – 31 Dec 2011). Drain discharge was 20% of precipitation, flow to ditches 18% of precipitation, groundwater outflow 15% of precipitation, and storage change 7% of precipitation.

During the model validation period (6 May 2008 – 31 Dec 2009), the correspondence of simulated and observed hourly drain discharges were comparable to calibration with the N-S_m values of 0.51 and 0.38 in Sections B and D, respectively. The D values of drain discharge were in the same order of magnitude as during calibration in the autumn periods of 2008 (1 mm in Section B and 10 mm in Section D) and 2009 (-5 mm in Section B and 10 mm in Section D). The model overestimated most outflow events in the spring 2009, probably due to the inaccuracies in the TLR measurements and the slightly inaccurate amount and timing of simulated maximum SWE during the winter period (Figure 19).

During the validation period, the cumulative corrected precipitation was 1023 mm. Compared to calibration, evapotranspiration increased to 55% of precipitation, drain discharge decreased to 15% and flow to ditches to 10%, while groundwater outflow (15%), and storage change (6%) compared to validation in the whole field area (Sections A–E). In Section D, during the validation period, the D values of TLR (22 mm in autumn 2008, 32 mm in spring 2009, and -15 mm in autumn 2009) were comparable to calibration. In Section B, TLR measurement devices did not function in autumn 2008. During the spring 2009 the simulations underestimated the observed amount likely due to measurement problems similar to those during the spring 2011. In Section B in the autumn 2009, both simulated and observed amounts of TLR were 0 mm. During validation, the simulations reproduced the observed LGT values qualitatively similarly as during the calibration period. Simulated LGT values resided between the observed minimum and maximum values 73% and 46% of the time in Section D and Section B, respectively.

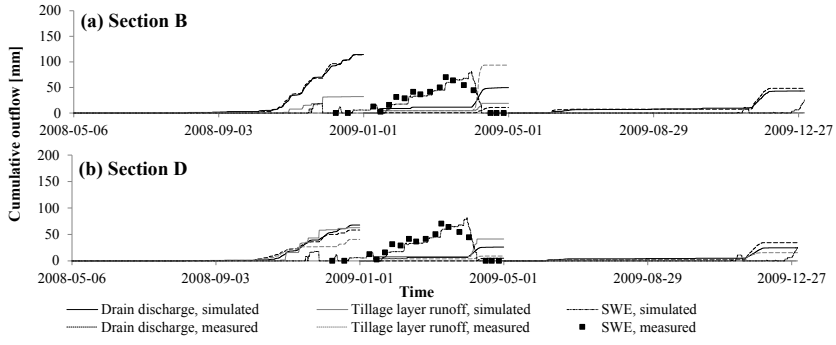

Figure 19. Simulated and measured snow water equivalent (SWE), and cumulative simulated and measured drain discharge and tillage layer runoff in field Sections (a) B and (b) D of the Nummela experimental site in the validation period 6 May 2008 – 31 Dec 2009. (Paper II)

3.2.2 Evapotranspiration scenarios

The simulations were run with the three different PET estimates (see Section 2.3). PET_{ClassA} and PET_o estimates resembled each other with a difference of 3% (sums from May–Dec in 2008–2009 and 2011) (Figure 20). Since the Class A observations were available annually only from 1 May onwards, the measurements before the date were replaced with the PET_o estimate. Accumulations of the three different PET estimates and PET_o in 2008–2009 are shown in Figure 20. PET calculated with the MACRO model is shown for reference. PET_{ClassA} resulted in the highest annual evapotranspiration of the tested approaches. PET_{o7} (calibrated constant crop coefficient) gave the lowest estimate. PET calculated with the MACRO model was found to qualitatively resemble the PET_o estimate, except for the late autumn periods (Figure 20). The hourly and daily simulated and measured radiation components and PET_o values are shown in Annex II.

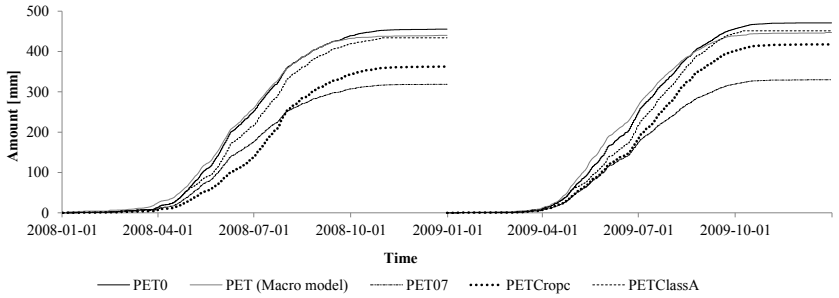

Figure 20. Accumulated potential evapotranspiration estimated with different methods at the Nummela experimental site in 1 Jan 2008 – 31 Dec 2009. (Paper II)

The magnitude of the PET had a direct impact on the simulated water outflow components of the studied field sections (Figure 21). When the model was run with PET_{Cropc} or PET_{ClassA} estimates, the simulated drain discharge events during early autumn periods occurred later than the measured events in 2008 and 2011 and were low compared to the measured values in 2009 (Figure 21). Additional tests (not shown) suggested that recalibration of the model parameters (θ_s and macroporosity below the subsurface drain depth and root growth speed and development stages) did not improve the correspondence of the simulated and observed events in the autumn periods of 2008 and 2011 with the relatively high PET estimates. The different PET estimates had a lower impact on TLR than on drain discharge, but the lowest PET estimate (PET_{o7}) resulted in the highest TLR during all autumn periods (Figure 21). Overestimation of the simulated TLR in Section D during autumn periods of model calibration and validation were likely caused by underestimated PET during the late growing season or autumn periods. A comparison between simulated and observed LGTs revealed that during the growing seasons simulations with PET_{Cropc} and PET_{ClassA} produced a closer correspondence with the observations than with PET_{o7}. However, simulations with PET_{Cropc} and PET_{ClassA} resulted in low simulated LGTs compared to the observations during the autumn periods.

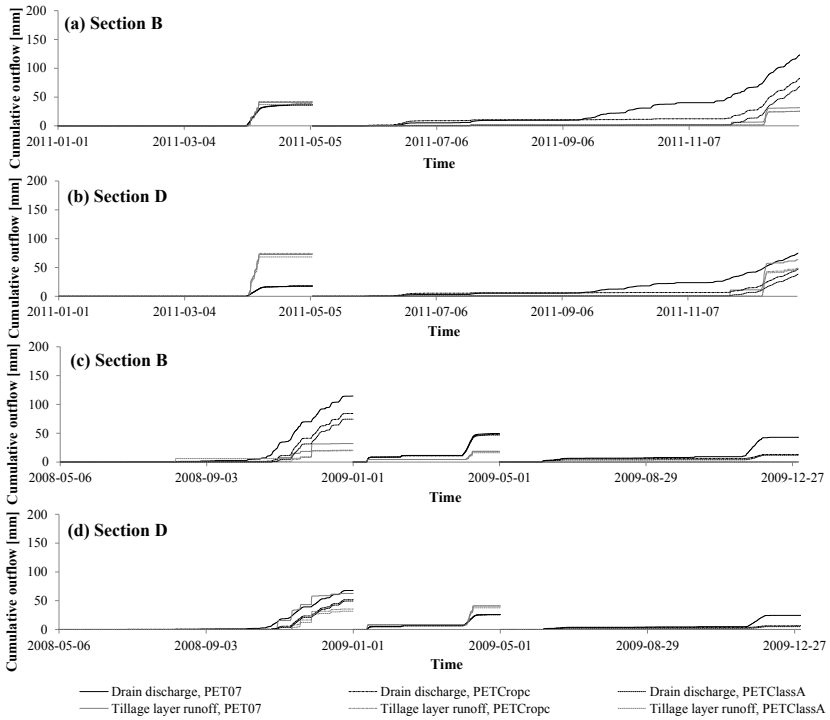

Figure 21. Accumulated simulated drain discharge and tillage layer runoff results with different evapotranspiration estimation methods in field Sections (a) B and (b) D of the Nummela experimental site in Jan – Dec 2011 as well as (c) B and (d) D in May – Dec 2009. (Paper II)

Even though the range of tested PET estimates in the validation period (2008–2009) was 595–818 mm and the range of actual evapotranspiration was 547–666 mm, the amount of groundwater outflow with the different evapotranspiration rates varied only between 127 and 157 mm (Table 11). The results demonstrate that evapotranspiration and groundwater outflow are interlinked, but changes in the evapotranspiration estimate are only partly reflected in the estimate of the amount of groundwater outflow. The magnitude of PET had a higher relative impact on all other water outflow components (from -31% to -23%) than on groundwater outflow (-19%) in 2008–2009. Note also that evaporation from snow cover (13 mm) comprised only a relatively small fraction of the water balance (1% of precipitation).

Table 11. Components of the simulated water balance [mm] with different potential evapotranspiration estimates at the Nummela experimental site during the validation period 6 May 2008 – 31 Dec 2009. (Paper II)

	PET_{07}	PET_{Cropc}	PET_{ClassA}
Precipitation	1023	1023	1023
Potential evapotranspiration	595	741	818
Actual evapotranspiration	547	647	666
Evaporation from snow cover	13	13	13
Flow to open ditches	105	83	81
Drain discharge	157	117	108
Groundwater outflow	157	137	127
Change of storage	59	40	42
Mass balance error	-13	-15	-13

3.3 Paper III: Effects of terrain slope on long-term and seasonal water balances

In this application, the model was applied in two field sections with the slope of 1% and 5% at the Gårdskulla Gård experimental site (Section 2.4.2.1). Long-term simulations were conducted to assess the seasonal and annual differences in the water balances of the sections. A simulation scenario was conducted to assess the impacts of water influx to the monitored area from the upslope area of Section 1. A scenario was also conducted to assess the impacts of the chosen topography of the impermeable bottom boundary condition on the simulation results (Figure 11).

3.3.1 Calibration and validation

The model calibration (2008–2010) resulted in the model evaluation criteria presented in Table 12, which indicated a correspondence between the dynamics of simulated and observed variables. In terms of the criteria (Table 12), model performance during the validation period (2011–2012) was comparable to calibration. Regarding the magnitude of the components, in Section 2, the D value of drain discharge was -40 mm during calibration and 57 mm during validation. For reference, precipitation during the calibration and validation was 3662 mm.

The higher D value during validation than during calibration in Section 2 was likely caused by underestimating TLR (-104 mm during validation) during the spring 2012 (Figure 22c). During the calibration period in Section 2, the D value of TLR was -21 mm. The difference between the simulated and measured accumulated TLR during the spring of 2012 was likely caused by the soil frost impact on water infiltration, which was not taken into account in the model structure.

In Section 1, where the adjacent hill area was presumed to induce an influx of water to the field area, the D values of drain discharge were low (-169 mm during calibration and -226 mm during validation) compared to Section 2, which demonstrated the need to include the uphill contributing area to the simulations. The hydrological impact of the uphill boundary condition was further assessed in the simulation Scenario 2 (Section 3.3.2). The D value of TLR was -60 mm and -59 mm during calibration and validation, respectively. As shown in Figure 22a, the

D value of TLR was particularly high during the spring snowmelt period 2010 in Section 1, which was assumed to be due to the frost-induced changes in the soil hydraulic properties. In contrast to Section 2, the difference between the simulated and measured TLR during spring 2012 was comparable to the other spring periods (except for spring 2010).

Table 12. Modified Nash-Sutcliffe coefficient (N-S_m) and mean absolute error (MAE) for the calibration and validation periods. Average absolute deviation of measurement results are in parentheses. (Modified from Paper III)

		Calibr. Section 1	Calibr. Section 2	Valid. Section 1	Valid. Section 2
N-S_m	DD [-]	0.5	0.55	0.45	0.44
	TLR [-]	0.45	0.43	0.5	0.54
MAE	DD [mm]	0.02 (0.04)	0.02 (0.04)	0.03 (0.06)	0.03 (0.04)
	TLR [mm]	0.003 (0.005)	0.003 (0.005)	0.004 (0.008)	0.007 (0.015)
	SWE [mm]	30.65 (45.00)	22.85 (44.75)	24.36 (21.50)	19.78 (16.38)
	GW_{mt} [m]	0.27 (0.17)	0.42 (0.42)	0.26 (0.13)	0.35 (0.36)
	GW_{mc} [m]	0.11 (0.17)	0.34 (0.42)	0.10 (0.13)	0.33 (0.36)

DD = Drain discharge.
TLR = Tillage layer runoff.
SWE = Snow water equivalent.
GW_{mt} = Level of the groundwater table in soil matrix (median of monitoring tubes 1–3).
GW_{mc} = Level of the groundwater table in soil macropores (median of monitoring tubes 1–3).

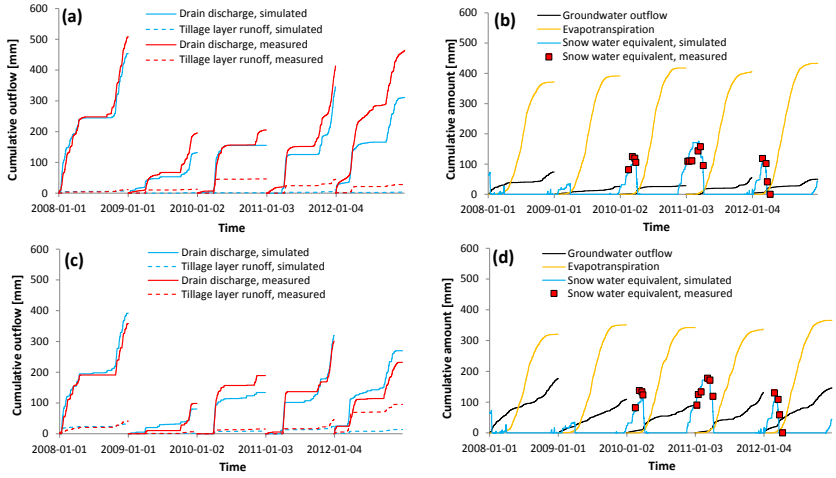

Figure 22. Annual dynamics of the accumulated water balance components in field sections (a–b) 1 and (c–d) 2 during the model calibration (2008–2010) and validation periods (2011–2012) at the Gårdskulla Gård experimental site. (Paper III)

The simulated long-term water balance components are presented in Table 13. In this application, groundwater outflow was defined as the seepage of water into the Kirkkojoki stream below the other drainage systems (subsurface drains and open ditches). Drain discharge and groundwater outflow were the dominant outflow components in both field sections in 2008–2012 (Figure 22). The amount of groundwater outflow was 419 mm (178%) higher in Section 2 (slope 5%) than in Section 1 (slope 1%). Correspondingly, drain discharge was 181 mm lower in Section 2 than in Section 1. Evapotranspiration dominated the water balance in both field sections (Figure 22, Table 13), and flow to open ditches comprised only 4–6% of the water balance. The amount of actual evapotranspiration was higher in Section 1 (57% of precipitation), than in Section 2 (49% of precipitation) and the difference was explained by the low LGT and low root zone soil moisture in the upper parts of the steep Section 2, which limited the amount of evapotranspiration in the area.

Table 13. Simulated water balance components from 1 Jan 2008 to 31 Dec 2012 at the Gårdskulla Gård experimental site. (Paper III)

	Proportion of precipitation [%]		Amount [mm]	
Year	2008–2012		2008–2012	
Field section	1	2	1	2
Precipitation	100	100	3662	3662
Evapotranspiration	56.9	48.6	2085	1780
Flow to open ditches	4.3	5.5	156	201
Drain discharge	34.1	29.2	1250	1069
Groundwater outflow	6.4	17.9	235	654
Change of storage	-0.9	-1	-35	-37
Mass balance error	-0.8	-0.2	-29	-6

Figure 23 presents the simulated water balance components during spring (1 Mar – 31 May), summer (1 Jun – 31 Aug), autumn (1 Sep – 30 Nov) and winter (1 Dec – 28/29 Feb) seasons in both of the field sections. Evapotranspiration dominated the water balance during summer periods, but was relatively low during autumn and winter periods, and varied less than the other studied components. During the winter seasons, the dominating water balance components were drain discharge, SWE and groundwater outflow. During the spring and autumn seasons the water balance was more evenly distributed to different components (Figure 23). The variation in the amount of drain discharge was higher than the variation of the other water balance components during all seasons except summer, when the amount of drain discharge was minimal. Moreover, as shown in Figure 22 and Figure 23, the subsurface flow components exceeded the amount of TLR during all studied seasons and years.

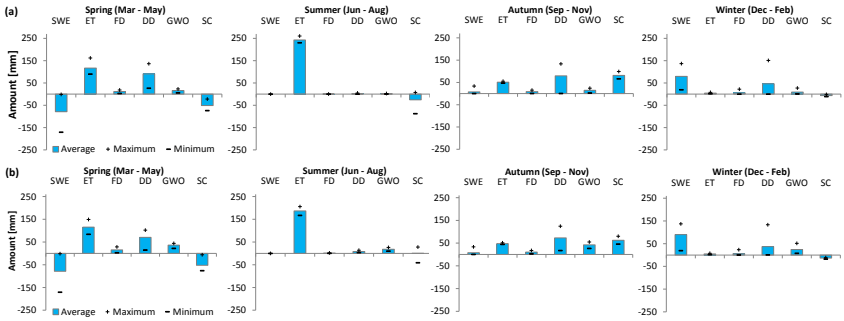

Figure 23. Simulated seasonal water balance components and their variation in 2008–2012 in (a) Section 1 (slope 1%) and (b) Section 2 (slope 5%) of the Gårdskulla Gård experimental site. SWE = snow water equivalent, ET = evapotranspiration, FD = flow to open ditches, DD = drain discharge, GWO = groundwater outflow, SC = soil water storage. (Paper III)

During the winter periods with a permanent snow cover on the ground and minimal evapotranspiration, LGT was often observed to decline below the drain depth in Section 2 (slope 5%) (Figure 24). This supports the simulation results of the occurrence of groundwater outflow in the deep soil layers, since during the time periods when LGT resided below the drain depth, other outflow pathways (subsurface drains and open ditches) remained inactive. In Section 1 (slope 1%), LGT stayed approximately at the drain depth during these time periods (Figure 24), which is in line with the simulation results showing a lower amount of groundwater outflow in Section 1 than in Section 2. Figure 24 presents also the simulated LGTs in the monitoring tubes 1–3 (see Figure 4). The observed LGT was constantly the lowest in the monitoring tubes located closest to the Kirkkojoki stream (tube 1 in Sections 1 and 2, Figure 4). In these locations, the differences between the observed and simulated LGTs were higher than in the locations of tubes 1 and 2 (Figure 23). This indicated that the hydrogeological assumptions related to the horizontal homogeneity of the soil properties and the topography of the impermeable bottom boundary were not valid in the vicinity of the stream. The hydrological impacts of the topography of the impermeable bottom boundary condition were further assessed with a simulation scenario (Section 3.3.2).

A correspondence was observed between the temporal variation of TLR and LGT, which suggested that near-saturated soil surface conditions triggered most TLR runoff events.

The recession of both simulated and measured drain discharge peaks was longer in the flat Section 1 than in Section 2, which corresponded to the slower decline of LGT and lower amount of groundwater outflow in Section 1 than in Section 2. According to additional simulations tests, the differences in the soil hydraulic properties between the field sections did not explain the differences in the drain discharge recession. However, the influx of groundwater across the field borders might have also contributed to the slower recession in Section 1, and it was further assessed in a simulation scenario (Section 3.3.2).

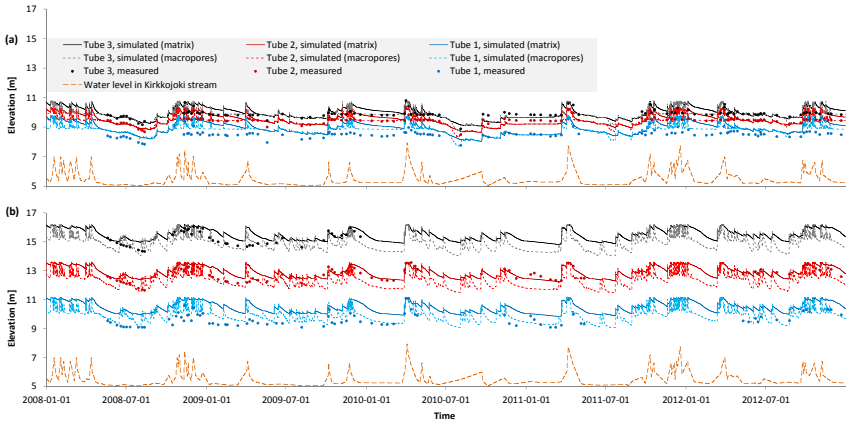

Figure 24. The measured and simulated (soil matrix and macropores) groundwater table elevations in monitoring tubes 1–3 (Fig. 1b) as well as the measured water level in the Kirkkojoki stream in (a) Section 1 and (b) Section 2 of the Gårdskulla Gård experimental site. (Paper III)

3.3.2 Simulation scenarios

In Scenario 1, the soil profile depth was set to gradually increase downslope towards the stream, as presented in Figure 11. The results of this simulation scenario showed that the water balance of Section 2 (slope 5%) was sensitive to the spatial difference in the depth of the conductive soil profile (Table 14). This change in the hydrogeological model structure decreased average LGTs, increased the amount of groundwater outflow, and decreased the amount of other outflow components (Table 14). In Section 1 (slope 1%), the profile depth change induced smaller changes to the LGTs and outflow components (Table 14) due to the lower terrain slope of the simulated field and lower macroporosity in the deep soil layers (see Table 3 in Turunen et al. 2015a). Scenario 1 did not provide an explicit explanation for the low LGTs observed in the monitoring tubes in the vicinity of the stream (tubes nr. 1, Figure 4), but the results from Section 2 (Table 14) indicated that the thicker depth of the conductive soil profile in the location of tube 1 would explain the phenomena.

In Scenario 2, the simulated area of Section 1 was extended south to the top of the adjacent hill area (Figure 4), as shown in Figure 11. The simulation results of this scenario showed an increase in the water outflow components of the field section due to the influx of water to the field area from the adjacent area (Table 14). The influx had the highest impact on flow to open ditches in the south border of the field and also a relatively high increase in the amount of drain discharge (Table 14). As presented earlier, in the model calibration and validation the simulated annual amount of drain discharge was systematically lower than the observed amount in Section 1 (Figure 22a). The influx of water across the field borders also provided an explanation for the difference during spring 2012 when the model mismatch was highest. The inclusion of the water influx to the field also improved the correspondence of observed and simulated drain discharge values during recession of the peak values. Due to the change in model structure, the N-S_m values

increased from 0.45–0.5 to 0.52 in 2008–2010 and also in 2011–2012. However, the accumulated amount of drain discharge increased even above the observed amount, which indicated that the calibrated macroporosity value in the soil layers beneath the subsurface drain depth (1 m) was too small. According to additional tests (not shown), a higher macroporosity value in the soil layers beneath the drain depth would decrease the amount of drain discharge and increase groundwater outflow.

Table 14. Change of water balance components (outflow volume) and level of the groundwater table in simulation Scenario 1 (soil profile depth increases gradually from upslope to downslope) and 2 (extended field area) compared to model calibration and validation (2008–2012) at the Gårdskulla Gård experimental site. (Paper III)

	Scenario 1		**Scenario 2**
	Change [%]		Change [%]
Field section	1	2	1
Flow to open ditches	-1	-57	66
Drain discharge	-2	-27	37
Groundwater outflow	11	68	1
Average level of the groundwater table (matrix)	-3	-58	0
Average level of the groundwater table (macropores)	-1	-46	0

3.4 Paper IV: Sediment balances and structural uncertainties in sediment transport models

In this application, the erosion and sediment transport model was applied on top of the hydrological model derived from Paper III (Section 2.4.2.2). Three different model structures (Models A–C) with different assumptions of subsurface sediment connectivity were applied to assess structural uncertainties in sediment transport models and to quantify erosion processes, sediment balances and transport pathways.

3.4.1 Calibration and validation

Models A–B (Figure 12) resulted in a comparable correspondence against the observed values in terms of the evaluation criteria (Table 15). These models were also able to reproduce the distribution of sediment load to TLR and drain discharge components (Figure 25). In both field section and models during calibration, the D values of load via drain discharge were from -7% to 3% of the observed drain discharge loads, which demonstrates a correspondence with the observed values. The D values of TLR loads were comparable to the drain discharge load D values during calibration (Table 15).

Table 15. Results of the model evaluation criteria during the model calibration and validation period in Sections 1 (slope 1%) and 2 (slope 5%) with the Models A, B and C. (Paper IV)

			Model	Accumulated load D [kg ha^{-1} a^{-1}]	Accumulated load M [kg ha^{-1} a^{-1}]	Load N-S_m [-]
Calibration	Drain discharge	Section 1	A	21	1418	0.21
			B	40	1418	0.21
			C	-6	1418	0.29
		Section 2	A	-61	2416	0.13
			B	-181	2416	0.18
			C	-923	2416	0.30
	Tillage layer runoff	Section 1	A	-6	54	-0.26
			B	-5	54	-0.27
			C	238	54	-6.51
		Section 2	A	-80	232	-0.42
			B	-82	232	-0.40
			C	-168	232	-0.47
			Model	Accumulated load D [kg ha^{-1} a^{-1}]	Accumulated load M [kg ha^{-1} a^{-1}]	Load N-S_m [-]
Validation	Drain discharge	Section 1	A	-25	382	-0.30
			B	-13	382	-0.34
			C	-119	382	-0.15
		Section 2	A	100	469	0.63
			B	76	469	0.68
			C	-153	469	0.79
	Tillage layer runoff	Section 1	A	-28	29	-0.26
			B	-28	29	-0.26
			C	-27	29	-0.24
		Section 2	A	-48	74	0.15
			B	-49	74	0.14
			C	-51	74	0.12

D = difference between the simulated and measured annual accumulations.
M = measured annual accumulation.
N-S_m = the modified Nash-Sutcliffe coefficient.

In contrast to Models A–B, the simulated loads with Model C did not correspond to the magnitude of the observed loads (Table 15, Figure 25). Model C underestimated the load via drain discharge by -923 kg ha^{-1} a^{-1} (-38%) in Section 2 (slope 5%) and overestimated the load via TLR by 238 kg ha^{-1} a^{-1} (441%) in Section 1 (slope 1%). Since the differences were high compared to Models A–B, Model C was not considered as a plausible representation of the transport processes. However, in Model C the simulated drain discharge load in Section 1 corresponded to

the observations qualitatively similarly as the results of Models A–B (Table 15). The results suggest that due to the differences in the hydraulic gradient and the higher amount of groundwater outflow, lateral fluxes had a bigger role in sediment transport in the steep field section compared to the flat field section.

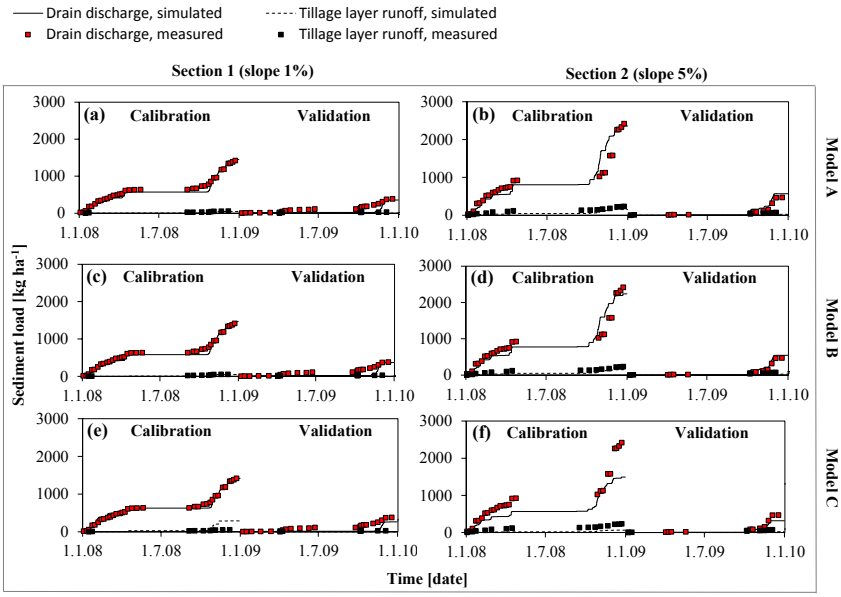

Figure 25. Measured and simulated accumulated annual sediment loads via drain discharge and tillage layer runoff during the calibration and validation periods of (a) Model A in Section 1, (b) Model A in Section 2, (c) Model B in Section 1, (d) Model B in Section 2, (e) Model C in Section 1 and (f) Model C in Section 2 of the Gårdskulla Gård experimental site. (Paper IV)

As shown in Table 15 and Figure 25, the D values of drain discharge and TLR during validation were comparable to those of calibration. During the entire studied period, most of the load occurred outside the growing season and most of the load occurred via drain discharge in both field sections (Figure 25).

Regarding drain discharge load dynamics during calibration, the positive N-S_m values (0.13–0.21) in Models A–B indicate a correspondence between the simulated and observed temporal variations in load generation. In Section 2, the model reproduced the load dynamics more accurately during the validation period (N-S_m values 0.63–0.68) than during calibration (N-S_m values 0.13-0.18). In Section 1, the N-S_m values for drain discharge load dynamics with Models A–B were negative during validation. However, the MAE between the simulated and measured values was lower during validation (18–19 kg ha^{-1}) than during calibration (26 kg ha^{-1}) in Section 1. Thus, the negative values were caused by low variability of the loads during the validation period (Figure 25). Furthermore, the model performance was generally better during high loads than during low loads, as also demonstrated by the negative N-S_m values of TLR load dynamics (Table 15).

Regarding TSS concentration, the N-S_m values of drain discharge and TLR dynamics were all negative. When those simulated concentrations which occurred

during the time periods that generated a minor share of the loads (concentration <20 g m^{-3} and <1% of the load) were neglected, the average measured TSS concentrations (228 g m^{-3} in Section 1 and 480 g m^{-3} in Section 2) in drain discharge were comparable to the simulated values (206–207 g m^{-3} in Section 1 and 506–521 g m^{-3} in Section 2 with Models A–B) during the entire studied period. Also the simulated (338–341 g m^{-3} in Section 1 and 802–810 g m^{-3} in Section 2 with models A–B) and measured (456 g m^{-3} in Section 1 and 851 g m^{-3} in Section 2) mean TSS concentrations in TLR were on the same order of magnitude. The correspondence of the simulated and observed TSS concentration levels explains the capability of the model to reproduce the observed loads, since the simulated and measured drain discharge (D 6–37 mm or 1–5% of measured discharge) and TLR (D -23 to -6 mm or -49 to -26% of measured TLR) were comparable during the studied time period.

3.4.2 Sediment balances and sensitivity analyses

The simulated sediment balance and load components with the three model structures (A–C) are shown in Table 16. As presented also in Figure 26, load via subsurface drains dominated the loads with all of the applied models and in both field sections. The simulation results from Model A and B also suggested that 8–9% of the load occurred via seepage to open ditches and 10–21% via groundwater outflow (seepage flux into the Kirkkojoki stream). Due to the higher amount of groundwater outflow in Section 2 (slope 5%) than in Section 1 (slope 1%), the load via groundwater outflow was higher in the steep field section. In the simulations, the majority of the detached particles at the soil surface infiltrated the subsurface domains (Table 16). Load via overland flow composed the lowest load component in the simulations and the majority (>80%) of the load via overland flow was collected by the Kirkkojoki stream. Simulation results from Model C are shown for reference in Table 16 and Figure 26.

The amount of eroded sediment with Models A and B (3104–3317 kg ha^{-1} a^{-1} in Section 1 and 3879–4171 kg ha^{-1} a^{-1} in Section 2) was higher than the simulated sum of the load components (1028–1077 kg ha^{-1} a^{-1} in Section 1 and 1756–2022 kg ha^{-1} a^{-1} in Section 2) (Table 16). Sediment retention and deposition on the field surface removed 37–52% and 10–18%, respectively, of the eroded sediment in the simulations. With Model C the amount of retained sediment was even higher (Table 16), since the sediment infiltrating the subsoil domain between the drain lines was not transported horizontally in the simulations, and thus it did not form load. Note also that the simulated load with the Model C were partly not consistent with the load data and thus the sediment balance simulation results with Model C may not be physically plausible.

Table 16. The simulated mean annual sediment balance components [kg ha^{-1} a^{-1}] in Sections 1 and 2 with Models A–C at the Gårdskulla Gård experimental site. (Paper IV)

	Model	A	B	C
Section 1 (slope 1%)	Erosion	3104	3317	11312
	Deposition (field surface)	560	561	1168
	Infiltration to the soil	2486	2698	9957
	Retention	1467	1729	9164
	Overland flow	58	58	187
	Seepage to open ditches	88	90	52
	Subsurface drains	770	773	737
	Groundwater outflow	161	107	5

	Model	A	B	C
Section 2 (slope 5%)	Erosion	3870	4171	12527
	Deposition (field surface)	410	433	695
	Infiltration to the soil	3327	3604	11595
	Retention	1439	1983	10715
	Overland flow	134	134	238
	Seepage to open ditches	167	147	74
	Subsurface drains	1288	1201	785
	Groundwater outflow	433	274	20

In the simulations, the higher amount of erosion and load in Section 2 compared to Section 1 (Table 16) was explained by differences in soil hydraulic properties of the topsoil layers of the field sections. Particularly the difference in macroporosity of the topsoil promoted more rapid water infiltration to the subsurface domain in Section 2 than in Section 1, and thus in Section 1 the overland water had a higher protective impact against the erosive force of the raindrops (Eq. 6).

The sensitivity analysis, where the calibrated parameter values were altered by +20% and -20%, demonstrated that the parameter changes had the highest impact on load via subsurface drains (Figure 26). As shown in Figure 26, the model structure selection (Model A vs. Model B) had a higher impact on the groundwater outflow component than the parameter alterations.

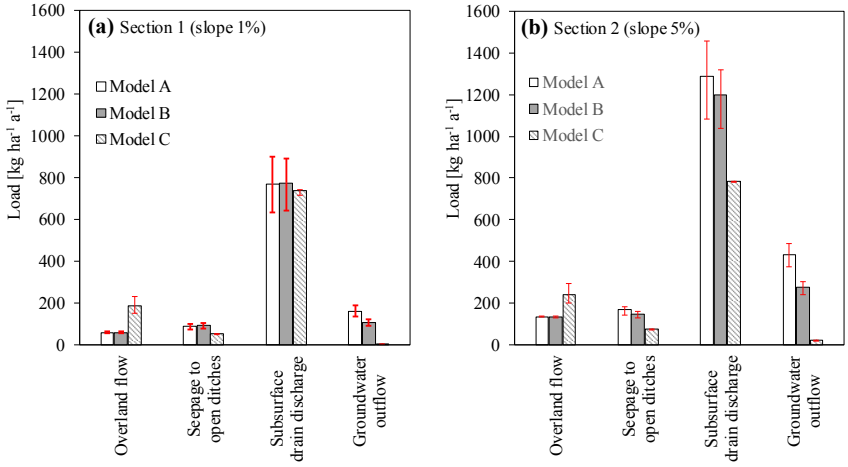

Figure 26. The simulated mean annual sediment load components computed with Models A–C in (a) Section 1 and (b) Section 2 of the Gårdskulla Gård experimental site. The error bars denote the minimum and maximum loads from the parametric sensitivity analysis, where parameters values were increased and decreased by 20%. (Paper IV)

The simulation scenario where Section 1 was simulated with the soil hydraulic parameters of Section 2, and vice versa, was conducted to study the sensitivity of the model to the soil parameters. The water flow model was found to be less sensitive to the soil parameterization than the erosion and sediment transport model (Figure 27). The erosion and sediment transport model was the most sensitive to the changes in soil macroporosity.

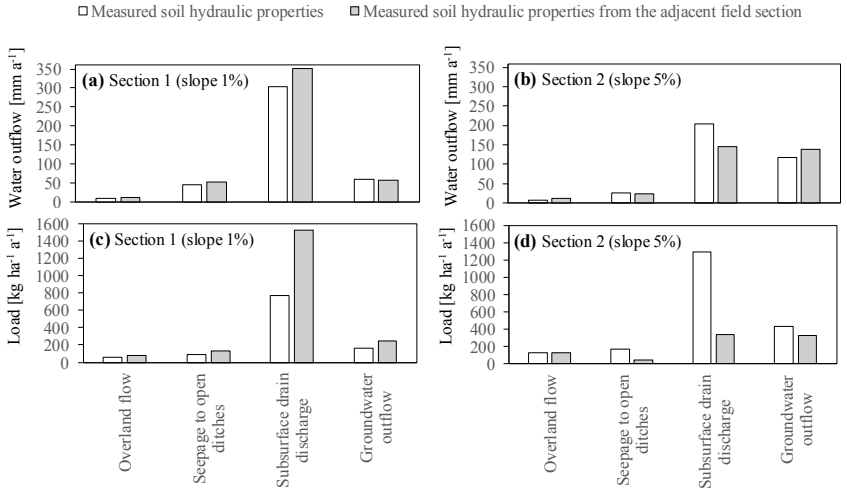

Figure 27. Simulated mean annual water outflow components (Model A) in (a) Section 1 and (b) Section 2 and simulated sediment load components in (c) Section 1 and (d) Section 2 with the measured soil hydraulic properties swapped between the field sections in the Gårdskulla Gård experimental site. (Paper IV)

4. Discussion

4.1 Water flow and drainage

The field-scale datasets and 3D simulations covered a range of experimental conditions, including different drainage methods, terrain topographies and hydrometeorological circumstances. The results produced a rare computational closure and a quantification of the water balance in clayey high-latitude agricultural fields. During the growing seasons, evapotranspiration dominated the annual water balance in all studied conditions, and clearly most of the water outflow occurred outside the growing season. Drain discharge was the largest water balance component during the dormant seasons and also showed the highest interannual variation of the water balance components. Groundwater outflow in the deep soil layers beneath the drain depth stayed active also during the growing seasons and formed the largest outflow component during the studied summer periods. The magnitude of the subsurface outflow pathways exceeded the amount of TLR. As noted previously by Deelstra et al. (2009), a major share of annual water outflow can occur during winter seasons in high-latitude conditions. The results of this thesis also demonstrated how water balance components can be distributed during winter periods and that drain discharge may typically form the highest outflow component during winter seasons.

The water balance components of this study can be compared against previous studies, although such studies typically consider only drain discharge and TLR. Turtola et al. (2007) observed drain discharge to be on average 25% of precipitation in a field with heavy clayey soil and a slope of 2% in southern Finland. Bechmann (2012) observed on average 27% of precipitation to form drain discharge in a silt soil in southern Norway. A monitoring study by Øygarden et al. (1997) showed that 24% of precipitation converted to drain discharge in a silty clay loam soil with a slope of 8–9% in southern Norway. Jin and Sands (2003) noted that drain discharge was 30–40% of precipitation in a field with a clay loam soil in southern Minnesota. In the conditions of the current study, the observed drain discharge component was 18–34% of precipitation, being the highest in the flat field section of Gårdskulla Gård and lowest at the Nummela site. The relatively low proportion of drain discharge in the Nummela field was due to the wide drain spacing (approximately 32 m) in Section D and groundwater outflow via the adjacent steep slope. At the Nummela site, the magnitude of the drain discharge component was the lowest in the poorly drained Section D (10%) and highest in Section C (32%). As compared to the previous studies, the magnitude of the observed drain discharge component in the studied fields of the current study can be considered typical for high-latitude conditions.

The amount of subsurface outflow exceeded the amount of TLR in the conditions of the current study. The proportion of drain discharge to the sum of TLR and drain discharge (DD/TD) values was observed to be 0.85–0.93 in the field sections of Gårdskulla Gård and 0.53–0.87 in the sections of the Nummela site. Previously, Seuna and Kauppi (1981) observed DD/TD of 0.77 in a clayey field in southern Finland. Uusitalo et al. (2007) reported DD/TD values of 0.5–0.8 in subdrained field plots with heavy clayey soil. Bechmann (2012) reported a value of 0.77 and Øygarden et al. (1997) a value of 0.49 in an agricultural field in Norway. Also Jin and Sands (2003) reported clearly higher drain discharge than TLR amounts in long-term simulations in Minnesota. Compared to these previous studies, the measured amount of drain discharge and DD/TD values appeared to be partly higher than in the previous studies but are likely representative for a range of well-drained high-latitude clay soils.

The results of this thesis showed that groundwater outflow can form a major water balance component in clayey fields. Even though previous simulation studies (e.g. Hintikka et al. 2008; Gärdenäs et al. 2006; Larsson and Jarvis 1999; Mohanty et al. 1998) suggested that groundwater outflow may impact the hydrology of clayey fields, the quantification of the seasonal and long-term amount of groundwater outflow has not been previously conducted. The results suggested that groundwater outflow can be active even in relatively flat fields with a slope of ≥1%. The magnitude of groundwater outflow was shown to be controlled by the terrain slope and the topography of the underlying impermeable bottom boundary. An increase in terrain slope was found to result in a decreased amount of drain discharge due to the increased amount of groundwater outflow. The results demonstrate that in this sense the hydrological impact of the terrain slope in structured soils can be analogous to the impact of the slope in frictional soils (Fipps and Skaggs 1989). Thus, as demonstrated in Paper I and III, steep field sections typically require less efficient subsurface drainage methods than flat sections or sections located adjacent to a slope. Furthermore, the studied fields were shown to share a hydrological connection with the surrounding areas through groundwater flow, and this connection was found to impact the water balances of the fields. In practice, the results indicate that field topography as well as the topography of the surrounding field areas should be taken into account when designing drainage systems for sustainable and productive crop production. Such connections should also be taken into account in empirical paired catchment studies (e.g. Äijö et al. 2014; Seuna and Kauppi 1981) and the hydrological impacts of connectivity via groundwater outflow have not been previously quantified on a field and field section scale in structured soils. Even though the studied range of terrain slopes was representative of the majority of Finnish agricultural fields, the studied range was partly limited when compared with the wide range of terrain slopes in the high-latitude areas. However, the results conceptualize the slope impact on lateral preferential flow processes and can be considered to be applicable also in areas with a higher slope.

As shown in previous studies (e.g. Appels et al. 2011), field areas can also share a lateral hydrological connection through overland flow. In the current study the amount of overland flow was smaller than the amount of groundwater outflow,

and thus the hydrological connection of groundwater flow was shown to have a higher impact on the water balance than surface runoff. Based on the results, this can be assumed to be a common feature in well-drained high-latitude clayey fields where subsurface outflow pathways dominate. Furthermore, open ditches are a common and relatively easy method to direct surface runoff, whereas groundwater outflow is more difficult to control and quantify.

In order to improve the understanding of hydrological processes of clayey agricultural fields, it would be beneficial to further study the soil hydraulic properties and preferential flow paths in the deep soil layers beneath the subsurface drains. A few empirical studies (Kessler et al. 2012; Yli-Halla et al. 2009; Knud and Gravesen 1999) have demonstrated that lateral preferential flow paths, such as layers of coarse material embedded in the soil matrix, can reside in the deep soil layers. As pointed out by Nielsen et al. (2010), vertical macropores can also be directly connected to lateral preferential flow paths, which allow a rapid flow of water from the field surface to the horizontal pathways. Lorente and Bejan (2006) and Sidle et al. (2001) also suggested that preferential flow paths can have a tendency to self-propagate in the down-slope direction. Kessler et al. (2012) further noticed that sand lenses embedded in clayey soils can be discontinuous. However, Nieber and Sidle (2010), who simulated water flow in a soil with disconnected macropores in 3D, noticed that even disconnected preferential flow pathways can form preferential flow networks in saturated soils. Based on the literature, it can be assumed that the groundwater outflow in clayey fields is generated in lateral and partly discontinuous preferential flow paths. A comprehensive understanding of the groundwater outflow generation processes in high-latitude clayey fields would require detailed observations of the subsoil hydraulic properties. The results of this thesis demonstrate that understanding the role of the different subsoil hydraulic properties in water balances would further benefit of 3D hydrological model applications, which have rarely been conducted before in high-latitude clayey soils. Also, it would be worthwhile to consider the validity and importance of the fill and spill hypothesis (Tromp-van Meerveld and MacDonnell 2006), which suggests a threshold-like response to subsurface outflow generation.

In addition to groundwater outflow, terrain topography is known to affect surface runoff generation (Appels et al. 2011; Freer and Bay 1969), although soil frost and farming operations also have an impact on its generation (e.g. Turtola et al. 2007; Stähli et al. 2001). Stähli et al. (1996), who simulated water flow in frozen structured soil, noted that if soil was not saturated during freezing, soil preferential flow paths stayed air-filled and conducted water effectively during snowmelt. This suggests that even though frost can have an impact on surface runoff generation in clayey fields (Seuna and Kauppi 1981), the potential may be lower in well-drained fields. Hydrological processes during snowmelt, however, are highly complex and infiltration of meltwater is also affected by preferential flow paths in the snowpack (Waldner et al. 2004). Infiltration into frozen soil can be also spatially highly variable and dependent on the soil micro-topography (French 1999). Soil frost can also have an impact on soil hydraulic properties and pore size distribution (e.g. Lundin 1990). Furthermore, formation of an ice layer on the soil surface

or topsoil layer can also affect infiltration of water to the soil profile during snowmelt (Jones and Pomeroy 2001). In this thesis, the simulated TLR with the model that excluded the frost-induced impacts on water flow were compared to the TLR observations in order to assess the frost-induced impacts on water balance. The results suggested that even though the impact of frozen soil conditions occasionally increased the amount of TLR, frozen soil conditions typically did not have a substantial effect on the distribution of the water balance component. However, the variation of observed TLR during those spring periods when frost affected TLR generation, was higher than the variation during other spring and autumn periods. The applied model without computational schemes of frost-induced impacts on water flow was able to reproduce the measured magnitude of the drain discharge during spring periods. The results suggest that despite the complexity of outflow generation during snowmelt periods, soil frost may typically have only a minor effect on the distribution of water balance components in well-drained structured soils with a slope of ≤5%.

It was also noted that annually TLR events were mostly triggered by the saturation-excess mechanism in the studied conditions, which is in line with the findings of Needelman et al. (2004), who studied surface runoff generation in Pennsylvania (USA). However, Needelman et al. (2004) were unable to study winter conditions due to equipment limitations. Even though there also were equipment limitations in the current study, the simulation and observations of this thesis suggested that TLR events were mostly triggered by a saturation-excess mechanism also during spring periods. Furthermore, although the field slope increased the amount of TLR, the terrain slope had a higher impact on the amount of groundwater outflow than TLR. The results have novelty value because the field slope impact on both groundwater outflow and TLR has not been previously studied simultaneously in high-latitude structured soils.

Although the effects of the changes in tillage operations were not included in the model, the model was able to reproduce the observed hydrological variables. This indicates that tillage operations may not have a high impact on the water balance components in well-drained soils, which is in line with the findings of the meta-analysis of Sun et al. (2015), who claimed that tillage does not have a significant impact on runoff generation in fields with a gentle slope (<5%) and high clay content (≥33% clay). In contrast to the findings of this thesis, Turtola et al. (2007) noted that tillage had a high impact on the distribution of water balance components in subsurface drained field plots with a heavy clay soil and a slope of 2%. It can be assumed that unknown site-specific features can cause differences in runoff generation under the impacts of tillage operations. Furthermore, as pointed out by Sun et al. (2015), the effect of tillage on runoff generation can be higher in fields with a moderate slope (5–10%). Also other factors, such as rainfall intensities are likely to have an impact on how surface runoff is generated under the influence of different soil tillage conditions.

The water balance simulations with different PET estimates suggested that the standard methods had limitations in describing evapotranspiration in the agricultural fields with a temporally varying crop cover. Even though the methods were

able to take into account various hydrometeorological variables and their temporal changes, the PET estimates had to be adjusted to adequately describe evapotranspiration in the applications. The crop coefficient approach (PET_{Cropc}) was capable of taking into account the temporal variations in crop cover, but led to an overestimation of the amount of evapotranspiration in the model. The calibrated constant crop coefficient approach (PET_{07}) appeared to adequately describe the amount of evapotranspiration in the model, as the simulated and observed discharges corresponded with each other after the growing seasons. However, the PET_{07} approach did not adequately describe the impact of the crop cover changes on PET. The results highlight the need to determine crop coefficients in high-latitude conditions, e.g. with empirical lysimeter data. It would be further beneficial to study the impacts of different stress factors on transpiration (e.g. Lhomme et al. 1998) and compensatory root water uptake processes (Jarvis 2011) in the evapotranspiration simulations. The simulations also showed that the magnitude of the evapotranspiration estimate had a higher impact on drain discharge and TLR components than on groundwater outflow. The climate change is expected to increase evapotranspiration rates in high-latitude conditions (e.g. Xu 2000). Johnsson and Jansson (1991) also noted that evapotranspiration in grass-covered fields can be clearly higher than in plots cultivated with barley. The results of this thesis can give an insight into how the increase in evapotranspiration due to climatic or land-use change can affect field water balances. The effects of increasing evapotranspiration on different outflow components have not been quantified previously in subdrained clayey high-latitude fields. Moreover, the results highlight the fact that outflow components during spring periods are practically unaffected by the evapotranspiration estimate.

The drain installation method was found to have an impact on drain discharge dynamics of the studied field sections. The trenchless installation method had a more pronounced impact on drain discharge dynamics than the trench installation method, which is line with the findings of previous studies in clayey soils (e.g. Boels 1978). However, the simulation results also suggested that, although the trenchless method lowered the peak drain discharge values, it also increased the length of drain discharge events. The impact of the drain installation method has been rarely studied in the context of field water balance. The results of this thesis suggest that the choice of drain installation method had a minor impact on the water balance of the clayey field. According to the simulations, drain spacing and terrain topography had a higher impact on drain discharge generation than the studied differences in the drain installation method, drain depth and envelope material. However, it should be noted that the installations in this study were conducted in dry soil moisture conditions and that the hydrological impact of drain installation in clayey soils is dependent on prevailing soil moisture conditions at the time of the installations (e.g. Spoor and Fry 1983). Furthermore, the impact of trenchless drain installation on soil hydraulic properties may be highest approximately for one year after the drainage and may gradually diminish during the following years (Olesen 1978).

4.2 Erosion and sediment transport

The results of this thesis underlined the fact that the largest portion of suspended sediment load in clayey agricultural fields can occur via subsurface drains. Also, many previous studies (Warsta et al. 2013b; Bechmann 2012; Turtola et al. 2007; Uusitalo et al. 2001; Øygarden et al. 1997) have observed subsurface drains to convey a major share of the loads from clayey fields in different hydrometeorological circumstances. Climate change is expected to reduce the amount of SWE (Räisänen et al. 2008) and to increase sediment loads in Finland (Puustinen et al. 2007); and the results of this thesis demonstrate how the loads may be distributed in conditions with low snow cover. Distribution of the loads to different components, including load via groundwater outflow, has not been previously quantified in subdrained high-latitude clay fields. Based on the results, it is suggested that sediment load studies and mitigation attempts should focus more on subsurface load pathways, even though methods to decrease subsurface loads may not currently exist. Previously, also Deasy et al. (2009) suggested that load mitigation should focus more on subsurface loads. While buffer strips at field boundaries can retain suspended sediment load from surface runoff (Uusikämppä and Jauhiainen 2010), the strips cannot have a high impact on total load when the majority of the load bypasses them via subsurface pathways.

In this thesis, three model structures (Models A–C, Figure 12) were applied to study sediment balances and suspended sediment transport pathways in the two field sections of the Gårdskulla Gård experimental site. The results demonstrated that lateral sediment transport was essential for describing subsurface sediment transport in the clayey soils. When lateral transport pathways were excluded in the subsurface domain in the model, the simulation results were inconsistent with the data. Previously Øygarden et al. (1997), who empirically studied erosion and sediment transport in a subdrained silty clay loam soil, also claimed that suspended sediment can be transported in soil profile via lateral and vertical transport pathways. The results of this thesis suggest that the effect of lateral connections on sediment transport was more pronounced in the steep field section (slope 5%) where the amount of groundwater flow was higher than in the flat field section. In the models where lateral transport was allowed (Models A and B), load via groundwater outflow formed 10–21% of the load in the field sections. The impact of slope on the load via groundwater outflow has not been quantified previously in high-latitude subdrained clay fields. As the impacts of different drainage and management methods on loads are often evaluated by monitoring subsurface drain discharge and TLR (e.g. Turtola et al. 2007; Øygarden et al. 1997), such a monitoring approach may result in a biased estimate of the impacts of the management methods on total loads when part of the load occurs via groundwater outflow.

Transport of suspended solids in soil is a complex process. In addition to continuous biopores (e.g. Nielsen et al. 2010) discontinuous macropores and the interface between the plough layer and the underlying soil profile can allow a preferential flow of water (Alberti and Cey 2011; Nieber and Sidle 2010; Haria et al. 1994) and thus also enable preferential transport pathways for small particles.

Transport of particles in the soil domain can also be impacted by sieving and retention processes (van den Bogaert et al. 2016; Burkhardt et al. 2008; Turtola et al. 2007; Jarvis et al. 1999), although the majority of TSS in drain discharge may be of colloid size and not sensitive to sieving (Ulén 2004). The computational approach of this thesis produced an estimate of the dominating components of the sediment balance, suggesting that the major share of detached particles stayed in the field and did not form load due to retention (Table 16). Even though the processes affecting load generation have also been studied previously, the quantification of the role of the different processes in sediment balances has been rarely conducted and therefore has novelty value. According to the simulations, a share (10–18% with Models A–B) of the eroded sediment also settled on the field surface and thus did not form load. However, it also needs to be noted that the results of this thesis apply particularly to well-drained fields with a slope of ≤5%. In areas with a steeper slope some processes, for example surface runoff and hydraulic erosion, may be more dominant, and induce dissimilar distribution of sediment components as compared to the results of this thesis.

The simulation results showed that the erosion and sediment transport model was highly sensitive to changes in soil hydraulic properties whereas the water model was clearly less sensitive to the changes (Figure 27). The sensitivity of the transport model to the changes in soil hydraulic properties was attributed particularly to the changes in soil macroporosity. In a previous empirical study Ulén et al. (2014) also noticed that the transport of substances in clayey soils can be highly sensitive to the characteristics of the soil structure.

4.3 Modelling water flow, erosion and sediment transport

FLUSH was found to be a useful tool in assessing the hydrological processes in clayey agricultural fields and it produced a closure of the water balance by describing the dominant water balance components. Moreover, the model was able to reproduce the magnitude and temporal variation of the observed hydrological variables in the various studied conditions. One of the benefits of the 3D modelling approach was the possibility to integrate different hydrological, soil and hydrometeorological data into a single modelling framework in the water balance assessment and to describe spatially varying hydrological processes more comprehensively than with the 1D and 2D approaches. The findings underline the necessity of including lateral flow processes in the structure of hydrological models if a comprehensive description of the water balance components is of interest. Even though previous modelling studies have indicated that lateral flow processes can have an impact on field hydrology (e.g. Gärdenäs et al. 2006; Mohanty et al. 1998), a computational estimate of lateral groundwater outflow in the water balance of clayey fields has not been previously conducted.

One of the main findings of the thesis was that different field areas can be hydrologically connected through groundwater flow processes, and hydrological processes of the fields can be linked to nonlocal processes. Water balance models

likely include structural uncertainty if they do not take into account such connections. This finding further indicates that in order to improve the accuracy of the water balance estimates, it would be beneficial to move from field-scale to catchment scale, as the regions surrounding the studied fields can impact the water balance of the fields. The finding has novelty value because previously the hydrological impacts of lateral preferential flow from surrounding field areas have been rarely assessed. The recent development of computational schemes that allow to the simulation of water flow in open channels (Haahti et al. 2016) enables the possibility to apply FLUSH in small catchments in the future.

Analysing field-scale water balances with long-term data and the 3D modelling approach provided a method to assess the dominating components in a way, that revealed such information of the lateral flow processes that would be challenging solely with empirical data. For example, even though dye tracers are commonly applied to visually assess the flow pathways in clayey soils, recent studies have found that the tracers possess sorptive properties, which highlights the fact that the visual tracer studies may not provide a complete understanding of the flow routes in structured soils (Morris et al. 2008; Ketelsen and Meyer-Winder 1999). Furthermore, TDR observations have been shown to include a high amount of uncertainty in clayey soils (Bittelli et al. 2008), and interpretating observations from groundwater monitoring tubes can be challenging in clayey soils (Bouma et al. 1980). Datasets can also include other kinds of uncertainties such as undocumented drainage networks, as found by Nousiainen et al. (2015). These examples underline the benefit and necessity of model applications when assessing hydrological processes and water balances in agricultural fields. Model scenarios also provided a method to quantify the hydrological impacts of different factors and interlinks of water balance components, which would not have been possible to assess with the data. Direct measurements of the amount of groundwater outflow using the method of Rozemeijer et al. (2010a) combined with a 3D modelling approach would likely provide an improved means to assess the groundwater outflow processes in clayey fields. Observations of within-field hydrological processes could further be beneficial in assessing the hydrological processes in more detail (Salo et al. 2017). Model applications could be further utilized to optimize the design of experiments for various tasks (e.g. Kikuchi et al. 2015).

Modelling techniques inevitably include both parametric and structural uncertainties (e.g. Refsgaard and Henriksen 2004) and the model had challenges in describing the TLR dynamics especially in the flat Nummela field. Though the amount of TLR was found to be small compared to the subsurface flow components, the improvement in the description of TLR in the model could further improve the model performance. As pointed out, e.g. by Appels et al. (2011), surface runoff models in relatively flat fields should include descriptions of the impacts of microtopography on the routing of surface runoff. However, incorporating these processes into computational models would be challenging because it may be difficult to interpret how the organization of microtopography is affected by different land-use conditions and farming operations. The inclusion of computational schemes to describe frost-induced impacts on soil hydraulic properties would further enhance the description of TLR and other interlinked hydrological processes

in FLUSH. Furthermore, such a scheme may be a necessity when applying the model for example in poorly drained areas where a higher amount of surface runoff can occur. The development task would likely require more detailed data on soil moisture, frost and overland flow dynamics.

In addition to TLR, the relative difference between the simulations and observations was often found to be worse during low-flow than high-flow events in drain discharge simulations. As pointed out by Wagener (2003), it is a common feature of computational models to be unable to reproduce both low-flow and high-flow events with a single parameter set. It can be argued that in low-flow conditions, water flow is sensitive to dynamic changes, e.g. in soil properties, whereas a higher amount of water flow may move in a more predictable manner in organized patterns and shapes (Savenije 2001). Agricultural field surfaces and soil structure are subject to a wide range of farming and weather conditions, which may make it difficult to interpret the impact on the flow of small amounts of water. However, the high-flow events typically contribute more to the water and sediment balance than the low-flow events, and thus the model appeared to be a suitable tool for analysing the balances. Overall, the application of multiple model parameterizations, e.g. with GLUE method (Beven and Binley 2014), would further help to assess the model uncertainties in more detail.

Further development of the subsurface water flow description would benefit of improved means to parameterize the soil preferential flow paths. As pointed out by Beven and Germann (2013) and Jarvis (2007), there are still challenges in process understanding and parameterization of preferential flow processes in computational models. The results of this study suggest that a 3D model could include spatially varying WRCs for soil preferential flow paths, since for example biopores above the subsurface drains likely have essentially different water retention properties than the layers of coarse material in the deeper soil layers (e.g. Kessler et al. 2012; Yli-Halla et al. 2009). Moreover, as pointed out by Nieber and Sidle (2010), some of the water conducting preferential flow paths can be discontinuous and describing water flow in those pathways in more detail should likely include threshold-like responses to the build-up of hydraulic water pressure in the macropores. Moreover, as pointed out by Tromp-van Meerveld and Weiler (2008) the parameterization of the bottom boundary condition in the simulations of hydrology in agricultural fields is challenging and should be further studied to improve the parameterization of the models. The results of this thesis point out the challenges related to setting up detailed hydrogeological model structures in water balance models in clayey areas.

Regarding sediment transport simulations, it was shown that different model structures (regarding subsurface connectivity, Figure 12) and parameterizations can results to qualitatively similar correspondence with the calibration variables, including load via TLR and drain discharge. However, it was shown that lateral transport in the subsurface domain is essential in describing sediment transport in structured soils. A computational assessment of the role of lateral preferential sediment transport in clayey high-latitude fields has not been conducted previously. According to the results, simulations with the different model structures

can expose uncertainties that parametric uncertainty analysis cannot reveal (Figure 26). Although structural uncertainties have been previously studied in hydrological models (e.g. Højberg and Refsgaard 2005; Butts et al. 2004), the impacts of different model structures related to subsurface sediment connectivity have rarely been quantified previously. These findings demonstrated that care should be taken when choosing a model structure and that lateral transport of suspended sediment in the soil domain should be included in simulations when assessing transport pathways. The simulations provided a rare quantification of the sediment balance components, although a more comprehensive assessment would require erosion and transport observations within the field (in addition to the outflow data).

It was also shown that, even though the model was able to reproduce the magnitude and temporal variation of the observed loads, there was a mismatch between the simulated and observed TSS concentrations dynamics. Previously, Rankinen et al. (2010), who simulated erosion and sediment transport in Finnish catchments with the Inca-Sed model, also was not able to reproduce the observed concentration dynamics in a catchment dominated by clayey soils. Based on the study of Rankinen et al. (2010) and the findings of this thesis, it is claimed that the dynamic erodibilities and aggregate stability processes (e.g. Bryan 2000) should be taken into account to be able to produce a more comprehensive computational description about the dominating erosion processes in structured soils. Furthermore, it would be beneficial to apply such models in fields with different characteristics to decipher the contribution of various erosion processes in different circumstances. It is also claimed that concentration data may encompass more information about the erosion processes than just the load data because the correspondence between simulated and observed concentrations can be poor while the model reproduces the loads adequately.

5. Conclusions

This thesis provided a rare computational quantification of the water and sediment balances in subdrained clayey agricultural fields with mean slopes of 1–5% in high-latitude conditions. Lateral preferential groundwater flow processes were shown to form a major water balance component in the studied conditions. The amount of groundwater outflow was shown to be controlled by the terrain slope and the topography of the underlying soil profile. An increase in the field slope resulted in a decreased amount of drain discharge due to the increased amount of groundwater outflow and its secondary drainage impact. Therefore drainage improvements were found to have a lower impact on field hydrology in sloping areas than in flat areas. Furthermore, the study demonstrates that field areas can be hydrologically connected to the surrounding field areas, which means that the nonlocal processes outside the fields can impact their water balance due to the groundwater flow processes. In practice, the results suggest that the slope of the arable fields and the surrounding areas should be taken into account when designing drainage procedures. It is suggested that sloping field areas require less efficient artificial drainage procedures as compared to a similar field with a flat topography. Conceptually the results of this thesis can also be beneficial for the design of hydrological measurement campaigns and interpretation of empirical field-scale data. Lateral preferential flow processes should also be taken into account in hydrogeological model structures. The hydrological impacts of lateral preferential flow have not been previously quantified in high-latitude clayey fields.

Evapotranspiration dominated the field water balances annually, and the largest share of the evapotranspiration occurred during growing seasons. The results suggest that standard methods (FAO-56) need to be adjusted in order to accurately describe evapotranspiration in the high-latitude conditions, where the crop coefficients have not been determined by intensive empirical studies. The magnitude of the PET was shown to have a major impact on water outflow components, although the impact was clearly the lowest on groundwater outflow. This suggests that an increase in evapotranspiration in a field area would have a higher impact on fast flow processes than on the slow flow processes via groundwater outflow. Quantification of the impacts of the changing amount of evapotranspiration simultaneously on all dominant water balance components has not been conducted in previous studies. During the growing seasons, groundwater outflow formed the highest outflow component. Drain discharge was the highest outflow component during the dormant season and had the highest interannual variation. Due to the effective percolation of water via soil macropores, tillage layer runoff occurred

mostly during the periods of high water table conditions (saturation excess) in the spring, autumn and winter periods. The results suggested that soil frost typically did not have a high impact on annual water balance, even though soil frost conditions intermittently led to an increased amount of tillage layer runoff in the fields.

Subsurface sediment transport pathways dominated the loads in the studied conditions, which suggested that water protection measures should focus more on subsurface load pathways. Load via subdrains formed the highest load component, whereas load via groundwater outflow also contributed to the load generation, especially in a steep field section (slope 5%). Load via groundwater outflow has not been previously taken into account in field-scale studies in clayey fields; and the results of this thesis suggested that a quantification of total loads may result in biased estimates if the load component is not taken into account. Furthermore, the simulations provided a rare quantification of the sediment balances and demonstrated that the majority of the detached particles may not form load due to the retention and settling processes. The erosion and sediment transport simulations also suggested that, in addition to hydraulic erosion and the kinetic force of raindrops, aggregate stability and breakdown processes should be taken into account in erosion models.

The 3D dual-permeability approach of FLUSH was found to be a suitable tool for water balance analysis and drainage procedure impact assessment in clayey fields. The 3D approach had the capability to take into account the spatially varying drainage systems and field characteristics more comprehensively than the widely applied 1D and 2D models. The 3D FLUSH model was able to reproduce the magnitude and temporal variation of the observed hydrological variables, and the water balance quantification was constrained by the information content of the various observed outflow and state variables. More detailed information about the hydraulic properties of the deep soil layers, more detailed observations of water flow processes within the field, and direct observations of the amount of groundwater outflow would be of benefit for further improved quantification of the water balances and determination of the model parameters. The 3D simulation approach provided novel process-based descriptions of the sediment transport mechanisms and quantification of the lateral preferential load component. More detailed sediment balance simulations would require data on erosion and sediment transport processes within the field, in addition to the outflow data. The sediment transport simulations further suggested that structural uncertainties regarding sediment transport pathways in the subsoil domain can induce higher uncertainties in the load simulations than parametric uncertainty. It is recommended that simulation strategies should apply different model structures in addition to the widely applied parameter sensitivity analyses.

References

Alberti, D.R., Cey, E.E., 2011. Evaluation of macropore flow and transport using three-dimensional simulation of tension infiltration experiments. Vadose Zone Journal 10, 603–617.

Allaire, S.E., Roulier, S., Cessna, A.J., 2009. Quantifying preferential flow in soils: A review of different techniques. Journal of Hydrology 378, 179–204.

Allen, R.G., Pereira, L.S., Raes, D.R., Smith, M., 1998. Crop evapotranspiration: guidelines for computing crop water requirements. In: FAO Irrigation and Drainage Paper No. 56. FAO, Rome, Italy, 300 pp.

Amézketa, E., 1999. Soil Aggregate Stability: A Review. Journal of Sustainable Agriculture 14, 83–151.

Antoine, M., Javaux, M., Bielders, C., 2009. What indicators can capture runoff-relevant connectivity properties of the micro-topography at the plot scale? Advances in Water Resources 32, 1297–1310.

Appels, W.M., Bogaart, P.W., van der Zee, S.E., 2011. Influence of spatial variations of microtopography and infiltration on surface runoff and field scale hydrological connectivity. Advances in Water Resources 34, 303–313.

Aura, E., 1990. Salaojien toimivuus savimaassa. MTT Agrifood Research Finland. Tiedote 10/90. MTT Agrifood Research Finland, Jokioinen, Finland, 93 pp.

Aura, E., Saarela, K., Räty, M., 2006. Savimaiden eroosio. MTT:n selvityksiä, 118 (2006). MTT Agrifood Research Finland, Jokioinen, Finland, 32 pp.

Äijö, H., Myllys, M., Nurminen, J., Turunen, M., Warsta, L., Paasonen-Kivekäs, M., Korpelainen, E., Salo, H., Sikkilä, M., Alakukku, L., Puustinen, M., 2014. PVO2-hanke, Salaojitustekniikat ja pellon vesitalouden optimointi Loppuraportti 2014. In: Salaojituksen tutkimusyhdistys ry:n tiedote 31. Finnish Field Drainage Association, Helsinki, Finland, 105 pp.

Bathurst, J.C., Cooley, K.R., 1996. Use of the SHE hydrological modelling system to investigate basin response to snowmelt at Reynolds Creek, Idaho. Journal of Hydrology 175, 181–211.

Bechmann, M., Deelstra, J., Stålnacke, P., Eggestad, H.O., Øygarden, L., Pengerud, A., 2008. Monitoring catchment scale agricultural pollution in Norway: policy instruments, implementation of mitigation methods and trends in nutrient and sediment losses. Environmental Science & Policy 11, 102–114.

Bechmann, M., 2012. Effect of tillage on sediment and phosphorus losses from a field and a catchment in south eastern Norway. Acta Agriculturae Scandinavica, Section B — Soil & Plant Science 62, 206–216.

Berisso, F.E., Schjønning, P., Keller, T., Lamandé, M., Simojoki, A., Iversen, B.V., Alakukku, L., Forkman, J., 2013. Gas transport and subsoil pore characteristics:anisotropy and long-term effects of compaction. Geoderma 195–196, 184–191.

Beven, K., Binley, A., 2014. GLUE: 20 years on. Hydrological Processes 28, 5897–5918.

Beven, K., Germann, P., 2013. Macropores and water flow in soils revisited. Water Resources Research 49, 3071–3092.

Bissonnais, Y.L., Singer, M.J., 1992. Crusting, runoff, and erosion response to soil water content and successive rainfalls. Soil Science Society of America Journal 56, 1898–1903.

Bittelli, M., Salvatorelli, F., Pisa, P R., 2008. Correction of TDR-based soil water content measurements in conductive soils. Geoderma 143, 133–142.

Blann, K.L., Anderson, J.L., Sands, G.R., Vondracek, B., 2009. Effects of agricultural drainage on aquatic ecosystems: a review. Critical Reviews in Environmental Science and Technology 39, 909–1001.

Boels, D., 1978. Installation methods. In: Proceedings of the International Drainage Workshop, ILRI, Wageningen, The Netherlands. Paper 3.0, pp. 39–49. Available at: http://content.alterra.wur.nl/Internet/webdocs/ ilri-publicaties/publicaties/Pub25/pub25-h3.0.pdf.

Bouma, J., Dekker, L.W., Haans, J.C.F.M., 1980. Measurement of depth to water table in a heavy clay soil. Soil Science 130, 264–270.

Bracken, L.J., Wainwright, J., Ali, G.A., Tetzlaff, D., Smith, M.W., Reaney, S.M., Roy, A.G., 2013. Concepts of hydrological connectivity: Research approaches, pathways and future agendas. Earth-Science Reviews 119, 17–34.

Bryan, R.B., 2000. Soil erodibility and processes of water erosion on hillslope. Geomorphology 32, 385–415.

Burkhardt, M., Kasteel, R., Vanderborght, J., Vereecken, H., 2008. Field study on colloid transport using fluorescent microspheres. European journal of soil science 59, 82–93.

Butts, M.B., Payne, J.T., Kristensen, M., Madsen, H., 2004. An evaluation of the impact of model structure on hydrological modelling uncertainty for streamflow simulation. Journal of Hydrology 298, 242–266.

Dalzell, B.J., King, J.Y., Mulla, D.J., Finlay, J.C., Sands, G.R., 2011. Influence of subsurface drainage on quantity and quality of dissolved organic matter export from agricultural landscapes. Journal of Geophysical Research 116, 1–13.

Deasy, C., Brazier, R.E., Heathwaite, A.L., Hodgkinson, R., 2009. Pathways of runoff and sediment transfer in small agricultural catchments. Hydrological Processes 23, 1349–1358.

Deelstra, J., Kværnø, S.H., Granlund, K., Sileika, A.S., Gaigalis, K., Kyllmar, K., Vagstad, N., 2009. Runoff and nutrient losses during winter periods in cold climates—requirements to nutrient simulation models. Journal of Environmental Monitoring 11, 602–609.

Deelstra, J., Iital, A., Povilaitis, A., Kyllmar, K., Greipsland, I., Blicher-Mathiesen, G., Jansons, V., Koskiaho, J., Lagzdins, A., 2014. Hydrological pathways and nitrogen runoff in agricultural dominated catchments in Nordic and Baltic countries. Agriculture, Ecosystems & Environment 195, 211–219.

Deelstra, J., 2015. Climate change and subsurface drainage design: results from a small field-scale catchment in south-western Norway. Acta Agriculturae Scandinavica, Section B—Soil & Plant Science 65, 58–65.

Devia, G.K., Ganasri, B.P., Dwarakish, G.S., 2015. A Review on Hydrological Models. Aquatic Procedia 4, 1001–1007.

Eriksson, J., Andersson, A., Andersson, R., 1999. Texture of agricultural topsoils in Sweden. In: Report, vol. 4955. Swedish Environmental Protection Agency, Stockholm, Sweden, 48 pp.

FAO, 2007. World reference base for soil resources 2006 first update. In: World Soil Resources Reports No. 103. FAO, Rome.

Farkas, C., Kværnø, S.H., Engebretsen, A., Barneveld, R., Deelstra, J., 2016. Applying profile-and catchment-based mathematical models for evaluating the runoff from a Nordic catchment. Journal of Hydrology and Hydromechanics 64, 218–225.

Feddes, R.A., Kowalik, P.J., Zaradny, H., 1978. Simulation of Field Water Use and Crop Yield. Pudoc, Wageningen, The Netherlands (1978) 189 pp.

Fipps, G., Skaggs, R.W., 1989. Influence of slope on subsurface drainage of hillsides. Water Resources Research 25, 1717–1726.

Førland, E.J., Allerup, P., Dahlström, B., Elomaa, E., Jónsson, T., Madsen, H., Perälä,J., Rissanen, P., Vedin, H., Vejen, F., 1996. Manual for Operational Correction of Nordic Precipitation Data (Report 24). Norwegian Meteorological Institute, Oslo, Norway, 66 pp.

Freer, G.R., Bay, C.E., 1969. Tillage and slope effects on runoff and erosion. Transactions of the ASAE 12, 209–2011.

French, H.K., van der Zee, S.E.A.T.M., 1999. Field observations of small scale spatial variability of snowmelt drainage and infiltration. Nordic Hydrology 30, 161–176.

Frey, S.K., Hwang, H.T., Park, Y.J., Hussain, S.I., Gottschall, N., Edwards, M., Lapen, D.R., 2016. Dual permeability modeling of tile drain management influences on hydrologic and nutrient transport characteristics in macroporous soil. Journal of Hydrology 535, 392–406.

Gallart, F., Latron, J., Llorens, P., Beven, K., 2007. Using internal catchment information to reduce the uncertainty of discharge and baseflow predictions. Advances in Water Resources 30, 808–823.

García-Ruiz, J.M., Beguería, S., Nadal-Romero, E., González-Hidalgo, J.C., Lana-Renault, N., Sanjuán, Y., 2015. A meta-analysis of soil erosion rates across the world. Geomorphology 239, 160–173.

Gerke, H.H., van Genuchten, M.T., 1993. Evaluation of a first order water transfer term for variably saturated dual-porosity flow models. Water Resources Research 29, 1225–1238.

Gerke, H.H., Köhne, J.M., 2004. Dual-permeability modeling of preferential bromide leaching from a tile-drained glacial till agricultural field. Journal of Hydrology 289, 239–257.

Gerke, H.H., 2006. Preferential flow descriptions for structured soils. Journal of Plant Nutrition and Soil Science 169, 382–400.

Gustafson, A., 1988. Simulation of nitrate leaching from arable land in southern Sweden. Acta Agriculturae Scandinavica 38, 13–23.

Gustafsson D, Lewan E, Jansson P-E., 2004. Modeling water and heat balance of the boreal landscape comparison of forest and arable land in Scandinavia. Journal of Applied Meteorology 43, 1750–1767.

Gärdenäs, A.I., Simunek, J., Jarvis, N., Genuchten, M.Th., 2006. Two-dimensional modelling of preferential water flow and pesticide transport from tile-drained field. Journal of Hydrology 329, 647–660.

Haahti, K., Warsta, L., Kokkonen, T., Younis, B. A., Koivusalo, H., 2016. Distributed hydrological modeling with channel network flow of a forestry drained peatland site. Water Resources Research 52, 246–263.

Haria, A.H., Johnson, A.C., Bell, J.P., Batchelor, C.H., 1994., Water movement and isoproturon behaviour in a drained heavy clay soil: 1. Preferential flow processes. Journal of Hydrology 163, 203–216.

Hintikka, S., Koivusalo, H., Paasonen-Kivekäs, M., Nuutinen, V., Alakukku, L., 2008. Role of macroporosity in runoff generation on a sloping subsurface drained clayfield – a case study with MACRO model. Hydrology Research 39, 143–155.

Højberg, A.L., Refsgaard, J.C., 2005. Model uncertainty – parameter uncertainty versus conceptual models. Water Science and Technology 52, 177–186.

Iglesias, A., Garrote, L., 2015. Adaptation strategies for agricultural water management under climate change in Europe. Agricultural Water Management 155, 113–124.

Ilola, A., Elomaa, E., Pulli, S., 1988. Testing of a Danish growth model for barley, turniprape and timothy in Finnish conditions. Journal of agricultural science in Finland 60, 631–660.

Istok. J.D., Boersma, L., Kling, G.F., 1985. Subsurface drainage: An erosion control practice for western Oregon? Special Report 729. Corvallis; Agricultural Experiment Station, Oregon State University. 43 pp.

Jarritt, N.P., Lawrence, D.S.L., 2007. Fine sediment delivery and transfer in lowland catchments: modelling suspended sediment concentrations in response to hydrological forcing. Hydrological Processes 21, 2729–2744.

Jarvis, N.J., Villholth, K.G., Ulén, B., 1999. Modelling particle mobilization and leaching in macroporous soil. European Journal of Soil Science 50, 621–632.

Jarvis, N.J., 2007. A review of non-equilibrium water flow and solute transport in soilmacropores: principles, controlling factors and consequences for water quality. European Journal of Soil Science 58 (3), 523–546.

Jarvis, N.J., 2008. Near-saturated hydraulic properties of macroporous soils. Vadose Zone Journal 7, 1302–1310.

Jarvis NJ., 2011. Simple physics-based models of compensatory plant water uptake: concepts and eco-hydrological consequences. Hydrology and Earth System Sciences Discussions 8, 6789–6831.

Jin, C.X., Sands, G.R., 2003. The long-term field-scale hydrology of subsurface drainage systems in a cold climate. Transactions of the ASAE 46, 1011–1021.

Johnsson, H, Jansson P-E., 1991. Water balance and soil moisture dynamics of field plots with barley and grass ley. Journal of Hydrology 129, 149–173.

Jones, H.G., Pomeroy, J.W., 2001. Early spring snowmelt in a small boreal forest watershed: influence of concrete frost on the hydrology and chemical composition of streamwaters during rain-on-snow events. Proceedings of the Eastern

Snow Conference, 58, 209-218. Available at: http://www.usask.ca/hydrology/papers/Jones Pomeroy 2001.pdf.

Kangas, A., Högnäsbacka, M., Kujala, M., Laine, A., Niskanen, M., Jauhiainen, L., Nikander, H., 2012. Results of official variety trials. MTT Raportti 75. MTT, Jokioinen,Finland, 234 pp. Available at:
http://www.mtt.fi/mttraportti/pdf/mttraportti75.pdf.

Kankaanranta, J., 1996. Veden virtaus ja ravinteiden huuhtoutuminen savimaassa. In: With an English Abstract: (Water flow and Nutrient Leaching in Clay Soils). Diplomityö. Helsinki University of Technology, Espoo, Finland, 79 pp.

Karvonen, T., 1988. A Model for Predicting the Effect of Drainage on Soil Moisture, Soil Temperature and Crop Yield. Doctoral Dissertation. Helsinki University of Technology, 215 pp.

Kätterer, T., Andrén, O., Jansson, P.E., 2006. Pedotransfer functions for estimating plant available water and bulk density in Swedish agricultural soils. Acta Agriculturae.Scandinavia Section B - Soil and Plant Science 56, 263–276.

Kessler, T.C., Klint, K.E.S., Nilsson, B., Bjerg, P.L., 2012. Characterization of sand lenses embedded in tills. Quaternary Science Reviews 53, 55–71.

Ketelsen, H., Meyer-Windel, S., 1999. Adsorption of brilliant blue FCF by soils. Geoderma 90, 131-145.

Kikuchi, C.P., Ferré, T.P.A., Vrugt, J.A., 2015. On the optimal design of experiments for conceptual and predictive discrimination of hydrologic system models. Water Resources Research 51, 4454–4481.

Kim, D.J., Vereecken, H., Feyen, J., Boels, D., Bronswijk, J.J.B., 1992. On the characterization of an unripe marine clay soil I. Shrinkage processes of an unripe marine clay soil in relation to physical ripening. Soil Science 153, 471–481.

King, K.W., Williams, M.R., Macrae, M.L., Fausey, N.R., Frankenberger, J., Smith, D.R., Kleinman, P.J., Brown, L.C., 2015. Phosphorus transport in agricultural subsurface drainage: A review. Journal of Environmental Quality 44, 467–485.

Kirchner, J.W., 2006. Getting the right answers for the right reasons: Linking measurements, analyses, and models to advance the science of hydrology. Water Resources Research 42, W03S04.

Kladivko, E.J., Willoughby, G.L., Santini, J.B., 2005. Corn growth and yield response to subsurface drain spacing on Clermont silt loam soil. Agronomy journal 97, 1419–1428.

Klint, K.E.S., Gravesen, P., 1999. Fractures and biopores in Weichselian clayey till aquitards at Flakkebjerg, Denmark. Nordic Hydrology 30, 267–284.

Knisel, W.G., Turtola, E., 2000. GLEAMS model application on a heavy clay soil in Finland. Agricultural Water Management 43, 285–309.

Knud, E.S., Gravesen, P., 1999. Fractures and biopores in Weichselian clayey till aquitards at Flakkebjerg, Denmark. Nordic Hydrology 30, 267–284.

Koestel, J.K., Moeys, J., Jarvis, N.J., 2012. Meta-analysis of the effects of soil properties, site factors and experimental conditions on solute transport. Hydrology and Earth System Sciences 16, 1647–1665.

Koivusalo, H., Karvonen, T., Paasonen-Kivekäs, M., 1999. Application of a two-dimensional model to calculate water balance of an agricultural hillslope. Physics and Chemistry of the Earth (B) 24, 313–318.

Koivusalo, H., Heikinheimo, M., Karvonen, T., 2001. Test of a simple two-layer parameterisation to simulate the energy balance and temperature of a snow pack. Theoretical and Applied Climatology 70, 65–79.

Koivusalo, H., Turunen, M., Salo, H., Haahti, K., Nousiainen, R., Warsta, L. 2015. FLUSH: 3D hydrological model for agricultural water management in high latitude areas. In: 20th International Northern Research Basins Symposium and Workshop, Kuusamo 16-21 Aug 2015, Finland: 14-23. Availabe at: http://www.syke.fi/download/noname/%7B8AE2852A-3B60-409A-BE52-574AB5085767%7D/111231

Kuhn, N.J., Bryan, R.B., 2004. Drying, soil surface condition and interrill erosion on two Ontario soils. CATENA 57, 113–133.

Larsson, M.H., Jarvis, N.J., 1999. Evaluation of a dual-porosity model to predict field-scale solute transport in a macroporous soil. Journal of Hydrology 215, 153–171.

Laubel, A., Jacobsen, O.H., Kronvang, B., Grant, R., Andersen, H.E., 1999. Subsurface Drainage Loss of Particles and Phosphorus from Field Plot Experiments and a Tile-Drained Catchment. Journal of Environment Quality 28, 576–584.

Legates, D.R., McCabe, G.J., 1999. Evaluating the use of "goodness of fit" measures in hydrologic and hydroclimatic model validation. Water Resources Research 35, 233–241.

Lemmelä, R., Sucksdorff, Y., Gilman, K., 1981. Annual Variation of Soil Temperature at Depths 20 to 700 cm in an Experimental Field in Hyrylä, South-Finland during 1969 to 1973. Geophysica 17, 143–154.

Lhomme JP, Elguero E, Chehbouni A, Boulet G. 1998. Stomatal control of transpiration: examination of Monteith's formulation of canopy resistance. Water Resources Research 34, 2301–2308.

Lorente, S., Bejan, A., 2006. Heterogeneous porous media as multiscale structures for maximum flow access. Journal of Applied Physics 100, 114909.

Lundin, L-C., 1990. Hydraulic properties in an operational model of frozen soil. Journal of Hydrology 118, 289–310.

Lundekvam, H.E., 2007. Plot studies and modelling of hydrology and erosion in southeast Norway. CATENA, Soil Water Erosion in Rural Areas 71, 200–209.

Matson, P.A., Parton, W.J., Power, A.G., Swift, M.J., 1997. Agricultural intensification and ecosystem properties. Science 277, 504–509.

McDowell, R., Sharpley, A., Folmar, G., 2001. Phosphorus Export from an Agricultural Watershed. Journal of Environment Quality 30, 1587–1595.

McMahon, T.A., Peel, M.C., Lowe, L., Srikanthan, R., McVicar, T.R., 2013. Estimating actual, potential, reference crop and pan evaporation using standard meteorological data: a pragmatic synthesis. Hydrology and Earth System Sciences 17, 1331–1363.

Mendez, A., Sands, G.R., Basin, B., Jin, C.X., Wotzka, P.J., 2004. Simulating the impact of drainage design in a cold climate with ADAPT. Journal of the American Water Resources Association 40, 385–400.

Merritt, W.S., Letcher, R.A., Jakeman, A.J., 2003. A review of erosion and sediment transport models. Environmental Modelling & Software 18, 761–799.

Mohtanty, B.P., Bowman, R.S., Hendrickx, J.M.H., Simunek, J., Van Genuchten, M.T., 1998. Preferential transport of nitrate to a tile drain in an intermittent-flood-irrigated field: model development and experimental evaluation. Water Resources Research 34, 1061–1076.

Monteith, J.L., 1965. Evaporation and the environment. In: The State and Movement of Water in Living Organisms, XIXth symposium. Swansea, UK: Society of Experimental Biology, Cambridge University Press.

Morris, C., Mooney, S.J., Young, S.D., 2008. Sorption and desorption characteristics of the dye tracer, Brilliant Blue FCF, in sandy and clay soils. Geoderma 146, 434–438.

Muukkonen, P., Hartikainen, H., Alakukku, L., 2009. Effect of soil structure disturbance on erosion and phosphorus losses from Finnish clay soil. Soil and Tillage Research 103, 84–91.

Mutziger, A.J., Burt, C.M., Howes, D.J., Allen, R.G., 2005. Comparison of measured and FAO-56 modeled evaporation from bare soil. Journal of. Irrigation and Drainage Engineering 131, 59–72.

Naarding, W.H., 1978. Trench versus trenchless drainage techniques. In: Proceeding of the International Drainage Workshop, ILRI, Wageningen, The Netherlands. Paper 3.07, pp. 543–555. Available at: http://content.alterra.wur.nl/Internet/webdocs/ilri-publicaties/publicaties/Pub25/pub25.pdf.

Nash, J.E., Sutcliffe, J.V., 1970. River flow forecasting through conceptual models. Part 1. A discussion of principles. Journal of Hydrology 10, 282–290.

Needelman, B.A., Gburek, W.J., Petersen, G.W., Sharpley, A.N., Kleinman, P.J., 2004. Surface runoff along two agricultural hillslopes with contrasting soils. Soil Science Society of America Journal 68, 914–923.

Nieber, J.L., Sidle, R.C., 2010. How do disconnected macropores in sloping soils facilitate preferential flow? Hydrological Processes 24, 1582–1594.

Nielsen, M.H., Styczen, M., Ernstsen, V., Petersen, C.T., Hansen, S., 2010. Field study of preferential flow pathways in and between drain trenches. Vadose Zone Journal 9, 1073–1079.

Nielsen, M.H., Petersen, C.T., Hansen, S., 2015. Identification of efficient transport pathways from the soil surface to field drains by smoke injection. European Journal of Soil Science 66, 516–524.

Nousiainen, R., Warsta, L., Turunen, M., Huitu, H., Koivusalo, H., Pesonen, L., 2015. Analyzing subsurface drain network performance in an agricultural monitoring site with a three-dimensional hydrological model. Journal of Hydrology 529, 82–93.

Nuutinen, V., Pöyhönen, S., Ketoja, E., Pitkänen, J., 2001. Abundance of the earthworm Lumbricus terrestris in relation to subsurface drainage pattern on a sandy clay field. European Journal of Soil Biology 37, 301–304.

Oades, J.M., 1993. The role of biology in the formation, stabilization and degradation of soil structure. Geoderma 56, 377–400.

Olesen, S.E., 1978. Trenchless drainage experiments in Denmark. In: Proceedings of the International Drainage Workshop, ILRI, Wageningen, The Netherlands, 527–535. Paper 3.05, pp. 527–542. Available at: http://content.alterra.wur.nl/ Internet/webdocs/ilri-publicaties/publicaties/Pub25/pub25.pdf.

Oreskes, N., Shrader-Frechette, K., Belitz, K., 1994. Verification, validation, and confirmation of numerical models in the earth sciences. Science 263, 641–646.

Øygarden, L., Kværner, J., Jenssen, P.D., 1997. Soil erosion via preferential flow to drainage systems in clay soils. Geoderma 76, 65–86.

Paasonen-Kivekäs, M., Peltomaa, R., Vakkilainen, P., Äijö, H. (ed.), 2009. Maan vesi- ja ravinnetalous: Ojitus, kastelu ja ympäristö [Water and nutrient balance of soils: drainage, irrigation and environment]. Helsinki: Salaojayhdisty ry. 452 pp.

Panagos, P., Van Liedekerke, M., Jones, A., Montanarella, L., 2012. European Soil Data Centre: Response to European policy support and public data requirements. Land Use Policy 29, 329–338.

Peltonen-Sainio, P., Rajala, A., 2008. Viljojen kasvun ABC. MTT Agrifood Research Finland, Jokioinen, Finland, 11 pp.

Pereira, L. S., Allen, R. G., Smith, M., Raes, D., 2015. Crop evapotranspiration estimation with FAO56: Past and future. Agricultural Water Management 147, 4–20.

Pietola, L., Alakukku, L., 2005. Root growth dynamics and biomass input by Nordic annual field crops. Agriculture, Ecosystems and Environment 108, 135–144.

Pietola, L., Horn, R., Yli-Halla, M., 2005. Effects of trampling by cattle on the hydraulic and mechanical properties of soil. Soil and Tillage Research 82, 99–108.

Puustinen, M., Merilä, E., Palko, J., Seuna, P., 1994. Kuivatustila, viljelykäytäntö ja vesistökuormitukseen vaikuttavat ominaisuudet Suomen pelloilla. In: With an English abstract: (Drainage Level, Cultivation Practices and Factors Affecting Load on Waterways in Finnish Farmland). Vesi- ja ympäristöhallinnon julkaisuja – sarja A 198. National Board of Waters and Environment, Helsinki, Finland, 319 pp.

Puustinen, M., Tattari, S., Koskiaho, J., Linjama, J., 2007. Influence of seasonal and annual hydrological variations on erosion and phosphorus transport from arable areas in Finland. Soil and Tillage Research 93, 44–55.

Puustinen, M., Turtola, E., Kukkonen, M., Koskiaho, J., Linjama, J., Niinioja, R., Tattari, S., 2010. VIHMA—A tool for allocation of measures to control erosion and nutrient loading from Finnish agricultural catchments. Agriculture, Ecosystems & Environment 138, 306–317.

Quinton, J.N., Catt, J.A., 2007. Enrichment of heavy metals in sediment resulting from soil erosion on agricultural fields. Environmental Science & Technology 41, 3495–3500.

Rankinen, K., Thouvenot-Korppoo, M., Lazar, A., Lawrence, D.S.L., Butterfield, D., Veijalainen, N., Huttunen, I., Lepistö, A., 2010. Application of catchment scale sediment delivery model INCA-Sed to four small study catchments in Finland. CATENA 83, 64–75.

Rawls, W.J., Pachepsky, Y.A., Ritchie, J.C., Sobecki, T.M., Bloodworth, H., 2003. Effect of soil organic carbon on soil water retention. Geoderma 116, 61–76.

Refsgaard, J.C., Henriksen, H.J., 2004. Modelling guidelines – terminology and guiding principles. Advances in Water Resources 27, 71–82.

Refsgaard, J.C., van der Sluijs, J.P., Brown, J., van der Keur, P., 2006. A framework for dealing with uncertainty due to model structure error. Advances in Water Resources 29, 1586–1597.

Rekolainen S., 1993. Assessment and mitigation of agricultural water pollution. In Publications of the Water and Environment Research Institute 12. Helsinki: National Board of Waters and the Environment. 33 pp.

Ritchie, J.T., 1972. Model for predicting evaporation from a row crop with incomplete cover. Water Resources Research 8, 1204–1213.

Ritzema, H.P., Nijland, H.J., Croon, F.W., 2006. Subsurface drainage practices: From manual installation to large-scale implementation. Agricultural Water Management 86, 60–71.

Rozemeijer, J.C., Broers, H.P., 2007. The groundwater contribution to surface water contamination in a region with intensive agricultural land use (Noord-Brabant, The Netherlands). Environmental Pollution 148, 695–706.

Rozemeijer, J.C., van der Velde, Y., van Geer, F.C., Bierkens, M.F.P., Broers, H.P., 2010a. Direct measurements of the tile drain and groundwater flow route contributions to surface water contamination: from field-scale concentration patterns in groundwater to catchment-scale water quality. Environmental Pollution 158, 3571–3579.

Rozemeijer, J.C., Van Der Velde, Y., McLaren, R.G., Van Geer, F.C., Broers, H.P., Bierkens, M.F.P., 2010b. Integrated modeling of groundwater–surface water interactions in a tile-drained agricultural field: The importance of directly measured flow route contributions. Water Resources Research 46, W11537, doi:10.1029/2010WR009155.

Räisänen, J., 2008. Warmer climate: less or more snow? Climate Dynamics 30, 307–319.

Saavalainen, J., 1984. Salaojittajan käsikirja, osa II A: Salaojituksen suunnitelu [Handbook of drainage designer, part II A: design of subsurface drainage]. Helsinki: Salaojakoulutuksen kannatusyhdistys. 167 pp.

Salo, H., Warsta, L., Turunen, M., Nurminen, J., Myllys, M., Paasonen-Kivekäs, M., Alakukku, L., Koivusalo, H., 2017. Simulating 3-D water flow in subsurface drain trenches and surrounding soils in a clayey field. Soil and Tillage Research 168, 20–32.

Sands, G.R., Canelon, D., Talbot, M., 2015. Developing optimum subsurface drainage design procedures. Acta Agriculturae Scandinavica, Section B—Soil & Plant Science 65, 121–127.

Satterlund, D.R., 1979. An improved equation for estimating longwave radiation from the atmosphere. Water Resources Research 15, 1649–1650.

Savenije, H.H., 2001. Equifinality, a blessing in disguise? Hydrological processes 15, 2835-2838.

Schoups, G., Van de Giesen, N.C., Savenije, H.H.G., 2008. Model complexity control for hydrologic prediction. Water Resources Research 44, W00B03.

Schulze-Makuch, D., Carlson, D.A., Cherkauer, D.S., Malik, P., 1999. Scale dependency of hydraulic conductivity in heterogeneous media. Ground Water 37, 904–919.

Seuna, P., Kauppi, L., 1981. Influence of sub-drainage on water quantity and quality in a cultivated area in Finland. Publications of the Water Research Institute 43, 32–47.

Sharpley, A.N., Bergström, L., Aronsson, H., Bechmann, M., Bolster, C.H., Börling, K., Djodjic, F., Jarvie, H.P., Schoumans, O.F., Stamm, C., Tonderski, K.S., 2015. Future agriculture with minimized phosphorus losses to waters: Research needs and direction. Ambio 44, 163–179.

Sidle, R.C., Noguchi, S., Tsuboyama, Y., Laursen, K., 2001. A conceptual model of preferential flow systems in forested hillslopes: Evidence of self-organization. Hydrological Processes 15, 1675–1692.

Silberstein, R.P., 2006. Hydrological models are so good, do we still need data? Environmental Modelling & Software 21, 1340–1352.

Šimůnek, J., Jarvis, N.J., Van Genuchten, M.T., Gärdenäs, A., 2003. Review and comparison of models for describing non-equilibrium and preferential flow and transport in the vadose zone. Journal of Hydrology 272, 14–35.

Skaggs, R. W., Tabrizi, A.N., Foster., G.R., 1982. Subsurface drainage effects on erosion. Journal of Soil and Water Conservation 37, 167–172.

Skaggs, R.W., Youssef, M.A., Chescheir, G.M., Gilliam, J.W., 2005. Effects of drainage intensity on nitrogen losses from drained lands. Transactions of the ASAE 48, 2169–2177.

Skaggs, R.W, Youssef, M.A., Chescheir, G.M., 2006. Drainage design coefficients for eastern United States. Agricultural water management 86, 40–49.

Soinne, H., Hyväluoma, J., Ketoja, E., Turtola, E., 2016. Relative importance of organic carbon, land use and moisture conditions for the aggregate stability of post-glacial clay soils. Soil and Tillage Research 158, 1–9.

Spoor, G., Fry, R.K., 1983. Field performance of trenchless drainage tines and implications for drainage system efficiency. Journal of Agricultural Engineering Research 28, 319–335.

Srinivasan, M.S., Gérard-Marchant, P., Veith, T. L., Gburek, W. J., Steenhuis, T. S., 2005. Watershed scale modeling of critical source areas of runoff generation and phosphorus transport. Journal of the American Water Resources Association 41, 361–377.

Stuyt, L.C.P.M., Dierickx, W., Martínez Beltrán, J., 2005. Materials for subsurface drainage systems. FAO irrigation and drainage paper 60, rev. 1. FAO, Rome, Italy, 202 pp. Available at: ftp://ftp.fao.org/agl/aglw/docs/idp60.pdf.

Stähli, M., Jansson, P-E., Lundin, L.-C., 1996. Preferential water flow in a frozen soil—a two-domain model approach. Hydrological Processes 10, 1305–1316.

Stähli, M., Nyberg, L., Mellander, P.E., Jansson, P-E., Bishop, K.H., 2001. Soil frost effects on soil water and runoff dynamics along a boreal transect: 2 Simulations. Hydrological.Processes 15, 927–941.

Sun, Y., Zeng, Y., Shi, Q., Pan, X., Huang, S., 2015. No-tillage controls on runoff: A meta-analysis. Soil and Tillage Research 153, 1–6.

Taskinen, A., Bruen, M., 2007. Incremental distributed modelling investigation in a small agricultural catchment: 2. Erosion and phosphorus transport. Hydrological Processes 21, 92–102.

Tattari, S., Bärlund, I., Rekolainen, S., Posch, M., Siimes, K., Tuhkanen, H.-R., Yli-Halla, M., 2001. Modeling sediment yield and phosphorus transport in Finnish clayey soils. Transactions of the ASAE 44, 297–307.

Thacker, B.H., Doebling, S.W., Hemez, F.M., Anderson, M.C., Pepin, J.E., Rodriquez, E.A., 2004. Concepts of model verification and validation, Technical Report, Los Alamos National Laboratory, Los Alamos, NM, USA, DOI: 102172/835920, 2004.

Tilman, D., Balzer, C., Hill, J., Befort, B.L., 2011. Global food demand and the sustainable intensification of agriculture. Proceedings of the NAS 108, 20260–20264.

Tromp-van Meerveld, H.J., McDonnell, J.J., 2006. Threshold relations in subsurface stormflow: 1. A 147-storm analysis of the Panola hillslope. Water Resources Research 42, W02410.

Turtola, E., Paajanen, A., 1995. Influence of improved subsurface drainage on phosphorus losses and nitrogen leaching from a heavy clay soil. Agricultural Water Management 28, 295–310.

Turtola, E., Alakukku, L., Uusitalo, R., 2007. Surface runoff, subsurface drainflow and soil erosion as affected by tillage in a clayey Finnish soil. Agricultural and Food Science 16, 332–351.

Ulén, B., 2004. Size and Settling Velocities of Phosphorus-Containing Particles in Water from Agricultural Drains. Water, Air, & Soil Pollution 157, 331–343.

Ulén, B., Bechmann, M., Øygarden, L., Kyllmar, K., 2012. Soil erosion in Nordic countries – future challenges and research needs. Acta Agriculturae Scandinavica, Section B — Soil & Plant Science 62, 176–184.

Ulén, B.M., Larsbo, M., Kreuger, J.K., Svanbäck, A., 2014. Spatial variation in herbicide leaching from a marine clay soil via subsurface drains. Pest Management Science 70, 405–414.

Uusi-Kämppä, J., Jauhiainen, L., 2010. Long-term monitoring of buffer zone efficiency under different cultivation techniques in boreal conditions. Agriculture, Ecosystem and Environment, Special section Harvested perennial grasslands: Ecological models for farming's perennial future 137, 75–85.

Uusitalo, R., Turtola, E., Kauppila, T., Lilja, T., 2001. Particulate Phosphorus and Sediment in Surface Runoff and Drainflow from Clayey Soils. Journal of Environment Quality 30, 589–595.

Uusitalo, R., Turtola, E., Lemola, R., 2007. Phosphorus losses from a subdrained clayey soil as affected by cultivation practices. Agricultural and Food Science 16, 352–365.

Vagstad, N., Stålnacke, P., Andersen, H.-E., Deelstra, J., Jansons, V., Kyllmar, K., Loigu,E., Rekolainen, S., Tumas, R., 2004. Regional variations in diffuse nitrogen losses from agriculture in the Nordic and Baltic regions. Hydrology and Earth System Sciences 8, 651–662.

Vakkilainen, P., Suortti-Suominen, T., 1982. Aurasalaojituksen käyttömahdollisuuksien tarkastelua [Assessing opportunities for the usage of trenchless

drain installation methods]. Vesitalous 1/82. Helsinki University of Technology, Espoo, Finland.

Vakkilainen, P., Alakukku, L., Myllys, M., Nurminen, J., Paasonen-Kivekäs, M., Peltomaa, R., Puustinen, M., Äijö, H., 2008. Pellon vesitalouden optimointi – Väliraportti 2008. Salaojituksen tutkimusyhdistys ry:n tiedote 29. Finnish Field Drainage Association, Helsinki, Finland, 100 pp.

Vakkilainen, P., Alakukku, L., Koskiaho, J., Myllys, M., Nurminen, J., Paasonen-Kivekäs,M., Peltomaa, R., Puustinen, M., Äijö, H., 2010. Pellon vesitalouden optimointi – Loppuraportti 2010. Salaojituksen tutkimusyhdistys ry:n tiedote 30. Finnish Field Drainage Association, Helsinki, Finland, 114 pp.

van Dam, J.C., Groenendijk, P., Hendriks, R.F., Kroes, J.G., 2008. Advances of modeling water flow in variably saturated soils with SWAP. Vadose Zone Journal 7, 640–653.

van den Bogaert, R., Cornu, S., Michel, E., 2016. To which extent do rain interruption periods affect colloid retention in macroporous soils? Geoderma 275, 40-47.

Van den Eertwegh, G.A.P.H., Nieber, J.L., De Louw, P.G.B., Van Hardeveld, H.A., Bakkum, R., 2006. Impacts of drainage activities for clay soils on hydrology and solute loads to surface water. Irrigation and Drainage 55, 235–245.

van der Velde, Y., Rozemeijer, J.C., de Rooij, G.H., van Geer, F.C., Broers, H.P., 2010. Field-scale measurements for separation of catchment discharge into flow route contributions. Vadose Zone Journal 9, 25–35.

van Genuchten, M.Th, 1980. A closed-form equation for predicting the hydraulic conductivity of unsaturated soils. Soil Science Society of America Journal 44, 892–898.

Vanmaercke, M., Poesen, J., Verstraeten, G., de Vente, J., Ocakoglu, F., 2011. Sediment yield in Europe: Spatial patterns and scale dependency. Geomorphology 130, 142–161.

Vereecken, H., Schnepf, A., Hopmans, J.W., Javaux, M., Roose, D., Vanderborght, J., Young, M.H., Amelung, W., Aitkenhead, M., Allison, S.D., Assouline, S., Baveye, P., Berli, M., Brüggemann, N., Finke, P., Flury, M., Gaiser, T., Govers, G., Ghezzehei, T., Hallett, P., Hendricks Franssen, H.J., Heppell, J., Horn, R., Huisman, J.A., Jacques, D., Jonard, F., Kollet, S., Lafolie, F., Lamorski, K., Leitner, D., McBratney, A., Minasny, B., Montzka, C., Nowak, W., Pachepsky, Y., Padarian, J., Romano, N., Roth, K., Rothfuss, Y., Rowe, E.C., Schwen, A., Šimůnek, J., Tiktak, A., Van Dam, J., van der Zee, S.E.A.T.M., Vogel, H.J., Vrugt, J.A., Wöhling, T., Young, I.M., 2016. Modeling Soil Processes: Review, Key Challenges, and New Perspectives. Vadose Zone Journal 15. doi:10.2136/vzj2015.09.0131

Villholth, K.G., Jensen, K.H., 1998. Flow and transport processes in a macroporous subsurface-drained glacial till soil II. Model analysis. Journal of Hydrology 207, 121–135.

Wagener, T., 2003. Evaluation of catchment models. Hydrological Processes 17, 3375–3378.

Waldner, P.A., Schneebeli, M., Schultze Zimmermann, U., Flühler, H., 2004. Effect of snow structure on water flow and solute transport. Hydrological Processes 18, 1271–1290.

Warsta, L., 2011. Modelling water flow and soil erosion in clayey, subsurface drained agricultural fields. Doctoral dissertation. Aalto University, School of Engineering, Department of Civil and Environmental Engineering, Espoo, Finland, 212 pp.

Warsta, L., Turunen, M., Koivusalo, H., Paasonen-Kivekäs, M., Karvonen, T., Taskinen, A., 2012. Modelling heat transport and freezing and thawing processes in a clayey, subsurface drained agricultural field. In: Proceedings of the 11th ICID Int. Drainage Workshop on Agricultural Drainage, Needs and Future Priorities, Cairo 23–27.9.2012, Egypt, 10 pp.

Warsta, L., Karvonen, T., Koivusalo, H., Paasonen-Kivekäs, M., Taskinen, A., 2013a. Simulation of water balance in a clayey, subsurface drained agricultural field with three-dimensional FLUSH model. Journal of Hydrology 476, 395–409.

Warsta, L., Taskinen, A., Koivusalo, H., Paasonen-Kivekäs, M., Karvonen, T., 2013b. Modelling soil erosion in a clayey, subsurface-drained agricultural field with a three-dimensional FLUSH model. Journal of Hydrology 498, 132–143.

Warsta, L., Taskinen, A., Paasonen-Kivekäs, M., Karvonen, T., Koivusalo, H., 2014. Spatially distributed simulation of water balance and sediment transport in an agricultural field. Soil and Tillage Research 143, 26–37.

Weiler, M., McDonnell, J.J., 2007. Conceptualizing lateral preferential flow and flow networks and simulating the effects on gauged and ungauged hillslopes. Water Resources Research 43, 1–13.

Wellen, C., Arhonditsis, G.B., Long, T., Boyd, D., 2014. Quantifying the uncertainty of nonpoint source attribution in distributed water quality models: A Bayesian assessment of SWAT's sediment export predictions. Journal of Hydrology 519, 3353–3368.

Wicks, J.M., Bathurst, J.C., 1996. SHESED: a physically based, distributed erosion and sediment yield component for the SHE hydrological modelling system. Journal of Hydrology 175, 213–238.

Widmoser, P., 2009. A discussion on and alternative to the Penman–Monteith equation. Agricultural Water Management 96, 711–721.

Wilson, B.N., 2000. History of drainage research at the University of Minnesota. University of Minnesota and Iowa State University Drainage Research Forum, St. Paul, Minnesota, US, 39 pp. Available at: https://wiki.umn.edu/pub/Wilson/DownloadReports/his_drain.pdf.

Wright, J., Sands, G., 2001. Planning an Agricultural Subsurface Drainage System. Pub. No. BU-07685. Minnesota Ext. Ser., University of Minnesota, St. Paul, MN, USA (2001).

Xu, C.Y., 2000. Modelling the effects of climate change on water resources in central Sweden. Water Resources Management 14, 177–189.

Yalin, M.S., 1963. An expression for bed-load transportation. Proceedings of the ACAE, Journal of the Hydraulic Division 89, 221–250.

Yalin, M.S., 1977. Mechanics of Sediment Transport. Pergamon Press, Toronto, 298 pp.

Yli-Halla, M., Mokma, D.L., Alakukku, L., 2009. Evidence for the formation of Luvisols/Alfisols as a response to coupled pedogenic and anthropogenic influences in a clay soil in Finland. Agricultural and Food Science 18, 388–401.

Youngs, E.G., 1991. Hydraulic conductivity of saturated soils. In: K.A. Smith, C.E. Mullins (Eds.), Soil Analysis – Physical Methods, Marcel Dekker, New York, USA (1991), 620 pp.

Zhang, M-K., Wang, K-P, He, Z-L., 2007. Spatial and temporal variation of nitrogen exported by runoff from sandy agricultural soils. Journal of Environmental Sciences 19, 1086–1092.

Annex I. Observed median groundwater depths in field sections A–D of the Nummela experimental site in (a) 2010, (b) 2011 and (c) 2012. Observations during those time periods when groundwater depth was below the tube depth (1.6 m) were assigned a depth of 1.6 in the calculation of the median values.

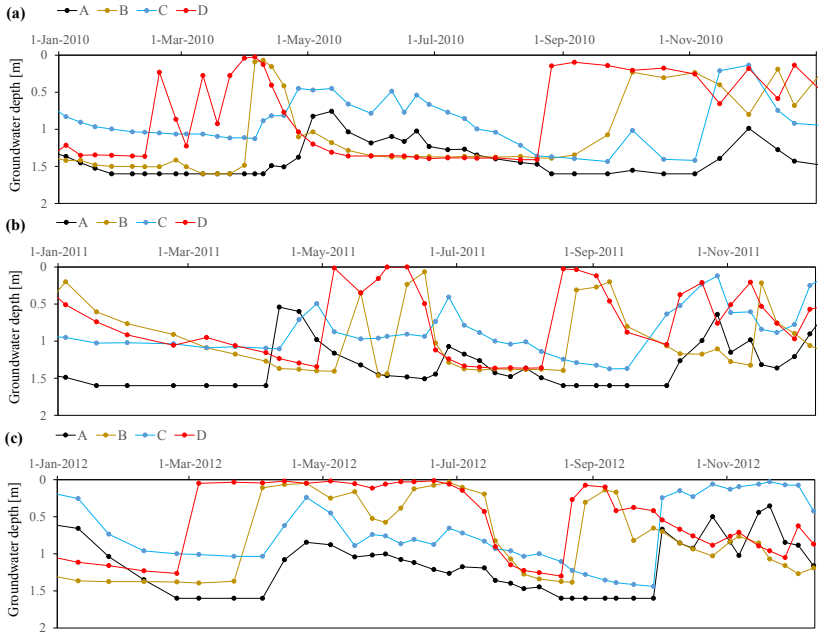

Annex II. (a) Hourly and (b) daily simulated and observed radiation components and (c) hourly and (d) daily potential evapotranspiration of the reference surface in the model application at the Nummela experimental site.

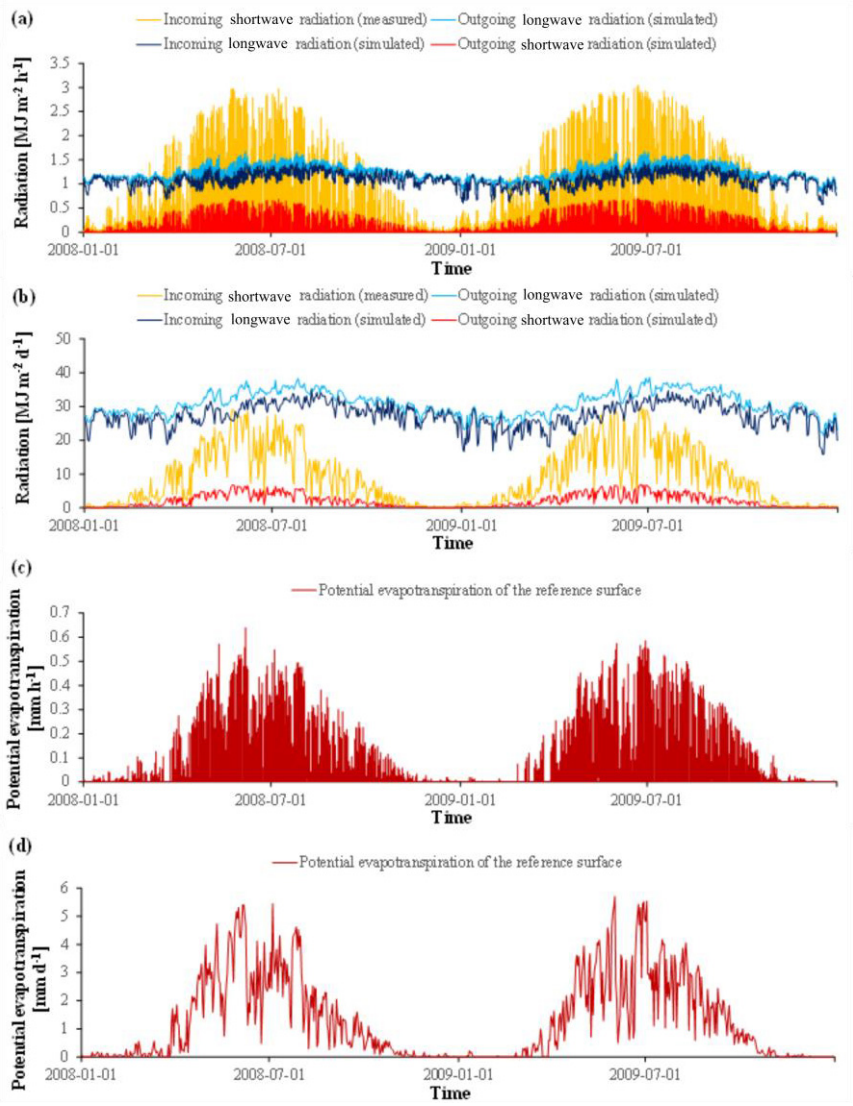

Aalto-DD 67/2017

ISBN 978-952-60-7379-8 (printed)
ISBN 978-952-60-7378-1 (pdf)
ISSN-L 1799-4934
ISSN 1799-4934 (printed)
ISSN 1799-4942 (pdf)

Aalto University
School of Engineering
Department of Built Environment
www.aalto.fi

BUSINESS +
ECONOMY

ART +
DESIGN +
ARCHITECTURE

SCIENCE +
TECHNOLOGY

CROSSOVER

DOCTORAL
DISSERTATIONS